ELECTRIC POWER
RESEARCH INSTITUTE

Program on Technology Innovation: State-of-Knowledge Review of Erosion-Resistant Coatings for Steam and Gas Turbine Applications

Program on Technology Innovation: State-of-Knowledge Review of Erosion-Resistant Coatings for Steam and Gas Turbine Applications

1017458

Final Report, August 2008

EPRI Project Manager
D. Gandy

ELECTRIC POWER RESEARCH INSTITUTE
3420 Hillview Avenue, Palo Alto, California 94304-1338 • PO Box 10412, Palo Alto, California 94303-0813 • USA
800.313.3774 • 650.855.2121 • askepri@epri.com • www.epri.com

DISCLAIMER OF WARRANTIES AND LIMITATION OF LIABILITIES

THIS DOCUMENT WAS PREPARED BY THE ORGANIZATION(S) NAMED BELOW AS AN ACCOUNT OF WORK SPONSORED OR COSPONSORED BY THE ELECTRIC POWER RESEARCH INSTITUTE, INC. (EPRI). NEITHER EPRI, ANY MEMBER OF EPRI, ANY COSPONSOR, THE ORGANIZATION(S) BELOW, NOR ANY PERSON ACTING ON BEHALF OF ANY OF THEM:

(A) MAKES ANY WARRANTY OR REPRESENTATION WHATSOEVER, EXPRESS OR IMPLIED, (I) WITH RESPECT TO THE USE OF ANY INFORMATION, APPARATUS, METHOD, PROCESS, OR SIMILAR ITEM DISCLOSED IN THIS DOCUMENT, INCLUDING MERCHANTABILITY AND FITNESS FOR A PARTICULAR PURPOSE, OR (II) THAT SUCH USE DOES NOT INFRINGE ON OR INTERFERE WITH PRIVATELY OWNED RIGHTS, INCLUDING ANY PARTY'S INTELLECTUAL PROPERTY, OR (III) THAT THIS DOCUMENT IS SUITABLE TO ANY PARTICULAR USER'S CIRCUMSTANCE; OR

(B) ASSUMES RESPONSIBILITY FOR ANY DAMAGES OR OTHER LIABILITY WHATSOEVER (INCLUDING ANY CONSEQUENTIAL DAMAGES, EVEN IF EPRI OR ANY EPRI REPRESENTATIVE HAS BEEN ADVISED OF THE POSSIBILITY OF SUCH DAMAGES) RESULTING FROM YOUR SELECTION OR USE OF THIS DOCUMENT OR ANY INFORMATION, APPARATUS, METHOD, PROCESS, OR SIMILAR ITEM DISCLOSED IN THIS DOCUMENT.

ORGANIZATION(S) THAT PREPARED THIS DOCUMENT

TurboMet International

Material Processing Technology, LLC

NOTE

For further information about EPRI, call the EPRI Customer Assistance Center at 800.313.3774 or e-mail askepri@epri.com.

Electric Power Research Institute, EPRI, and TOGETHER…SHAPING THE FUTURE OF ELECTRICITY are registered service marks of the Electric Power Research Institute, Inc.

Copyright © 2008 Electric Power Research Institute, Inc. All rights reserved.

CITATIONS

This report was prepared by

TurboMet International
8026 Winter Park
San Antonio, TX 78250

Principal Investigator
V. P. Swaminathan

Material Processing Technology, LLC
1965 Forest Park Road
Norton Shores, MI 49441

Principal Investigator
J. Smith

This report describes research sponsored by the Electric Power Research Institute (EPRI).

This report is a corporate document that should be cited in the literature in the following manner:

Program on Technology Innovation: State-of-Knowledge Review of Erosion-Resistant Coatings for Steam and Gas Turbine Applications. EPRI, Palo Alto, CA: 2008. 1017458.

PRODUCT DESCRIPTION

Solid particle erosion (SPE) and liquid droplet erosion (LDE) cause severe damage to turbine components, such as gas turbine compressor blades and vanes as well as steam turbine control stage and later stage low-pressure blades. This report will provide a comprehensive knowledge base to turbine users on erosion coating properties, methods of application, details about the various vendors and their experience as well as the tests conducted to evaluate and qualify erosion-resistant coatings.

Results and Findings

This state-of-knowledge literature review addresses the following topics:

- Coatings currently used in steam and gas turbines, such as nitriding, plasma spray, physical vapor disposition (PVD), and diffusion coatings
- Various methods of coating characterization and durability tests used in laboratories and in the field, including information about specific laboratories and original equipment manufacturer (OEM) test facilities
- Effects of processing methods and variables on coating quality and performance, with specific discussions of PVD processes, evaporation methods, sputtering methods, and coating growth
- LDE testing, with emphasis on test facilities and apparatus and a general discussion of LDE resistance
- SPE testing, including an overview of test apparatus and facilities as well as highlights of several methods referenced for characterization of the erosion performance of compressor materials and coatings
- An assessment of nanocoatings for potential use in gas and steam turbine applications

Challenges and Objective(s)

The goals of this report are twofold, as follows:

- To conduct a thorough state-of-the-art knowledge review of the erosion-resistant coatings produced and used in the industry as well as those under development and targeted for application to land-based gas and steam turbines
- To conduct a survey of the coating vendors who supply erosion-resistant coatings

Both goals were achieved through an in-depth literature survey, study of patents in this area, and direct survey of many coating vendors as well as several coating test facilities.

Applications, Value, and Use

Power producers will find this literature search particularly valuable to determine what coatings should be considered for steam and gas turbine applications where erosive conditions are a concern.

EPRI Perspective

EPRI and the power industry have realized for many years that improved coating technologies are needed to address erosive conditions in both steam and gas turbines. This report, along with other efforts aimed at developing nanostructured coatings, represents the first time in 20 years that EPRI has looked at coatings for erosive conditions associated with turbine blades. If successful, the technologies have potential to save the industry millions of dollars each year. Related EPRI work includes *Program on Technology Innovation: Erosion Resistant Coating Development and Vendor Coating Evaluation for Turbine Components* (1014277, March 2008).

Approach

Investigators conducted a thorough survey of the published literature on erosion-resistant coatings. They included a summary of the various traditional and advanced coating processes. In addition, they conducted other direct inquiries of coating vendors who provide conventional and advanced erosion-resistant coatings. These interviews provided information on state-of-the-art erosion coatings currently in development and in use throughout the industry. All current information about the various coatings used in gas and steam turbines was collected from the literature for a comprehensive study of their properties, application processes, microstructural characteristics, and resistance against SPE and LDE. Both aeroengine and land-based gas turbine experience are summarized in this report.

Keywords

Steam turbines
Gas turbines
Erosion-resistant coatings
Nanocoatings
Blades
Vanes
Coating methods

ABSTRACT

A thorough survey of the published literature on erosion-resistant coatings was conducted. Also, direct inquiries of coating vendors who provide conventional and advanced erosion-resistant coatings were conducted to gather additional information on state-of-the-art erosion coatings currently under development and in use. A summary of the various traditional and advanced coating processes are included here. All of the current information about the various coatings used in turbines (gas and steam) was collected from the literature for a comprehensive study of their properties, application processes, microstructural characteristics and resistance against solid particle and liquid droplet erosion (SPE and LDE) protection. Effects of the processing methods and variables on the quality and performance of these coatings are summarized. The coating processes include the conventional coatings currently used in steam and gas turbines such as nitriding, plasma spray, physical vapor deposition and diffusion coatings. Various methods of coating characterization and durability tests used by various laboratories (both SPE and liquid particle erosion [LPE]) were gathered and summarized. Information about these specific laboratories and original equipment manufacturer (OEM) test facilities are also included. A comprehensive listing of all the patents in the area of erosion coatings is provided in an appendix.

Several coating vendors were surveyed to gather information about their specific processes and experience in the area of erosion coating application and field operating experience. The experience base mainly addresses the erosion coatings applied to gas turbines. Both aeroengine and land-based gas turbine experience were received and summarized in this report. It is expected that this report will provide a comprehensive knowledge base to turbine users on the various erosion coating properties, methods of application, details about the various vendors and their experience, and the tests conducted to evaluate and qualify the erosion-resistant coatings.

CONTENTS

---

1 LITERATURE REVIEW 1-1
- 1.1 Introduction 1-1
- 1.2 Solid Particle Erosion Mechanisms 1-3
  - 1.2.1 Ductile Versus Brittle Coatings 1-3
  - 1.2.2 Solid Particle Erosion of Flight Engine Components 1-5
- 1.3 Liquid Droplet Erosion Mechanisms 1-8
- 1.4 Coating Methods and Coating Characteristics 1-11
  - 1.4.1 General Coating Process Categories 1-11
  - 1.4.2 Physical Vapor Deposition Processes 1-13
  - 1.4.3 Evaporation Methods 1-15
    - 1.4.3.1 Biased Activated Reactive Evaporation/Reactive Ion Plating 1-15
    - 1.4.3.2 Cathodic Arc Physical Vapor Deposition 1-17
  - 1.4.4 Sputtering Methods 1-22
  - 1.4.5 Coating Growth – Structure Zone Model 1-23
- 1.5 Coating Materials and Compositions 1-26
  - 1.5.1 Titanium Nitride, Titanium Aluminum Nitride, and Ti-Silicon Carbonitride 1-26

2 COATING VENDOR SURVEY 2-1
- 2.1 Overview of Nanocoating Gas Turbine Experience Base 2-1
- 2.2 Vendor Profiles 2-4
  - 2.2.1 Liburdi Engineering Limited 2-4
    - 2.2.1.1 Background 2-4
    - 2.2.1.2 Performance Testing and Field Service 2-8
    - 2.2.1.3 Land-Based Gas Turbine Applications 2-9
  - 2.2.2 Praxair Surface Technologies 2-10
    - 2.2.2.1 Background 2-10
    - 2.2.2.2 Praxair 24K Coating Structure and Coating Process 2-12
    - 2.2.2.3 Coating Equipment and Process 2-15

2.2.2.4 QC Metrics 2-17
2.2.2.5 Performance Testing and Field Service 2-18
2.2.2.6 Rain Erosion Testing 2-21
2.2.3 MDS-PRAD Technologies 2-21
2.2.3.1 Background 2-21
2.2.3.2 ER-7 Coating Structure and Coating Process 2-22
2.2.3.3 Performance Testing and Field Service 2-23
2.2.3.3.1 FCT Test Program 2-23
2.2.3.3.2 T64 Stage 1 Blade Erosion Wind Tunnel Testing – University of Cincinnati 2-25
2.2.3.3.3 T64 Engine Qualification Testing 2-26
2.2.3.3.4 Field Service Experience 2-30
2.2.3.3.5 T58 Sand Ingestion Testing 2-30
2.2.4 Performance Turbine Components 2-32
2.2.4.1 Coating Process 2-33
2.2.4.2 Field Experience 2-33
2.2.5 BryCoat, Inc. 2-34
2.2.6 Sputtek, Inc. 2-37
2.2.6.1 Coating Process 2-37
2.2.6.2 Testing and Validation 2-39
2.2.6.2.1 Microstructure of the Coating 2-40
2.2.6.2.2 Adhesion Scratch Tests 2-41
2.2.6.2.3 Sand Erosion Test Results 2-41
2.2.7 American Surface Modification, LLC (AMS) 2-43
2.2.8 Analytical Services and Materials 2-44
2.2.9 Chromalloy Nevada 2-46

***3* LIQUID DROPLET EROSION TEST FACILITIES 3-1**
3.1 Background 3-1
3.2 AFRL/UDRI Rain Erosion Testing 3-3
3.2.1 UDRI Rain Erosion Test Apparatus 3-3
3.3 ALSTOM Materials LDE Test System 3-5
3.4 Dynaflow, Inc., Test System 3-5
3.5 Skoda Turbine Blade Water Erosion Test Facility 3-6

4 **SOLID PARTICLE EROSION TESTING 4-1**
4.1 Overview of the Types of SPE Tests 4-1
4.2 ASTM G76, Standard Method for Conducting Erosion Tests by Solid Particle Impingement Using Gas Jets 4-2
4.2.1 Apparatus 4-2
4.2.2 Test Materials and Sampling 4-4
4.2.3 Calibration of Apparatus 4-4
4.2.4 Standard Test Conditions 4-5
4.2.5 Optional Test Conditions and Test Procedure 4-5
4.3 SPE Test Facilities 4-6
4.3.1 Metcut Research, Inc. 4-6
4.3.2 University of Dayton Research Institute Facility 4-6
Test Conditions 4-8
4.3.3 University of Cincinnati Erosion Facility Description 4-9
4.3.4 National Research Council of Canada SPE Test Facility 4-10

5 **REFERENCES 5-1**

A **APPENDIX A-1**

LIST OF FIGURES

Figure 1-1 Examples of solid particle (SPE) and liquid droplet erosion (LDE) damage to gas and steam turbine components 1-2

Figure 1-2 Examples of severe solid particle erosion environments in flight engines. Nano-scale PVD coatings have been used to improve turbine durability and reliability. 1-3

Figure 1-3 Erosive mass loss as a function of impact angle for al (ductile) and Al_2O_3 (brittle) substrates. The variation in response typifies the characteristic definitions of a “ductile” and a “brittle” response respectively. Note the variation in the magnitude of erosion In the Y-axis label. 1-4

Figure 1-4 Particle erosion mechanisms. a) Plowing and extrusion mechanism for ductile materials, b) Brittle material erosion proceeds through lateral and radial cracking around the crush zone 1-5

Figure 1-5 Compressor airfoil particle impact angles for flight engines 1-6

Figure 1-6 Schematic of gas turbine engine illustrating the effects of sand ingestion 1-7

Figure 1-7 V22 Osprey new and engine run compressor impellers showing effects of solid particle erosion on the component. Note the significant erosion loss of the vanes. 1-7

Figure 1-8 (a) Idealized diagram of early stage liquid drop impact and (b) a diagrammatic representation of some of the mechanisms by which an impinging liquid drop can damage a solid 1-8

Figure 1-9 Characteristic erosion versus time curves showing (a) cumulative erosion (mass or volume loss) versus exposure duration (time or cumulative mass or volume of liquid impinged); (b) corresponding instantaneous erosion rate versus exposure duration obtained by differentiating curve a 1-9

Figure 1-10 Schematics of the liquid impact erosion mechanism of TiN coating 1-10

Figure 1-11 PVD schematic depicting the elements of the biased activated reactive evaporation process 1-17

Figure 1-12 Industrial cathodic arc coating system with a 600 mm (23.6 in.) diameter x 1000 mm (39.37 in.) high coating zone 1-19

Figure 1-13 CA-PVD systems with cylindrical post style cathodes used to increase cathode spot velocity and minimize macroparticle formation 1-21

Figure 1-14 Schematic illustration of the sputtering process 1-22

Figure 1-15 Plasma enhanced magnetron sputtering (PEMS) system with two magnetrons 1-23

Figure 1-16 Structure zone models for PVD coating growth 1-25

Figure 1-17 Titanium - nitrogen phase diagram 1-27

Figure 2-1 Liburdi production erosion-resistant coating photomicrographs. a) RIC TiN monolayer, b) RIC TiN multilayer 2-5

Figure 2-2 Schematic of Liburdi Engineering Reactive Ion Coating (RIC) EB-PVD coating process 2-6

Figure 2-3 Liburdi RIC large production coating unit. Effective coating zone 1.2 x 1.2 x 1 m (3.9 x 3.9 x 3.3 ft). Capable of coating multiple larger IGT compressor blades. 2-6

Figure 2-4 Liburdi RIC multilayer (Ti, Al, Cr) metal - metal nitride coating under development for erosion/corrosion applications 2-7

Figure 2-5 Relative erosion performance of T64 turboshaft engines uncoated and Liburdi RIC TiN coated blades in service. The coated airfoils maintained engine power and stall margin ~2.5 times longer than the uncoated airfoils. 2-8

Figure 2-6 Comparison of Liburdi RIC TiN coated and uncoated blade profiles following field service. The uncoated blades show trailing edge thinning and chord loss while the coated blades have maintained their profile. 2-8

Figure 2-7 Component fatigue test data for Liburdi RIC TiN on coated and uncoated T58 stages 3 and 7 compressor blades 2-9

Figure 2-8 Frame 7EA VGV compressor inlet vane and Fr 7FA Row 0 compressor blade coated with Liburdi RIC erosion-resistant coating 2-10

Figure 2-9 Effect of TiNx coating nitrogen content on microhardness, residual compressive stress, crystallographic texture, and crystallite size 2-13

Figure 2-10 Erosion resistance as a function of TiNx nitrogen content at 30 and 90 degrees with 50 micron alumina at 80–120 m/s. The shaded area shows the region for optimum erosion performance. 2-14

Figure 2-11 Photomicrograph and schematic of PST 24K Type II TiN erosion-resistant coating architecture 2-15

Figure 2-12 Praxair CA-PVD coater # 3 with multiple arc cathodes, a load capacity of 400 lbs (181 kg) (rotation mode), and a coating zone 30 inches (76 cm) in diameter and 36 inches (91 cm) in height 2-16

Figure 2-13 Praxair chamber #4 multiple cathodes coating 2-16

Figure 2-14 Praxair 24K color comparison between sub-stoichiometric (left) and fully stoichiometric TiN (right). The coating color is used as a quality control metric. 2-18

Figure 2-15 PST 24K Type II erosion test results compared to Ti 6-4 and IN 718 uncoated alloys at 20 and 90 degree impingement angles. 50 micron alumina at 80–120 m/s (262–394 ft/s). 2-19

Figure 2-16 ASTM G76 modified erosion test of Praxair 24K Type II TiN multilayer coating data replotted to show relative improvement compared to uncoated Ti 6-4 and IN 718 alloys at 20 and 90 degree particle impact angles. 2-19

Figure 2-17 Comparison of various Praxair thermal spray and CA-PVD coatings in relative erosion resistance at 20 and 90 degrees 2-20

Figure 2-18 Compressor blade 20 degree erosion test comparing PST 24K Type II coating to uncoated blade after 2500 grams (5.5 lb) of Arizona Road Dust. The uncoated blade is completely eroded through the thickness (hole), but the coated blade is intact. 2-20

Figure 2-19 Praxair 24K+ Type 2 TiN coating rain erosion test sample after 450 minutes 2-21

Figure 2-20 Multilayer coating architecture of MDS-PRAD's ER-7 erosion coating................2-22

Figure 2-21 MDS-PRAD production facility in Prince Edward Island......................................2-23

Figure 2-22 Erosion performance of ER-7 coating compared to uncoated 17-4 PH, Custom 450, IN 718, and Ti 6-4 as a function of erosion angle. ASTM G76 50 micron alumina erosion testing. 2-24

Figure 2-23 Relative improvement in erosion performance of ER-7 coating compared to uncoated 17-4 PH, Custom 450, IN 718, and Ti 6-4 as a function of erosion angle. ASTM G76 50 micron alumina erosion testing..2-25

Figure 2-24 Particle erosion testing on T64 Stage 1, Ti 6-4 compressor blades in the University of Cincinnati erosion wind tunnel...2-26

Figure 2-25 HCF test results for ER-7 coated and uncoated IN 718, A286, and Ti 6-4 cylindrical test bars [74]..2-27

Figure 2-26 T64 compressor rotor at teardown following sand ingestion testing at Kirtland Air Force Base. ER-7 coated and uncoated blades were used in the rainbow rotor. Severe erosion of the uncoated airfoil trailing edge is particularly apparent. 2-28

Figure 2-27 Improved chord and trailing edge thickness retention seen for ER-7 coated compressor blades and vanes compared to uncoated parts following teardown of the T64 sand ingestion test engine. 2-29

Figure 2-28 T58 ER-7 coated and uncoated first stage blades showing differences in degree of leading edge curl...2-31

Figure 2-29 T58 ER-7 coated rotor showing erosion patterns following sand ingestion testing...2-32

Figure 2-30 T-Armor coated Frame7 FA R0 compressor blade row.......................................2-34

Figure 2-31 Condition of the leading edge of R0 blade from Frame 7FA engine coated with T-Armor coating after 15,000 hours of operation. 1300 hours with fogging (wet) operation. 2-34

Figure 2-32 Sputtek's CA-PVD coating deposition systems located in Toronto, Canada. Bottom photo shows a close-up of the new system. 2-38

Figure 2-33 Metallurgical cross section of Sputtek's TiAlN coating 2-40

Figure 2-34 Microhardness indentations (left) and hardness profile (right) of the ion nitrided sublayer (0.5N load) in the duplex coating (TiAlN + ion nitriding) 2-40

Figure 2-35 Adhesion scratch test of TiAlN coating on AM350 steel; coating thickness is 15 microns; average microhardness is 2720 HV50; critical load for coating crack is 60N. 2-41

Figure 2-36 Sand erosion test results of TiAlN coating by the University of Cincinnati showing 37 times improvement at 20 degree impingement and 18 times improvement at 90 degree impingement...2-42

Figure 2-37 Results of rainbow tests on aeroengine compressor blades showing a factor of 7 times improvement in erosion resistance over uncoated substrate 2-42

Figure 2-38 Aerocoat K coating has a tough nano-composite polymeric matrix, designed to absorb and dissipate the impact energy without tearing or debonding. 2-45

Figure 2-39 Erosion test results for AS&M's Aerocoat K polymeric coating with 120 grit alumina at 600 ft/s (183 m/s) in ASTM G 76 test 2-46

Figure 2-40 ASTM G 32 cavitation test results for Aerocoat K compared to various substrate materials. Testing was performed at 20 kHz, at 500 watts in de-ionized water with a pulsed cycle of 4 s on/1 s off for times ranging from 2–20 hours. 2-46

Figure 3-1 Graphic of relative water droplet sizes 3-2

Figure 3-2 AFRL/UDRI rain erosion test facility schematic 3-4

Figure 3-3 Water droplet erosion test rig at ALSTOM in Switzerland 3-5

Figure 3-4 Test systems used at Dynaflow for water droplet erosion and cavitation erosion testing 3-6

Figure 3-5 Erosion test stand at Skoda 3-7

Figure 4-1 ASTM G76 solid particle erosion test rig schematic 4-3

Figure 4-2 ASTM A76 solid particle erosion test rig at SwRI. Photo at right shows a coated disc sample and the nozzle aimed at 90 degree impact angle 4-4

Figure 4-3 UDRI particle erosion rig (From UDRI Facility Description) 4-7

Figure 4-4 Schematic of gas jet particle erosion test showing particle impact angle (From UDRI Facility Description) 4-8

Figure 4-5 University of Cincinnati high-velocity erosion test facility schematic 4-9

Figure 4-6 S.S. White Industrial Airbrasive unit for erosion tests at NRC Canada 4-10

LIST OF TABLES

Table 1-1 Coating deposition methods (after Bunshah) 1-12
Table 1-2 Some traditional erosion coating methods and vendors...1-13
Table 1-3 Movchan-Demchishin structure zone model of PVD. Zone transitions as a function of the homologous temperature Ts/Tm determined for metal and oxides. 1-24
Table 1-4 Transition temperatures for thermal evaporation..1-26
Table 2-1 Summary of thin erosion-resistant coating vendor survey..2-2
Table 2-2 Relative erosion performance at 30 and 90 degrees for several D-Gun carbide-based coatings compared to CA-PVD TiN and ZrN coatings.............................2-11
Table 2-3 Coating chemistries, thickness, and temperature limits..2-43
Table 4-1 ASTM G76 particle erosion standard test conditions..4-11
Table A-1 Listing of erosion coating patents (1979 to 2007) A-1

1

LITERATURE REVIEW

1.1 Introduction

The main purpose of this report is to provide a summary of survey of the published literature as well as direct inquiries with the various commercial coating vendors conducted to gather additional information on the state-of-the-art erosion coatings in development and in use. All of the current information about the various coatings used in turbines (gas and steam) was collected for a comprehensive study of their properties, coating application processes, microstructural characteristics, and resistance against solid particle erosion (SPE) and liquid particle erosion (LPE) protection. These include the conventional coatings currently used in steam and gas turbines such as nitriding, plasma spray, physical vapor deposition (PVD), and diffusion coatings. Various methods of coating characterization and durability tests used in laboratories (both SPE and LPE) and in the field are also gathered and summarized.

SPE and liquid droplet erosion (LDE) cause severe damage to turbine components such as gas turbine compressor blades and vanes and steam turbine control stage and later stage low-pressure (LP) blades. Some examples of such damage are shown in Figure 1-1. In the case of gas turbines operating on land in power generation and mechanical drive applications, dust ingestion and other small particles from the environment lead to erosion and impact damage to the airfoils. Some of the large frame and smaller aeroderivative engines incorporate front end fogging systems and water spray directly in the path of the air intake as well as inside the compressor path. This is done to increase the mass flow to improve the power output and efficiency of the engines. However, such operation has inadvertent negative consequences. Solid particles and liquid droplets cause erosion of the airfoils and reduce engine efficiency and reliability, potentially leading to catastrophic failures during service. At the inlet end of the high-pressure (HP) and intermediate-pressure (IP) steam turbines, particulate matter such as oxides from the steam paths lead to SPE of the blades and nozzles as shown in Figure 1-1. In addition to SPE, LDE in the steam path of steam turbines near the exhaust end of the low-pressure turbines leads to damage to the blades [1]. For LM6000 SPRINT gas turbines using water injection inside the compressor, significant LDE damage was observed on the leading edge of some of the compressor blades [2]. Similar damage to Frame FA engine R-0 compressor blades was reported [3]. Such erosion damage could act as high-cycle fatigue crack initiation sites and lead to blade failures when the blades have marginal design allowance for frequency and stress amplitudes.

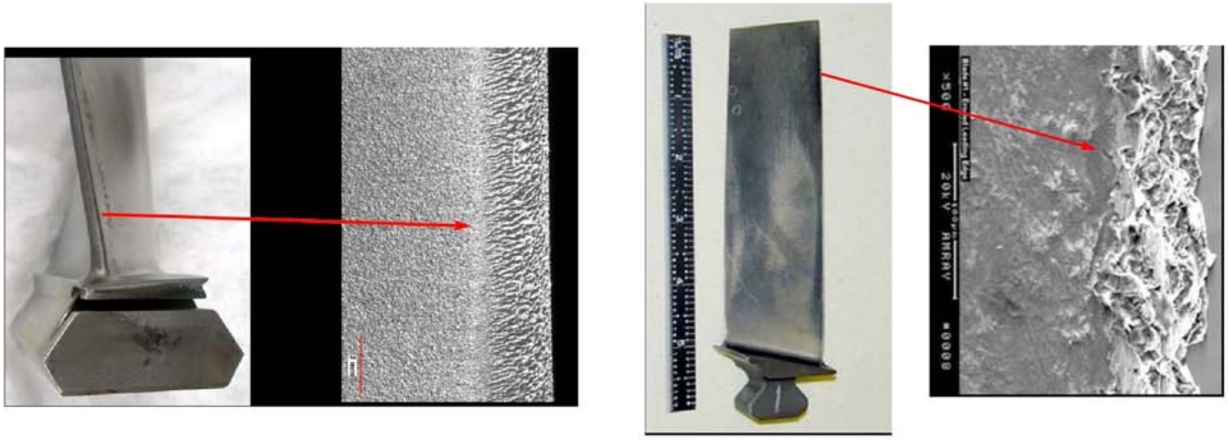

a) LDE Damage to 7FA Engine R-0 Compressor Blade

b) LDE Damage to HP Compressor Blade in LM6000 SPRINT Engine Compressor Blade

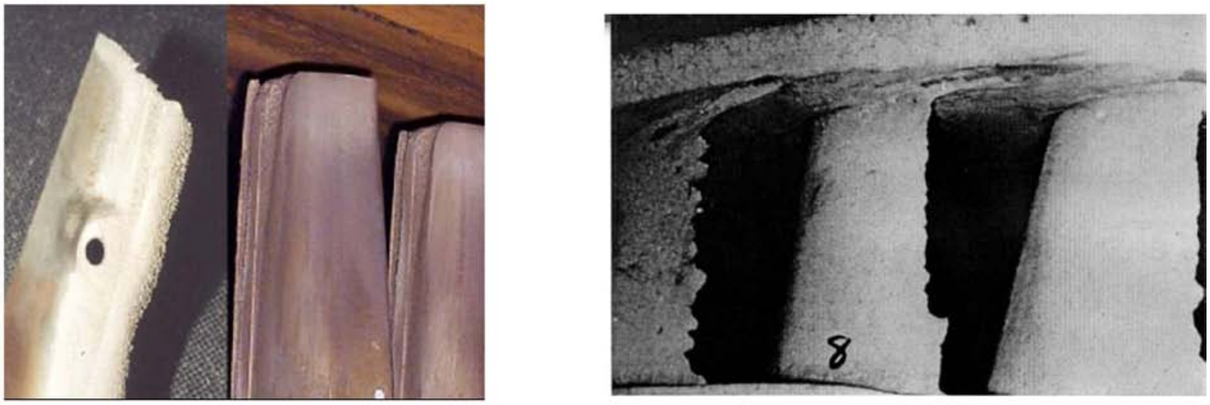

c) LDE Damage to LP Steam Turbine Blades

d) SPE Damage to Steam Turbine IP Blade

Figure 1-1
Examples of solid particle (SPE) and liquid droplet erosion (LDE) damage to gas and steam turbine components

The problem of solid particle erosion in both fixed wing airplane and helicopter engines is well known. Operation in desert environments or from unimproved airstrips has been identified as a cause of rapid deterioration of gas turbine engine performance due to the accelerated wear of compressor airfoils. Figure 1-2 dramatically illustrates the issue. In the case of flight engines, it may endanger the lives of the crew and passengers, especially for flight engines operated in dusty environments [4, 5]. Engine durability has been reduced in some instances from a design life of 3000 hours to less than 100 hours time on wing before removal for loss of power or lack of stall margin occurs. Nano-scale erosion-resistant PVD coatings for gas turbine compressor airfoils have been found to significantly improve compressor durability and have largely replaced traditional coating methods for these applications.

Figure 1-2
Examples of severe solid particle erosion environments in flight engines. Nano-scale PVD coatings have been used to improve turbine durability and reliability.

1.2 Solid Particle Erosion Mechanisms

1.2.1 Ductile Versus Brittle Coatings

The topic of solid particle erosion has been studied by numerous researchers over the years. Several good reviews of the particle erosion literature can be found in articles by Wright [6], Finnie [7], and Mathews [8]. One of the key concepts that have been identified is the difference in the erosion behavior of ductile materials, such as metals, and that of brittle materials, such as most ceramics. With ductile materials, the erosion response as a function of particle impact angle has been shown to approach zero at very low angles of attack; it increases to a maximum as the angle of incidence is between 15–20 degrees and then drops to 1/2 to 1/3 of the maximum erosion rate as the particles impacting the surface approach 90 degrees. The erosion rate of brittle materials is at a maximum at 90 degrees with the rate decreasing continually to a negligible mass loss at very low angles of impact. This response reflects fracture-induced mass loss where the extent of the erosion is dependent on the normal component of the particle impact energy. This difference in ductile and brittle material behavior is plotted in Figure 1-3.

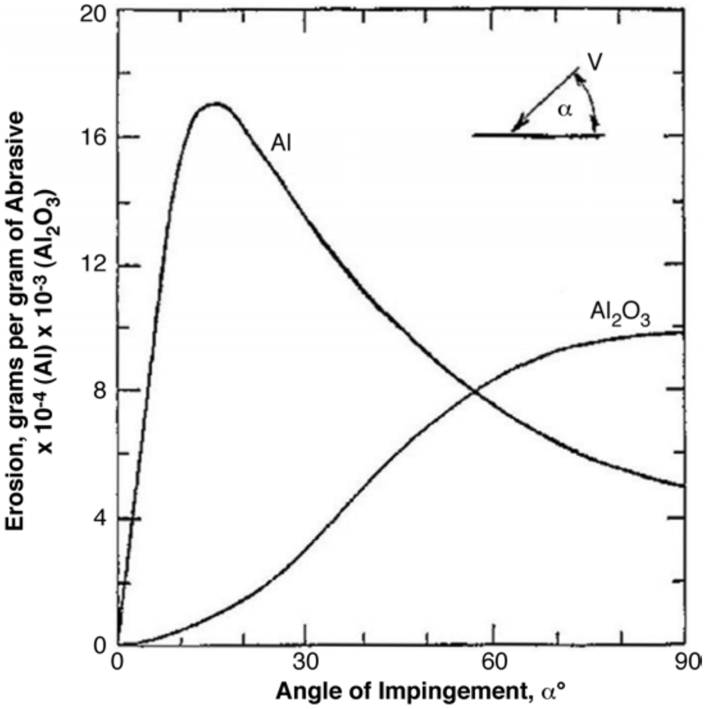

Figure 1-3
Erosive mass loss as a function of impact angle for al (ductile) and Al_2O_3 (brittle) substrates. The variation in response typifies the characteristic definitions of a “ductile” and a “brittle” response respectively. Note the variation in the magnitude of erosion In the Y-axis label. [7, 8]

In ductile erosion, the metal is indented by the particles impacting the surface, and material is extruded around the indentation. At high angles, the energy of the particle is dissipated through ductile deformation and is more resistant to erosive wear than at low angles where the metal indentation proceeds by a plowing or micromachining action. At high angles, the material removal mechanism is thought to proceed by work hardening of the extruded material by repeated impacts, leading to local fracture-based loss of material. With brittle materials, the particle impact generates brittle fracture within the near surface zone of the material, with cracks radiating outward and downward from the point of impact. These behaviors are illustrated in Figure 1-4.

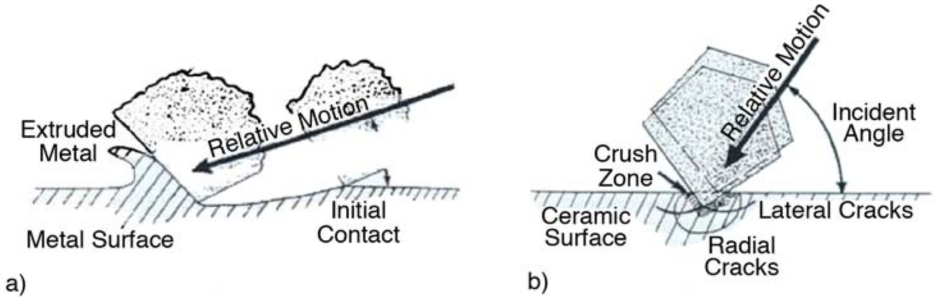

Figure 1-4
Particle erosion mechanisms. a) Plowing and extrusion mechanism for ductile materials, b) Brittle material erosion proceeds through lateral and radial cracking around the crush zone [9]

The factors that have been found to affect erosion rate in addition to particle impact angle are [10]:

- Particle size
- Size distribution
- Shape (angularity)
- Hardness
- Friability
- Composition
- Erodent flux
- Erosion temperature

Toughness and hardness are the dominant substrate properties controlling erosion behavior. Erosion performance has been found to scale with increasing material hardness for low and high impingement angles, while higher toughness reduces the threshold for brittle fracture, which improves 90-degree erosion resistance [11, 12]. The test results reported by the various coating manufacturers and test laboratories vary significantly, making meaningful comparison and relative performance of the various coatings difficult.

1.2.2 Solid Particle Erosion of Flight Engine Components

For gas turbine engines, operation in dust-laden environments can lead to several forms of erosive wear on the compressor airfoils. As shown in Figure 1-5, the angle of impact of an erodent particle varies from ~ 75–90 degrees at the leading edge of the airfoil to low-angle attack on the pressure face. This is especially pronounced at the trailing edge. Due to the geometry of compressor airfoils and the high rate of erosion of metals at low-particle impact angles, trailing edge thinning and resultant chord loss has been found to be the primary mechanism for loss of turbine compressor efficiency in aero engines. Leading edge thinning also occurs, but generally to a lesser extent. The first few stages of the compressor are more likely to experience leading edge curl due to ductile deformation of a thinned leading edge by the ballistic impact of larger sand particles.

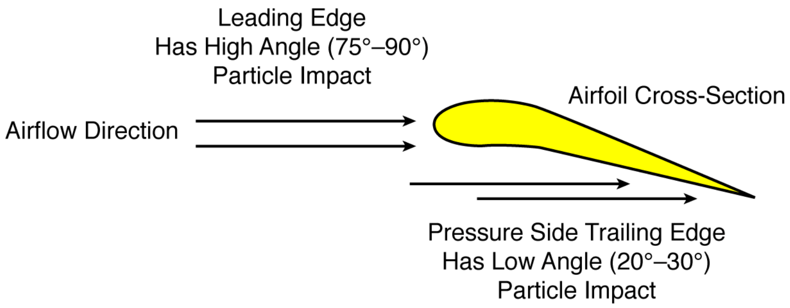
Leading Edge
Has High Angle (75°–90°)
Particle Impact
Airfoil Cross-Section
Airflow Direction
Pressure Side Trailing Edge
Has Low Angle (20°–30°)
Particle Impact

Figure 1-5
Compressor airfoil particle impact angles for flight engines

Chord loss is typically greater in the middle stages of the compressor due to the sand particles concentrated toward the outer portion of the gas path by the centrifugal action of the rotating blades. As shown in Figure 1-6 the eroded profile of a mid-stage compressor blade has incurred a significant amount of chord loss in the outer third of the airfoil at the trailing edge. Figure 1-7 shows a compressor impeller that was damaged in service by solid particle erosion. Such erosion of the compressor components leads to the deterioration of engine efficiency with operating time, increased specific fuel consumption (SFC), and reduced reliability of the engines. It is reported that by applying a multilayer TiN-based PVD coating to the compressor blades, time on wing (TOW) was increased from 100 to 200 hours on military aircraft.

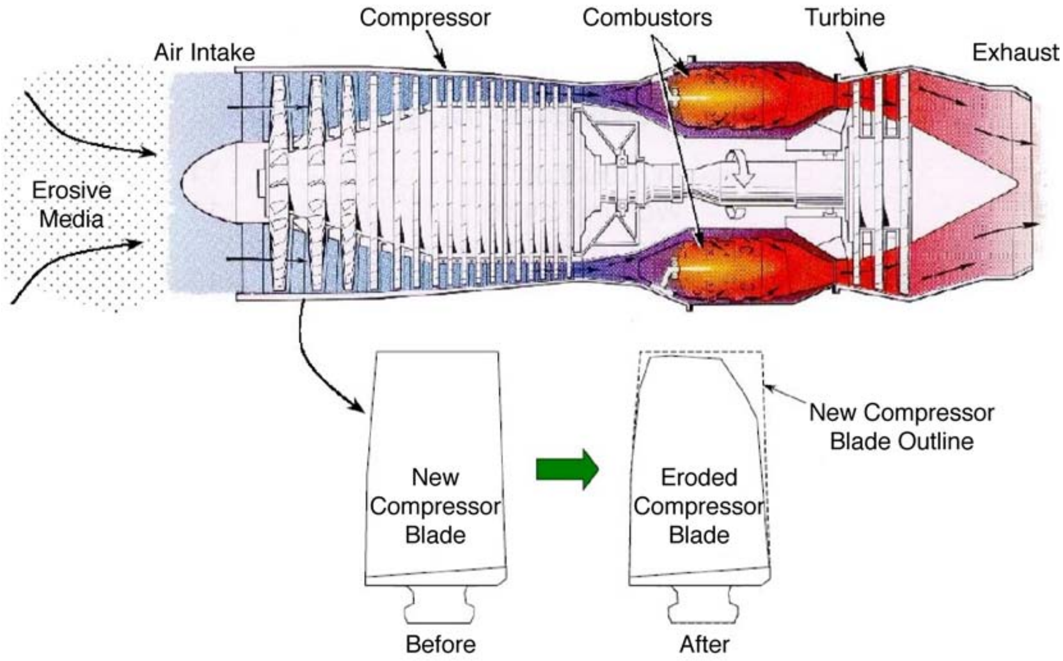
Compressor
Combustors
Turbine
Air Intake
Exhaust
Erosive Media
New Compressor Blade
Eroded Compressor Blade
New Compressor Blade Outline
Before
After

Figure 1-6
Schematic of gas turbine engine illustrating the effects of sand ingestion [72]

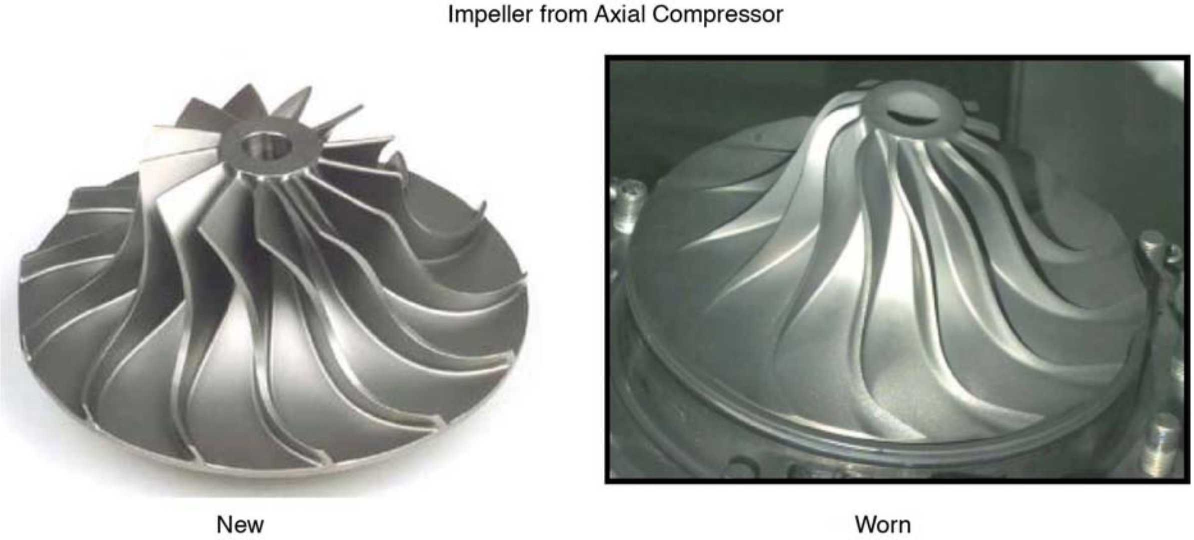
Impeller from Axial Compressor
New
Worn

Figure 1-7
V22 Osprey new and engine run compressor impellers showing effects of solid particle erosion on the component. Note the significant erosion loss of the vanes. [79]

1.3 Liquid Droplet Erosion Mechanisms

A drop of liquid impinging at a high speed onto the surface of a solid can exert enough force to permanently deform and fracture the solid. The type and extent of impact damage depends primarily on the size, density, and velocity of the drop of liquid and the strength of the solid. Considerable research has been conducted to characterize the mechanism of liquid droplet erosion (LDE) [13]. A report issued by EPRI [1] has a section on liquid droplet erosion of rotating and stationary blades that summarizes the mechanisms and results on various materials under droplet impingement and cavitation erosion tests. An idealized diagram of the early stages of liquid droplet impact is shown in Figure 1-8a, and the damage mechanisms shown in 1-8 (b) are from References 13 and 14.

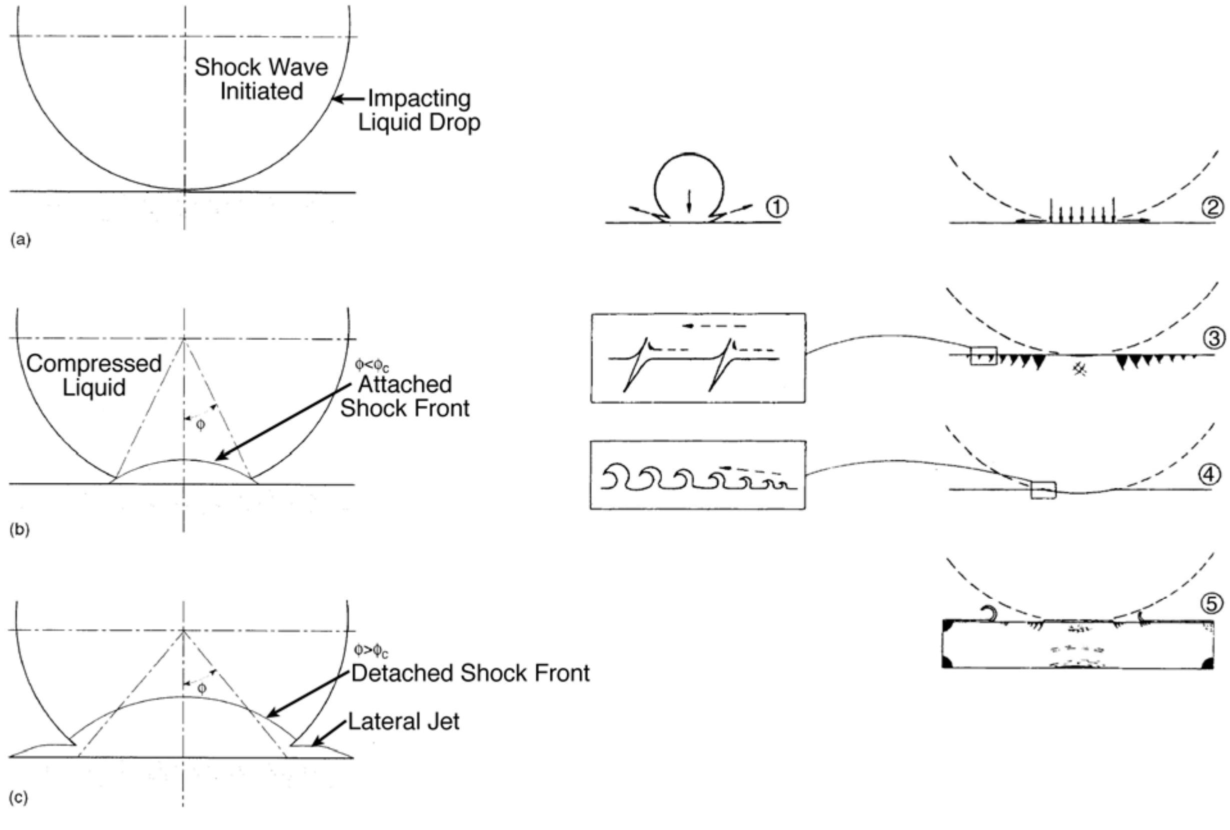
Shock Wave
Initiated
Impacting
Liquid Drop
(a)
Compressed
Liquid
$\phi<\phi_c$
Attached
Shock Front
ϕ
(b)
$\phi>\phi_c$
Detached Shock Front
ϕ
Lateral Jet
(c)
①
②
③
④
⑤

a) b)

Figure 1-8
(a) Idealized diagram of early stage liquid drop impact and (b) a diagrammatic representation of some of the mechanisms by which an impinging liquid drop can damage a solid

After the droplet makes initial contact with the solid surface, a shock wave is imitated from the compressed liquid, and a lateral jet forms. The surface loading has both normal and shear components. In brittle solids (such as hard coatings), circumferential cracks form around the central compressed region (Figure 1-8b, Inset 3). In ductile metals, a smaller depression forms, with erosion occurring at surface wavelets formed around the rim of the depression by the outward flow of the lateral jet (Inset 4). In a hard, brittle solid surface with a soft rubbery coating, the central area of the coating is initially undamaged. Stress wave damage occurs in the form of multiple spalling of the surface and an outer ring of damage on the impact surface (Inset 5).

The LDE process is highly nonlinear as illustrated in Figure 1-9 [13]. The erosion rate is time-dependent as shown in this figure. The damage accumulation occurs from thousands of droplet impacts before a particle is dislodged.

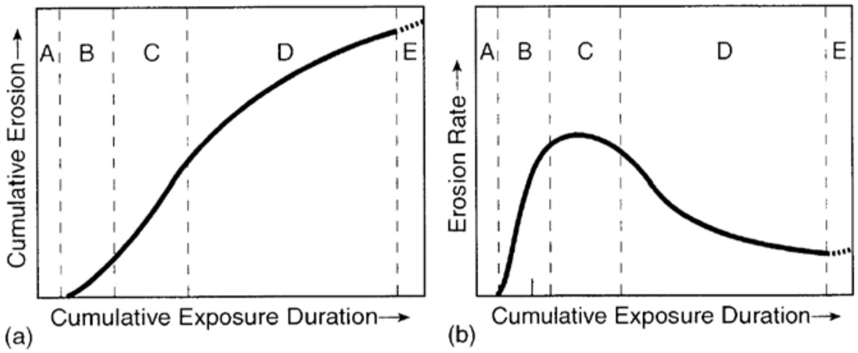

Figure 1-9
Characteristic erosion versus time curves showing (a) cumulative erosion (mass or volume loss) versus exposure duration (time or cumulative mass or volume of liquid impinged); (b) corresponding instantaneous erosion rate versus exposure duration obtained by differentiating curve a [13]

There are typically several stages of this erosion behavior as illustrated in Figure 1-9:

A) Incubation stage

B) Acceleration stage

C) Maximum rate stage

D) Deceleration stage

E) Terminal or steady state stage

By differentiating the curve shown in Figure 1-9 (a) above, the instantaneous erosion rate can be obtained as shown in (b). Due to this nonlinear behavior, an absolute prediction of the liquid droplet erosion rates is very difficult.

Liquid impact erosion mechanisms on TiN coated and uncoated 12 Cr stainless steel and Stellite 6B were studied by Lee et al. [15]. They used a pulsed water jet at speeds of up to 380 m/s (1247 ft/s) and used multiple impacts during testing of TiN-coated 12 Cr and TiN-coated Stellite 6B. The coating thickness was 11 microns. The damage produced by the water impacts appeared as isolated depressions. The density of these depressions (pit-like damage) increased with the number of impacts. The TiN coating fractured circumferentially by the plastic deformation of more ductile substrates, as schematically illustrated in Figure 1-10. The erosion rate of coated 12 Cr substrates was reported to be “much smaller” than that of uncoated specimens. It is also reported that an optimum coating thickness of 24 microns provided the best erosion resistance without negatively affecting the fatigue strength of the 12 Cr base alloy.

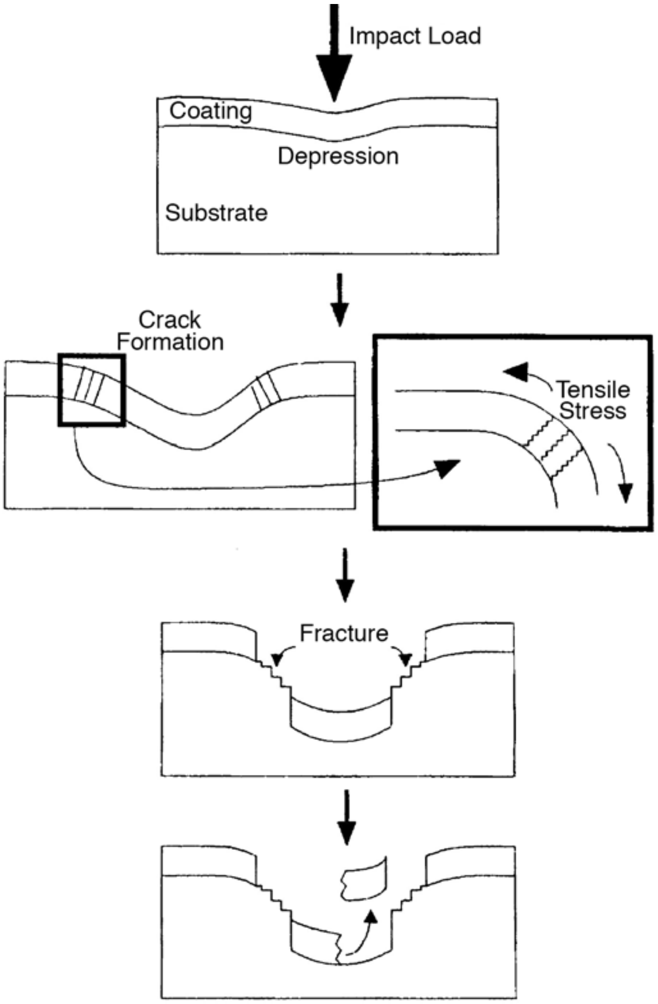
Impact Load
Coating
Depression
Substrate
Crack Formation
Tensile Stress
Fracture

Figure 1-10
Schematics of the liquid impact erosion mechanism of TiN coating [15]

1.4 Coating Methods and Coating Characteristics

1.4.1 General Coating Process Categories

In general, coating processes can be divided in to several classifications shown in Table 1-1. Bunshah divides deposition processes into four broad categories [16]:

- Surface modification methods are those where the surface characteristics are altered without buildup of an external coating, for example, ion implantation, surface nitriding, or boronizing.
- Atomistic deposition processes are those involving atom-by-atom buildup of the coating on the substrate surface, such as the PVD processes of evaporation, ion plating, sputtering, chemical vapor deposition, and electrodeposition.
- Particulate deposition methods are those involving droplet transfer such as plasma spraying, arc spraying, wire spraying, high velocity oxygen fuel (HVOF), and detonation gun coating.
- Bulk deposition is when the surface is altered by generally much thicker layers as in explosive cladding or roll forming, weld overlays, and more recently laser cladding, where a liquid interfacial layer is created by the process.

Table 1-1 summarizes these broad categories and the specific methods of traditional (conventional) coating applications. Depending on the final service requirements, the selection of the processes, the coating thickness, and the specific chemical composition of the coatings vary a great deal. The coating suppliers have developed their own proprietary processes and chemical compositions targeted for specific applications.

Table 1-1
Coating deposition methods (after Bunshah [16])

Surface Modification	Atomistic Deposition	Particulate Deposition	Bulk Coatings
Chemical Conversion Electrolytic anodization CVD Diffusion coatings Nitriding Boriding	**Vacuum Environment** Thermal evaporation EB-PVD Ivadizing (vapor aluminide)	**Thermal Spraying** Flame spray Wire spray D-Gun HVOF Plasma spraying LPPS	**Wetting Processes** Painting Dip coating Spraying
Mechanical Shot peening Burnishing Laser peening (high and low-intensity)	**Vacuum/Partial Pressure Environment - Plasma Enhanced Deposition** Sputter deposition Ion plating Cathodic arc PA-CVD PEMS	**Electrostatic Spraying** Printing Spin coating	**Cladding** Roll bonding Explosive
Ion Implantation	**Atmospheric or Low Pressure** CVD		**Overlaying** Weld overlay Laser cladding

Table 1-2 lists some of the traditional coating methods that have been used or are currently in used for erosion protection of gas or steam turbine compressor components. Weld overlays and Stellite are used on low-pressure steam turbine blades to mitigate LDE. Tungsten, chrome carbides, and borides are used in the inlet side of the high-temperature steam turbines. These coatings are considered very thick and will add significant weight to the components they coat; also, they introduce dimensional changes to the components as well as to the gas and steam flow paths.

Table 1-2
Some traditional erosion coating methods and vendors

Coating Vendor	Coating Designation	Coating Process	Coating Type	Thickness range in microns	Approximate Coating Temperature Limit in °C (°F)
Praxair Surface Technologies Sulzer Sematech		Weld overlay	Stellite 6	1/8–1/4 inch (3–6 mm)	
Praxair Surface Technologies Sulzer		Laser cladding	Stellite 6	1/8–1/4 inch (3–6 mm)	
Chromalloy	Boride	Pack cementation (CVD)	Boriding	25–50 microns (25–50 µm)	
Praxair Surface Technologies	WT-1	D-Gun	83(W, Ti) carbide 17Ni	75–250 µm	525 (977)
Praxair Surface Technologies	LC-1C LC-1H	D-Gun	NiCr Chrome Carbide 80 (92Cr-8C) 20 (80Ni-20Cr)	75–250 µm	750 (1382)
BryCoat	W and Cr Carbides	HVOF	WC and CrC	0.005–0.010 in. (0.127–0.25 mm)	815 (1499)
ASM, LLC	CrC-NiCr	HVOF	CrC-NiCr	0.020 µm Max	982 (1800)
ASM, LLC	WC-Co	HVOF	WC-Co	0.050 µm Max	649 (1200)

1.4.2 Physical Vapor Deposition Processes

Several coating methods are used to deposit relatively thin, hard coatings to mitigate erosion of turbine components. The deposition processes considered in this review for erosion-resistant coatings are physical vapor deposition (PVD) processes carried out inside vacuum chambers. Regardless of process used, there are three steps in the formation of any PVD coating that involve: 1) the phase transformation from a condensed state (either solid or liquid) to a vapor, 2) transport of the vapor to the substrate, and 3) condensation of the vapor on the substrate as detailed below:

- Synthesis of the material to be deposited - Transition from a condensed phase (solid as in sputtering or cathodic arc or liquid as in electron beam (EB) to the vapor phase though heat (EB or arc) or momentum transfer (sputtering).
- Transport of the vapors between the source and the substrate - For reactive deposition of compounds, a reaction between the components of the compound, some of which may be introduced into the chamber as a gas (Ti evaporation with a partial pressure of nitrogen gas to create titanium nitride coatings). In some cases, this reaction also occurs at the source and the substrate.
- Condensation of the vapor on the substrate to form a coating - The structure of the coating is dependent on the adatom energy and the substrate temperature.

PVD can be understood most simply as condensation of a vapor on a substrate that is at a temperature below the freezing point of the vapor. This can be observed inside freezer compartments on the walls; in northern climates, we observe this when frost forms on our car windshields. Similarly, in industrial PVD, the deposit can be thought of as a high-temperature metallic or ceramic frost.

For industrial scale PVD, the vapor is created by one of two major processes: evaporation or sputtering. Both are carried out in vacuum chambers and are atomistic deposition processes. The processes are all line of sight, so to obtain uniform coatings, the substrates must be rotated by fixtures inside the coating chamber. The coating microstructure, grain size, crystal structure, crystal orientation, residual stress, adhesive strength, and other properties are a function of the coating process parameters and the substrate temperature. Reactive gases can be introduced to create carbides, nitrides, silicides, or oxides from metal vapors. These same compounds can be deposited directly from a nonmetallic source with certain processes that do not need a conductive target material. RF sputtering of alumina and electron beam PVD (EB-PVD) of zirconia are two examples. Generally, reactive evaporation is the most common, effective, and economical process for producing hard coatings for tribological applications.

Traditional chemical vapor deposition (CVD) processes are used for applying wear-resistant coatings (for example, TiC, TiN, or alumina, generally in combination) on carbide cutting tool inserts, but CVD is a thermally driven process requiring temperatures on the order of 1000°C (1832°F). Being able to deposit hard, adherent coatings at low temperature (400–600°C [752–1112°F]) is a critical requirement for most applications where the properties of the substrate are sensitive to the processing condition (for example, high-speed steel cutting tools or compressor airfoils). The tooling industry has led the commercial development of industrial deposition processes that can create quality coatings. Mattox provides an excellent review of the history of the development of vacuum coating technologies that may be of interest to some readers [17].

For gas turbine compressor coating applications that are erosion resistant, the deposition methods have centered on reactive ion coating (RIC) (Liburdi) and cathodic arc deposition (Praxair, MDS-PRAD, SPUTTEK, and Performance turbine components). These coatings are based on TiN, modified TiN, and TiAlN applied as a monolithic (single layer) or multilayer coating with alternate soft and hard phases. Under funding from the Electric Power Research Institute (EPRI), TurboMet International and the Southwest Research Institute (SwRI) are currently developing a plasma enhanced magnetron sputtering (PEMS) process for advanced hard nano-composite (TiSiCN) coatings. Further details of these processes are covered later in this report.

1.4.3 Evaporation Methods

In evaporation, a heat source is used to create a vapor cloud in which the parts to be coated are held in order to allow the vapor to condense on the surface of the substrate to be coated. Bunshah [18] has thoroughly described the many variations of evaporative coating methods and the advantages and limitations of each. The major categories of evaporation have been classified by Bunshah as falling into four broad groupings as follows:

1. Thermal evaporation - The material is evaporated in a vacuum or inert gas.
2. Reactive evaporation - A gas is introduced into the coating chamber to react with the vapor and deposit a compound (for example, Ti metal vapor plus nitrogen gas, forming a TiN coating).
3. Activated reactive evaporation - Plasma is created inside the chamber to increase the reactivity of the gas via ionization.
4. Biased activated reactive evaporation - An electric potential is applied to the substrates to be coated in order to alter the film growth characteristics in the presence of an ionized vapor with a reactive gas present. By using a bias potential to substantially increase adatom energy, dense coatings can be produced at lower temperatures than is achievable with thermal evaporation.

1.4.3.1 Biased Activated Reactive Evaporation/Reactive Ion Plating

Figure 1-11 is a schematic of the biased activated reactive evaporation (BARE) process. Ion plating is a term that Mattox [21] developed to describe a PVD deposition process in which a substrate is bombarded with high-energy ions before and during deposition to alter the film adhesion and growth characteristics. Often, the terms *reactive ion plating* and *BARE* are used interchangeably for the same process. Liburdi uses the term *reactive ion coating* (RIC) to describe their company's process.

Lowden et al. [22], Parameswaran et al. [23], and Nagy et al. [24] have described the basic elements of the Liburdi RIC process for forming TiN coatings on turbine hardware. The parts to be coated are supported from a rack suspended above a titanium-filled crucible. During operation, the titanium is melted by a focused electron beam deflected magnetically into the crucible. A shutter blocks spits (liquid droplets) from reaching the parts during startup and stabilization of the melt pool.

One of the unique features of the RIC process is the use of a tungsten filament thermionic emitter to inject extra electrons into the titanium vapor cloud and process gas, increasing the stability and density of the plasma. Nitrogen and argon are the working gases; they are metered into the chamber via mass flow controllers. Prior to the start of the deposition cycle, the chamber is backfilled with Ar or Ar and H.

The parts are preheated via radiation and plasma to 400°C (752°F) and then sputter cleaned. Part temperature is monitored via a thermocouple attached to a reference part. At the end of the sputtering process, the part temperature is ~ 500°C (~ 932°F).

Following sputter cleaning, the hydrogen gas flow is turned off, and the electron beam gun Ti melting cycle is initiated. The bias voltage, nitrogen flow, and emission currents are adjusted to the desired levels. As the titanium is melted, it evaporates from the surface of the crucible, passes through the plasma generated by the thermionic emitter, and reacts with the nitrogen in the chamber to form TiN. The TiN condenses on the parts, fixtures, and chamber walls.

Chamber pressure is maintained in the 5×10^{-3} mbar (0.00375 torr) range helping improve coating coverage and uniformity through gas scattering. Part temperature is controlled to 400–600°C (752–1112°F). TiN stoichiometry is determined by the nitrogen partial pressure, other variables being constant. In operation, the parts have an applied bias in the range of 0–300 volts.

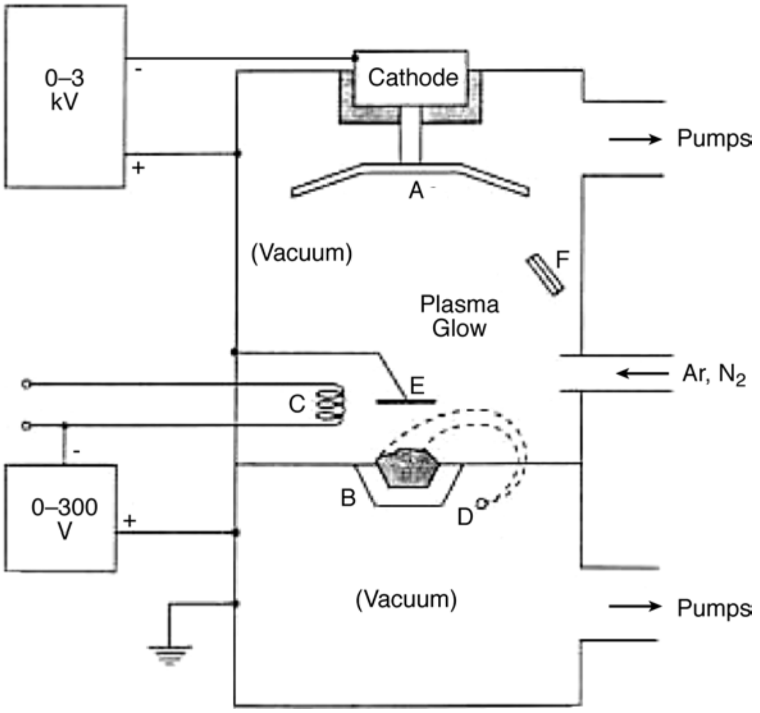

Figure 1-11
PVD schematic depicting the elements of the biased activated reactive evaporation process [23]

A) Parts are racked on fixtures suspended over the pool. B) The EB vapor source where the evaporant is loaded. C) The thermionic emitter that increases the degree of ionization in the vapor cloud. D) The electron beam vapor source. E) A shutter to shield the components from liquid spits during startup. F) A coating rate monitor. Reactive gas injection and a bias power supply for accelerating ions in the plasma to the substrate are also depicted [23]

1.4.3.2 Cathodic Arc Physical Vapor Deposition

Cathodic arc physical vapor deposition (CA-PVD) is a vacuum coating process that uses a low-voltage direct current to form cathode spots on the surface of the solid target material (for example, titanium) to “flash” evaporate the cathode material, forming a highly ionized vapor flux (Ti ++). Cathode spot size is on the order of 10 microns in diameter and has a current density in the range of 10^6 to 10^8 A/cm-^{2}. The local temperature at the surface of the spot is estimated to be on the order of 15,000 K.

Unlike ion plating or sputtering, a high percentage (~ 95%) of the vaporized material is ionized in the arc, and the ions are often multiply charged. A partial pressure of a reactive gas can be introduced via mass flow controllers into the vacuum chamber (for example, nitrogen or methane) to form metal nitrides or carbides. In order to form a dense coating at low temperatures (400–600°C [752–1112°F]), a bias voltage is used to increase the adatom energy of the depositing material as in ion plating or sputtering. Due to the significantly higher ionization level realized with the cathodic arc process, lower bias voltages (50–250 V) will typically be used, compared to sputtering and ion plating, to alter the film growth.

CA-PVD began to become a commercially significant process for industrial coating during the early 1980s [26], following inventions in the United States [27] and Russia [28] related to the basic cathodic arc deposition technology. CA-PVD overcame composition limitations inherent in thermal evaporation and rate limitations encountered with sputtering [27, 28]. Brown [29] reports that a wide range of coatings can be produced using arc. Among those listed are:

- TiN
- AlN
- VN
- ZrN
- Al_2O_3
- SiO_2
- TiO_2
- VO_2
- $Y2O_3$
- ZrO_2
- SiC
- TiC
- WC

Films of more complex composition such as TiCN, TiCrN, TiAlN, TiZrN, TiAlZrN, and others can be formed with an appropriate alloy cathode, with a background gas of the appropriate composition (for example, N or N plus methane).

The effect of preferential sputtering of the deposit may result in the composition of the coating differing from that of the cathode target alloy, dependent on the applied substrate bias. The effect of substrate bias is most noticeable on areas of the part with sharp edges where the current density effects are greatest. If the bias voltage is increased above that used during deposition, the adatoms may be so energetic that no coating is deposited, and the substrate material is removed by sputter of the substrate surface. This effect is often useful as part of the *in situ* cleaning of the substrate surfaces prior to the initiation of the coating process.

Although deposition rates of 1–10 microns per hour are typical, in industrial production of TiN coatings, deposition rates on the order of 3–4 microns per hour would be more common. Deposition rates are often limited to this range by substrate temperature considerations, regardless of the PVD process [42].

CA-PVD coatings in production for cutting tool applications include TiN, ZrN, CrN, TiAlN, and AlTiN in monolithic and multilayer architectures. Part A of Figure 1-12 shows an industrial scale CA-PVD production system. This system uses turbo pumps for the vacuum system and radiant heaters to bring the load to coating temperature; it has 24 separate cathodes for uniformity and multilayer coating deposition.

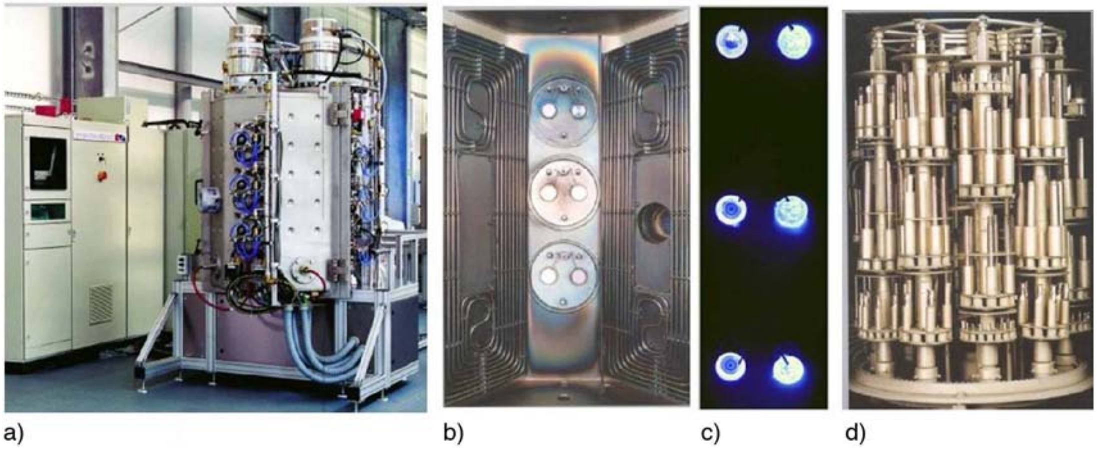

Figure 1-12
Industrial cathodic arc coating system with a 600 mm (23.6 in.) diameter x 1000 mm (39.37 in.) high coating zone [31]

a) Overall system view - 24 cathodes total arranged vertically on four of the eight chamber walls. b) View of radiant heaters used to preheat the load prior to coating and one panel of six evaporators in dual cathode arrangement c) Cathodes in operation – note bright tracks from cathode spot motion on the target and blue plasma of vapor being emitted. d) Part coating rack rotary turntable and planetary arrangement to provide uniform coating on each part.

The heater and six of the 24 cathodes can be seen in Figure 1-12 b. The individual cathodes are typically in the 2–4 inch (5.1–10.2 cm) diameter size range and are mounted vertically around the chamber walls. Large rectangular cathodes, similar to those used in planar magnetron sputtering, up to several feet in length, are used in some system designs. Figure 1-12 c shows one bank of six cathodes in operation with bright arc tracks and plasma of the vapor being emitted from the targets. A commonly used part fixturing rack is depicted in Figure 1-12 d. The parts are held in masking fixtures that keep the coating off areas that do not require coating and are rotated on a turntable and on satellite fixtures. A third axis is sometimes added with rotation of each part on its axis. The parts and turntable are connected electrically to the bias power supply. The rotation rate in front of each bank of cathodes can be used to adjust the layer spacing for multilayer coatings. For example, a TiN/CrN multilayer can be made with opposing banks of Ti and Cr cathodes. The substrates revolve in front of the cathodes, a layer of CrN is deposited, and 90 degrees later a layer of TiN is deposited.

By adjusting the cathode current setting and rotation rate, layer splicing on the order of 2-10 nm has been reported—the range of interest for superlattice coating effects. By modulating the nitrogen background pressure, the nitride stoichiometry can be affected, creating another type of multilayered structure. Metal/nitride and nitride/subnitrides have been produced in this manner;

the layer spacing is dictated by the ability of the chamber pumping system to modulate the nitrogen partial pressure and the extent to which the targets are “poisoned” with nitrides. Layers in the 100 nm range (0.004 mils) or greater are commonly generated by this technique [30].

One drawback to CA-PVD is that of macroparticles of target material that are emitted from the cathode as liquid droplets can become part of the growing film. Macroparticle emission has been shown to decrease with increasing melting point of the target material. When incorporated into the coating, they are typically observed as spherical inclusions in the coating. In a TiN coating, they would be Ti inclusions on the order of 0.5–5 microns or larger imbedded in the TiN matrix. Coating process parameters and cathode design can have a significant influence on the level of macroparticles. Rogozin and Fontana [32] has conducted compelling studies of minimizing macroparticles by controlling the location of nitrogen introduction during TiN coating so that TiN is evaporated from the cathode rather than Ti metal. He has called this process *reactive gas control of the arc* (RGCA).

Sue and Troue [33] has developed and patented a cathode source that also controls the reactive gas introduction and may offer similar benefits. Vergason [34] describes the use of cylindrical post style cathodes, and Welty [35] describes the use of magnetic fields to achieve higher arc spot velocities, minimizing macroparticles. Holubar and Cselle [36] claims to nearly eliminate macroparticles in the coatings. This is done by shielding the parts from the cathodes during arc startup and stabilization, where it has been shown that macroparticle generation is the greatest. This process also incorporates rotating post cathodes with large magnetic fields to further enhance cathode spot velocity. Figure 1-13 illustrates some of these concepts.

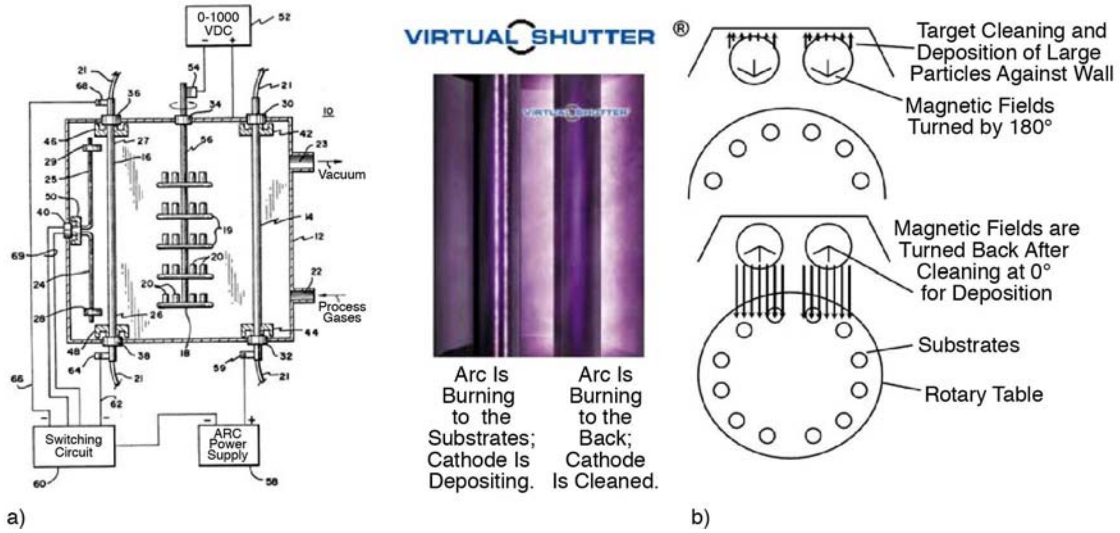
0-1000
VDC
52
54
21
68
36
34
21
30
10
46
27
56
42
23
Vacuum
29
16
25
50
40
19
14
12
69
20
24
20
22
Process
Gases
28
26
44
48
38
18
32
64
59
21
21
66
62
Switching
Circuit
ARC
Power
Supply
60
58
a)
VIRTUAL SHUTTER ®
Arc Is Burning to the Substrates; Cathode Is Depositing.
Arc Is Burning to the Back; Cathode Is Cleaned.
Target Cleaning and Deposition of Large Particles Against Wall
Magnetic Fields Turned by 180°
Magnetic Fields are Turned Back After Cleaning at 0° for Deposition
Substrates
Rotary Table
b)

Figure 1-13
CA-PVD systems with cylindrical post style cathodes used to increase cathode spot velocity and minimize macroparticle formation [34, 36]

a) CA-PVD process schematic depicting post style cathodes [34]. b) Arc system illustrating the use of shutters and high cathode spot velocity to minimize macroparticle deposition [36]

Filtered arc technology aimed at eliminating macroparticles has been reviewed by Brown [37]. While showing promise at creating completely macro-free films, deposition rates are significantly reduced, thus impacting commercial viability. EB-PVD coating processes can generate a different type of defect referred to as *spits*. Like macroparticles, they are liquid droplets that are sometime emitted from the vapor source during the coating process. Control of deposition conditions is essential to coating quality in any coating method.

In all vacuum deposition processes, attention to vacuum system, fixture, and tooling cleanliness is critical to coating quality. Condensate from multiple coating runs builds up on the chamber surfaces and part fixtures and may become dislodged in the form of fine dust, particles, or flakes that can become defects if they fall onto parts during a coating cycle.

DeMasi-Marcin and Gupta [38] noted the benefit to compressor blade life with CA-PVD TiN coatings in applications where runway sand ingestion was problematic. A 5 times improvement in relative erosion resistance was noted for a multilayer TiN system on Ti alloys compared to uncoated blades. Only a 1.5 times improvement was noted for an early version of a monolithic TiN coating. They attributed the dramatic increase in coating durability to interfacial impact energy scattering and/or absorption. It is also probable that the multilayer structure was more tolerant of macroparticles prevalent in some of the first generation arc deposited coatings. Improvements in arc deposition technology mentioned earlier have had a dramatic effect on the quality of the coatings from some suppliers.

1.4.4 Sputtering Methods

In sputtering, a vapor cloud is created by ions (usually of Ar) being accelerated into a target material, knocking atoms of the target material off the surface of the target by momentum transfer as shown in Figure 1-14. There are two main types of sputtering that are common: magnetron sputtering (MS) and radio frequency sputtering (RF-S). Metallic (conductive) targets can be sputtered by MS, but nonconductive target materials can be sputtered only using RF-S.

The rate for sputtering processes is typically lower than evaporation processes. By introducing a reactive gas such as nitrogen, compounds can be deposited while taking advantage of MS and metallic targets (for example, Ti, Al, Zr, Pt, stainless steel, etc.).

With the sputtering process, the target remains solid during the coating process, unlike the examples of electron beam evaporation described above. Consequently, the sputtering targets are often hung vertically on the interior walls of a vacuum chamber. An additional advantage of the sputtering process is that alloys can easily be deposited without consideration for the individual elements vapor pressure as in evaporation. The composition of the coating reflects that of the source.

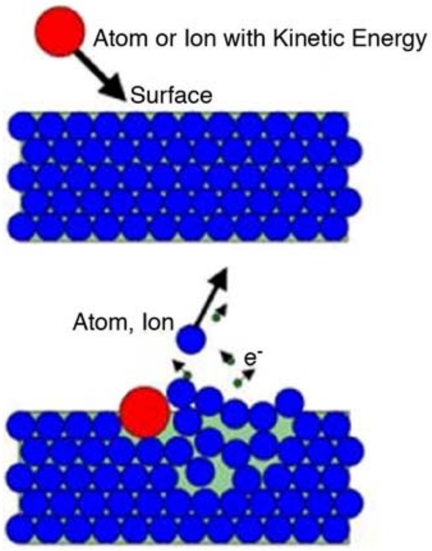

Figure 1-14
Schematic illustration of the sputtering process

Sputtering **is a term used to refer to a physical vapor deposition (PVD) technique wherein atoms or molecules are ejected from a target material by high-energy ion bombardment so that the ejected atoms or molecules can condense on a substrate as a film.**

One of the modifications of the MS method is to use an external filament to generate additional plasma to increase the energy of the ions to form very dense coatings. Southwest Research Institute (SwRI) has developed such a system and process. By introducing various gases such as nitrogen and/or trimethyl silane, the coating compositions can be modified from straight TiN or

TiSiCN [40, 41]. Such coatings have been found to have extremely fine grains. Figure 1-15 shows the plasma enhanced magnetron sputtering (PEMS) system configuration, which employs two magnetrons. Systems with four magnetrons are also used.

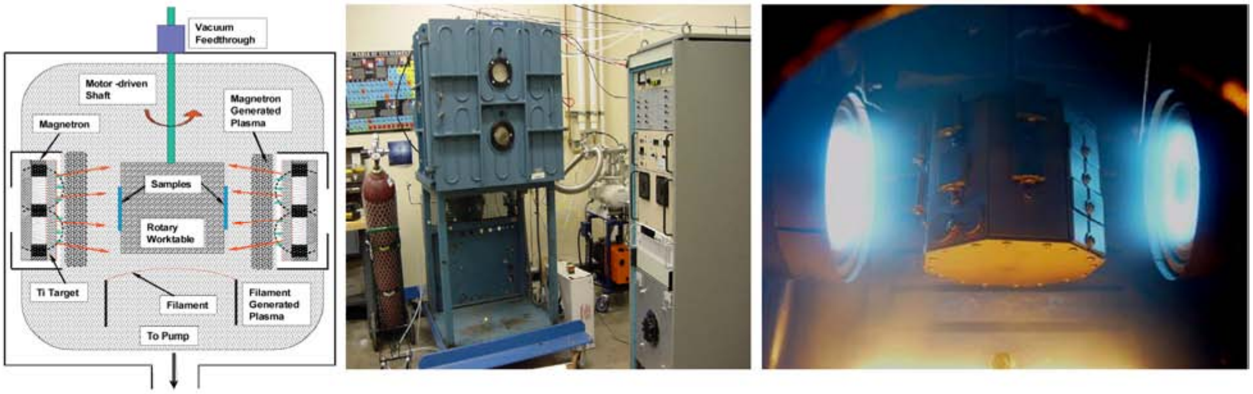

a) Schematic Diagram of the PEMS Chamber

b) PEMS Chamber and Control Module

c) Plasma During Coating

Figure 1-15
Plasma enhanced magnetron sputtering (PEMS) system with two magnetrons (Courtesy: Southwest Research Institute)

1.4.5 Coating Growth – Structure Zone Model

This section summarizes the mechanism of coating deposition in a vapor phase system [42, 43]. Atomistic film growth occurs as a result of the condensation of atoms (“adatoms”) on a surface of the substrate. The five stages of coating formation are:

1. Vaporization of the material (adatoms) to be deposited
2. Transport of the material to the substrate
3. Condensation and nucleation of the adatoms
4. Nuclei growth
5. Changes in structure during the deposition process at the coating substrate interface and during film growth

The qualities of the deposit have been found to be dependent on several key factors such as substrate temperature, chamber pressure, adatom arrival energy (bias voltage), and substrate rotation. Deposited films tend to grow as columnar grains, often with a strong crystallographic texture depending on growth conditions.

The structure zone model was developed by Movchan and Demchishin [44] as a way of describing changes in coating microstructure that they observed related to the ratio of the substrate temperature (Ts) to the melting point of the material being deposited (Tm) (also referred to as the homologous temperature) in thermal evaporation processes. With increasing substrate temperature, the atoms of material are able to have greater surface mobility and produce coatings of greater density. They classified the type of structure obtained into the three zones shown in Table 1-3.

Table 1-3
Movchan-Demchishin structure zone model of PVD. Zone transitions as a function of the homologous temperature Ts/Tm determined for metal and oxides.

Material	Zone 1	Zone 2	Zone 3
Metals	< 0.3	0.3–0.45	>0.45
Oxides	< 0.26	0.26–0.45	>0.45

Thornton [45] extended this model to include sputtering (in the absence of ion bombardment) and the associated reduction in adatom energy due to increase gas scattering as the chamber pressure is increased. Messier et al. [46] has further adapted this to include plasma enhanced deposition where the structure and properties of the coatings produced are shown to be a function of ion-bombardment-induced adatom mobility in addition to thermally induced mobility demonstrated in the previous studies. He has described substructures within Zone 1 and T that previously were unreported. Schultz et al. [47] has suggested that substrate rotation is also a factor affecting the structure of the coating produced and has proposed adding this as another axis to the structure zone model (SZM). Figure 1-16 depicts the structure zone models that have been developed.

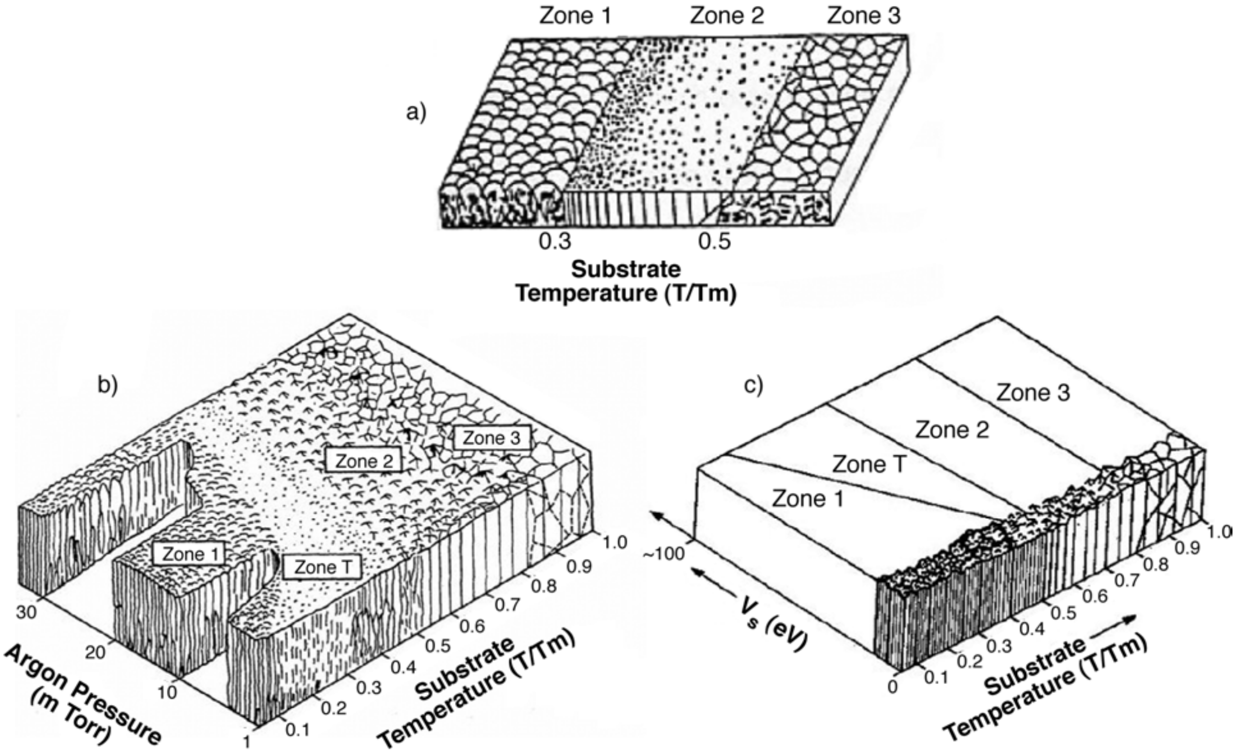
a)
Zone 1
Zone 2
Zone 3
0.3
0.5
Substrate Temperature (T/Tm)
b)
Zone 3
Zone 2
Zone 1
Zone T
30
20
10
1
Argon Pressure (m Torr)
0.1
0.2
0.3
0.4
0.5
0.6
0.7
0.8
0.9
1.0
Substrate Temperature (T/Tm)
c)
Zone 3
Zone 2
Zone T
Zone 1
~100
V_s (eV)
0
0.1
0.2
0.3
0.4
0.5
0.6
0.7
0.8
0.9
1.0
Substrate Temperature (T/Tm)

Figure 1-16
Structure zone models for PVD coating growth

a) Original SZM by Movchan and Demchishin [44] b) Schematic representation of the influence of substrate temperature and chamber pressure on the structure of coatings. T is the substrate temperature, and Tm is the melting point of the material being deposited [45].
c) SZM modified for ion-assisted deposition processes, showing the influence of thermally induced mobility and bombardment induced mobility [46].

Zone 1: Amorphous, porous film; the adatom surface diffusion is insufficient to overcome the geometrical shadowing by the surface features. The columns that are formed consist of dome-topped, tapered crystals separated by voided boundaries. The internal structure of the crystals, if formed, is poorly defined, with a high dislocation density.

Zone T: Small grains, relatively dense film; the coating has a fibrous morphology and is considered to be a transition from Zone 1 to Zone 2 observed at higher chamber gas pressure in the sputtering process.

Zone 2: Tall narrow columnar grains; the growth process is dominated by adatom surface diffusion. In this region, surface diffusion during deposition allows the densification of the inter-columnar boundaries. However, the basic columnar morphology remains. The grain size increases and the surface features tend to be faceted. It consists of dense columnar grains with smooth, sometimes faceted surfaces, resulting from surface diffusion dominant condensation. Preferred growth orientation of the columnar grains has been observed.

Zone 3: Bulk diffusion allows recrystallization, grain growth, and further densification of the coating. It consists of equiaxed grains with a bright surface.

Note: TiN deposition is in the 400–600°C (752–1112°F) temperature range for all vendors surveyed. This corresponds to a homologous temperature (Ts/Tm) of 0.21–0.27. The use of plasma-enhanced deposition with increased adatom mobility is important to increasing the quality of the deposit, lowering the transition temperature for dense Zone 2 coatings.

Table 1-4
Transition temperatures for thermal evaporation [46]

Material	Zone 1	Zone 2	Zone 3
TiN Thermal Evaporation Transition Temperatures	< 560°C (< 1040°F)	560–1170°C (1040–2138°F)	> 1170°C (> 2138°F)

1.5 Coating Materials and Compositions

1.5.1 Titanium Nitride, Titanium Aluminum Nitride, and Ti-Silicon Carbonitride

Titanium nitride (TiN) is widely used for erosion-resistant coatings. It must be understood that wide variation in the performance and properties of TiN coatings are realized, depending on the specific processing method and processing conditions utilized. As can be seen from Figure 1-17, TiN can exist over a very wide composition range, and as the nitrogen content is decreased, Ti_2N is the stable nitride.

Sue and Troue [66] has found that erosion performance can be optimized by controlling the nitrogen partial pressure during coating deposition with a substantial benefit to erosion properties [48]. Gupta and Freiling of Pratt and Whitney also describe the importance of controlling the titanium nitride stoichiometry [49]. They teach that a hyperstoichiometric TiN is preferred, specifying a N:Ti ratio or 1.05 to 1.15 for improving the fatigue life of titanium compressor components through increasing the coating compressive stress (similar to shot peening). A detailed review of titanium nitride has been compiled by LeClaire [50].

Titanium aluminum nitride (TiAlN) is also used by some of the commercial vendors for both wear and erosion-resistant applications (SPUTTEK). Titanium-silicon carbonitride (TiSiCN) type coatings are under development and testing by SwRI and TurboMet and have not yet been used in commercial applications [40, 41]. Some of the major gas turbine (aeroengine) manufacturers are currently evaluating these coatings.

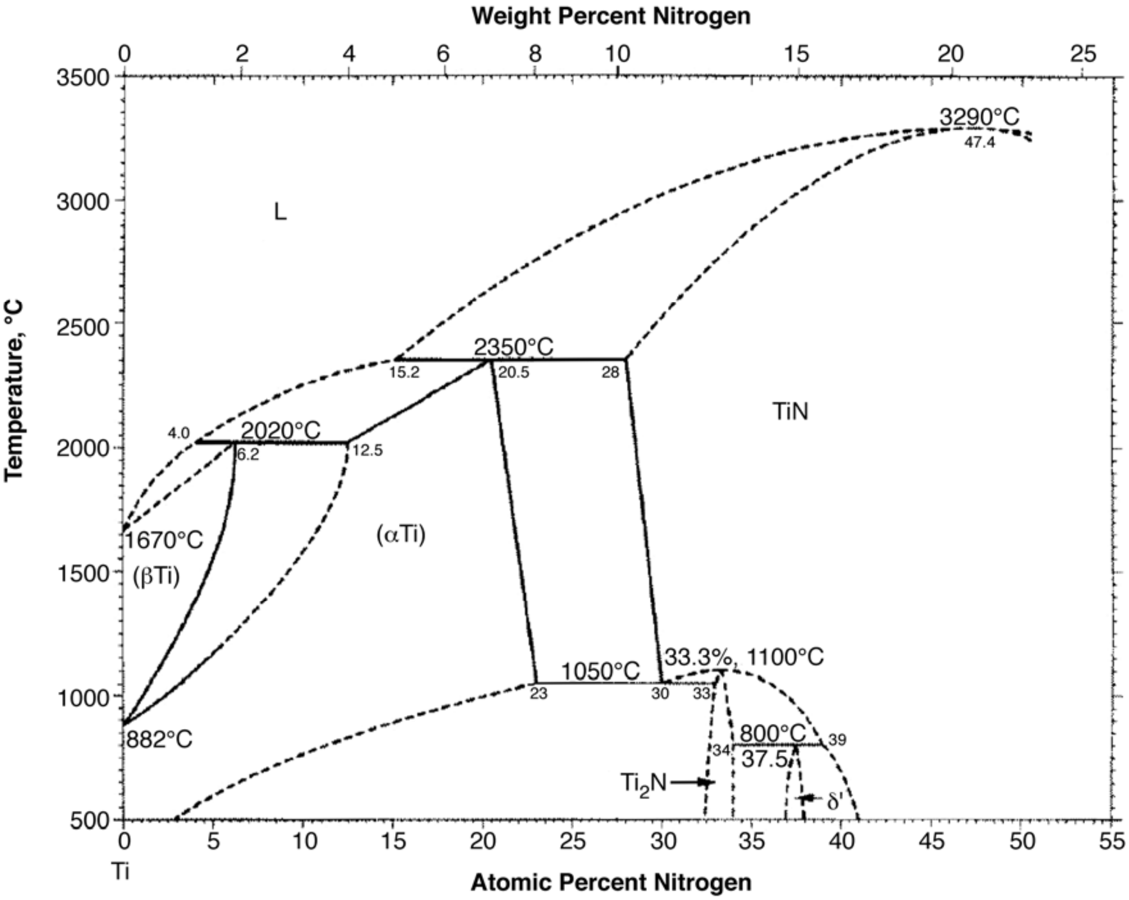

Figure 1-17
Titanium - nitrogen phase diagram [51]

2

COATING VENDOR SURVEY

2.1 Overview of Nanocoating Gas Turbine Experience Base

This review will focus on three suppliers that have successfully commercialized their erosion-resistant coating and manufacturing processes for gas turbine compressor applications. Each has been qualified for full scale production to aerospace quality standards and specifications. All three use proprietary variations of ion-assisted PVD to produce nominally TiN-based coatings in the range of 10–20 microns in thickness. As such these coatings are considerably thicker than the 2–5 micron films used for cutting tools, but thinner than the traditional 75–250 microns thick thermally sprayed erosion-resistant coatings. This can provide a benefit when applied on thin aerocompressor components in terms of minimizing weight and maintaining aerodynamic cross section. A fourth supplier AS&M is also profiled since they have also developed a nontraditional erosion-resistant polymeric coating with nano-scale filler. The coating has performed well in erosion trials and is currently undergoing evaluations in industrial gas turbine (IGT) compressor applications for water droplet erosion resistance. Polymeric materials have been found to perform well at high impact angles.

Table 2-1 below summarizes the coating supplier coating designations, methods of application, thickness ranges, and temperature capabilities. Except for the last company listed in this table, the others are commercial vendors providing coating services to diversified applications. The coating system at Southwest Research Institute (last row in this table) has a relatively small chamber that is used to develop various coatings (primarily TiSiCN targeted for application to turbine components). It has the capability to coat small batches of parts up to 7 in. (17.8 cm) in length.

Table 2-1
Summary of thin erosion-resistant coating vendor survey

Coating Vendor	Coating Designation	Coating Process	Coating Type	Thickness Range in Microns	Approximate Coating Temperature Limit in °C (°F)
Analytical Services & Materials Inc	Aerocoat K	Two-layer polymeric system	Siloxane polymer with nano-dispersed phases	25–50 bond layer 200–1000 top layer	200 (392)
Liburdi Engineering	RIC – Monolithic	Reactive ion plating	TiN based	10–25	550 (1022)
Liburdi Engineering	RIC Multilayer	Reactive ion plating	TiN based multilayer	10–25	550 (1022)
Liburdi Engineering	RIC Multilayer Erosion/ Corrosion Under Development	Reactive ion plating	TiN based multilayer	10–25	550 + (1022+)
MDS-PRAD Technologies Corp.	ER-7	CA-PVD	TiN + TiN based multilayer	10–30	550 (1022)
Performance Turbine Components (PTC)	T-Armor	CA-PVD	TiN based monolayer	5–15	550 (1022)
MDS-PRAD Technologies Corp.	NGC Under Development	CA-PVD	Proprietary multilayer compositions	10–30	650 + (1202 +)
Praxair Surface Technologies	24K Type I	CA-PVD	TiN Based	5–25	550 (1022)
Praxair Surface Technologies	24K Type II	CA-PVD	Sub stoichiometric TiN based multilayer	5–25	550 (1022)
Praxair Surface Technologies	24K Type II ZrN	CA-PVD	Sub stoichiometric ZrN based multilayer	5–25	650 (1202)
SPUTTEK	ERCOTEC	Modified CA-PVD	TiAlN monolayer	15–20	750 (1382)

Figure 2-1 (continued)
Summary of thin erosion-resistant coating vendor survey

Coating Vendor	Coating Designation	Coating Process	Coating Type	Thickness range (Microns)	Approximate Coating Temperature Limit in °C (°F)
BryCoat	TiN	CA-PVD	TiN monolayer	3–10	593 (1099)
BryCoat	TiN	CA-PVD	TiN multilayer	3–10	593 (1099)
* Southwest Research Institute	TiN and TiSiCN	Plasma enhanced magnetron sputtering (PEMS)	Monolayer and multilayer	10–20 microns	550 (1022)

* Research unit only, but capable of coating parts up to 7 in. (17.8 cm) long.

Richardson et al. [79] described a deposition process that is benign enough to avoid degrading the substrate materials and certain attributes that erosion-resistant coatings must possess in order to protect the substrate. Some of these attributes include:

- Strong adhesion to the substrate
- Hard and aerodynamically smooth surface
- High fracture toughness
- Low internal tensile residual stress
- Low-temperature processing to maintain substrate metallurgy
- Conformal coating methods
- Low erosion rate to significantly extend the product’s life

Nagy et al. [24] provided the following list of attributes to be considered:

- The coating must have good erosion resistance; with hardness greater than silica and toughness as high as possible to improve impact resistance at high angles.
- The coating must adhere well to the substrate.
- The coating should be smooth and uniform in thickness and capable of conforming to blade geometries (sharp edges, fillets, etc.).
- The application process should not damage the substrate alloy by exposure to excessively high temperatures or corrosive chemicals.

While not exhaustive, this is a good starting point for potential coatings and deposition methods. It should also be added that the process must also be economically viable, reproducible, and capable of production scale part processing.

The following section summarizes the information received from a survey of the coating vendors shown in Table 2-1.

2.2 Vendor Profiles

2.2.1 Liburdi Engineering Limited

2.2.1.1 Background

Liburdi Engineering Limited of Hamilton, Ontario, Canada, was established in 1979; they provide comprehensive metallurgical services aimed at extending the life of gas turbine equipment. Their services in the turbine industry complement those offered by the original engine manufacturers (OEMs) including advanced analysis techniques, refurbishment processes, and coatings [52].

Liburdi Engineering's proprietary Reactive Ion Coatings (RIC) are designed to protect turbine compressor airfoils from roughening and chord loss caused by sand and dust ingestion. The RIC process deposits extremely hard, erosion-resistant ceramic layers on the parts using an electron beam PVD process. The major difference from CA-PVD is that the coating vapor is created by the surface of a molten pool of metal rather than from solid targets as described in the earlier section on PVD methods. RIC coatings are recommended for turboprop, turboshaft, and turbofan engines operating in erosive environments. The processes and materials are compatible with a wide range of compressor alloys. Low-impact surface preparation and modest processing temperatures maintain base alloy strength without creating surface roughness or altering natural frequencies and fatigue life. The benefits claimed from the application of the RIC coating are retaining "new compressor" efficiencies beyond normal service intervals and extending compressor life and reducing overhaul frequency.

RIC coatings may be applied to the entire compressor gas path or selectively on an "as needed" basis to erosion-susceptible stages. RIC coatings are applied to new engine components and during overhaul. Exhausted RIC coatings can be safely stripped and re-applied during overhaul to extend aerofoil life.

Liburdi Engineering began working on erosion coating process development in the late 1980s initially with chemical vapor deposition (CVD) of TiN. They developed and patented a low-temperature CVD deposition process for producing TiN at 625°C (1157°F) that was effective for tool and die applications, but the deposition rate was deemed too low for compressor blade applications [56]. In 1988 they installed their first EB-PVD coating unit and began coating process development.

High-volume commercial coating commenced in 1997 with the T56 Stage 1 and 2 blades for C130 transport aircraft. They are qualified to Rolls-Royce's EPS 10705 specification and have coated over 2500 engine sets to date with the monolithic RIC coating. Development of a multilayer version of the RIC coating has been ongoing with recent successful rig and engine test results on Honeywell's AGT 1500 turbine engine for the Abrams M1 tank. Work is currently underway to assess the RIC coatings for industrial gas turbine applications where water droplet erosion is a concern [53]. Liburdi is certified to AS9001 and completed the National Aerospace and Defense Contractors Accreditation Program (NADCAP) coating supplier approval process in 2007.

Coating Structure and Coating Process: As described in the PVD process section earlier, Liburdi utilizes an electron beam PVD process to produce their Reactive Ion Coatings (RIC). Articles published in the open literature cover the initial process development work conducted in the late 1980s and early 1990s at Liburdi and in cooperation with the Canadian National Research Council. Lowden et al. [54], Liburdi et al. [55], Parameswaran et al. [56], D'Alessio and Nagy [57], and Nagy et al. [24] documented the initial parametric studies of the RIC EB-PVD process development work. Results for erosion, hardness, and fatigue testing from these early coating evaluations were presented. This early work ultimately led to the commercialization of the Liburdi monolithic RIC TiN coating. Recently, Liburdi introduced a multilayered version of their TiN coating shown in Figure 1-19.

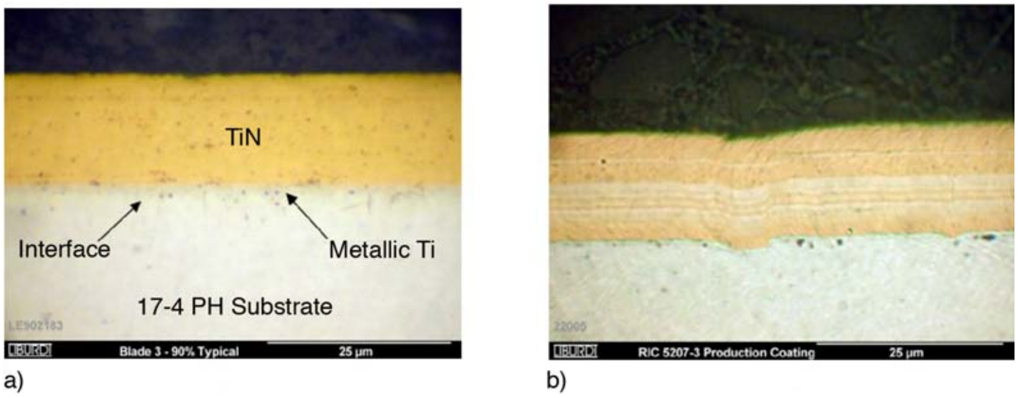

Figure 2-1
Liburdi production erosion-resistant coating photomicrographs. a) RIC TiN monolayer, b) RIC TiN multilayer [53]

Liburdi has three RIC coaters in operation today: one unit dedicated to development and two large coating units for production. The first large RIC coating unit was designed in 1998 and was qualified for production in 2001. The second large coater was qualified a year later, both primarily for Rolls Royce T56 blade applications. In moving to the larger units from the development coater described in an earlier section on PVD coating processes, Liburdi scaled the process up for longer, higher volume coating operations including moving to multiple wire fed EB evaporation sources. The production units have a coating zone 1.2 x 1.2 x 1.0 meters (3.9 x 3.9 x 3.3 ft) in size. Figures 2-2 and Figure 2-3 show a RIC coating process schematic and a photograph of a production RIC coating unit, respectively.

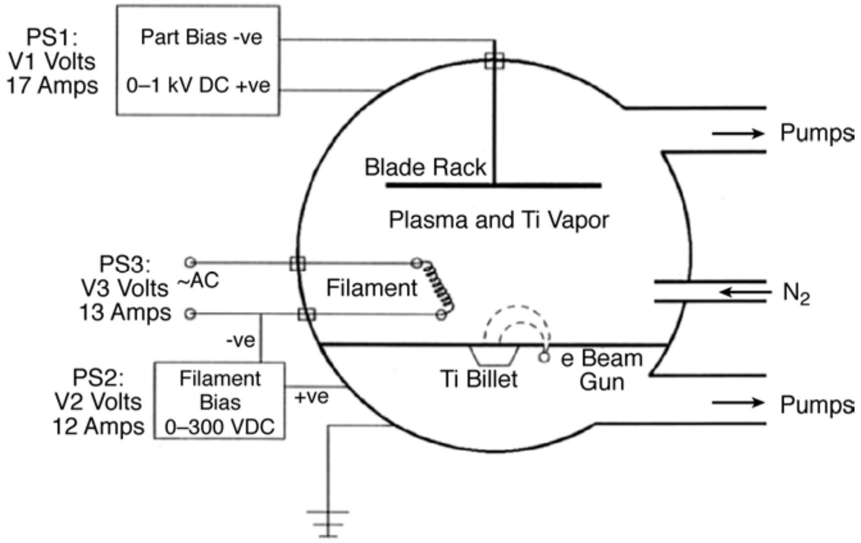
PS1:
V1 Volts
17 Amps
Part Bias -ve
0–1 kV DC +ve
Blade Rack
Plasma and Ti Vapor
Pumps
PS3:
V3 Volts
13 Amps
~AC
Filament
N$_2$
-ve
PS2:
V2 Volts
12 Amps
Filament
Bias
0–300 VDC
+ve
Ti Billet
e Beam
Gun
Pumps

Figure 2-2
Schematic of Liburdi Engineering Reactive Ion Coating (RIC) EB-PVD coating process

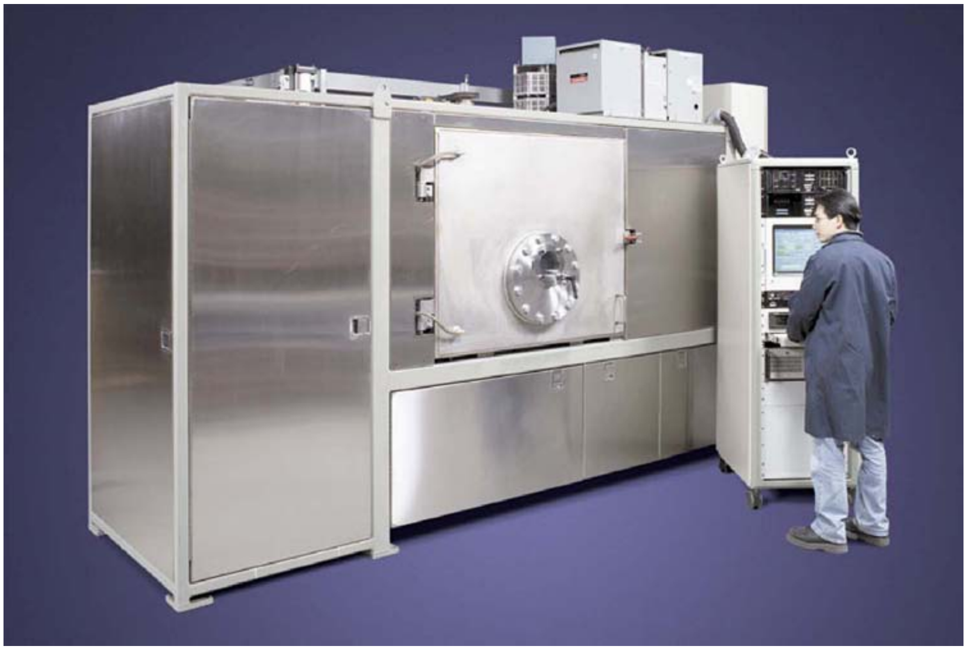

Figure 2-3
Liburdi RIC large production coating unit. Effective coating zone 1.2 x 1.2 x 1 m (3.9 x 3.9 x 3.3 ft). Capable of coating multiple larger IGT compressor blades.

Some of the features claimed for the RIC process are:

- The process deposits hard ceramic/metallic alloy thin coatings.
- *In situ* sputter cleaning enhances adhesion.
- Thermionic emitter allows control of plasma current independent of voltage and gas pressure.

- Plasma allows processing below thermodynamic equilibrium temperatures that are compatible with most compressor blade and vane alloys.
- Independent part bias allows control of microstructure and texture.
- EB evaporation coatings are dense and free of macro-particle defects that are typical of arc.
- A layering capability is provided by multiple evaporation sources and control of reactive gas partial pressure. Multiple wire-fed sources allow for a variety of coating chemistries within a single coating cycle.
- Coatings may be tailored on a stage-by-stage basis to address stage-specific wear mechanisms, such as high-angle vs. low-angle erosion.
- The process is environmentally friendly. No dangerous or corrosive effluents are used or generated.

Liburdi Engineering has also been conducting development trials on next-generation RIC multilayer coatings aimed at erosion/corrosion environments that go beyond the TiN composition. Uniform layered structures of Ti, Cr, and Al in ceramic and alloyed deposits by e-beam evaporation can provide superior performance in erosive/corrosive environments and are currently under development. An example of this developmental multilayer coating is shown in Figure 2-4.

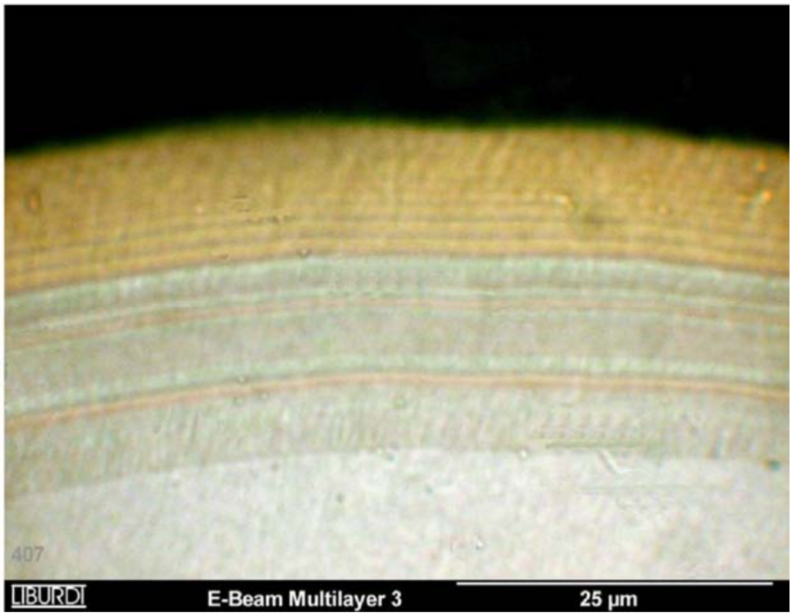

Figure 2-4
Liburdi RIC multilayer (Ti, Al, Cr) metal - metal nitride coating under development for erosion/corrosion applications

2.2.1.2 Performance Testing and Field Service

Erosion Performance: The results of T64 turboshaft engine field service evaluations of the RIC TiN coating are presented in Figures 2-5 and 2-6. The coated blades maintained power output and stall margin ~2.5 times longer than engines without the TiN coating. RIC-coated airfoils stayed smoother longer and also retained chord width over uncoated airfoils. The efficiency of RIC-coated compressors remained higher, preserving lower specific fuel consumption.

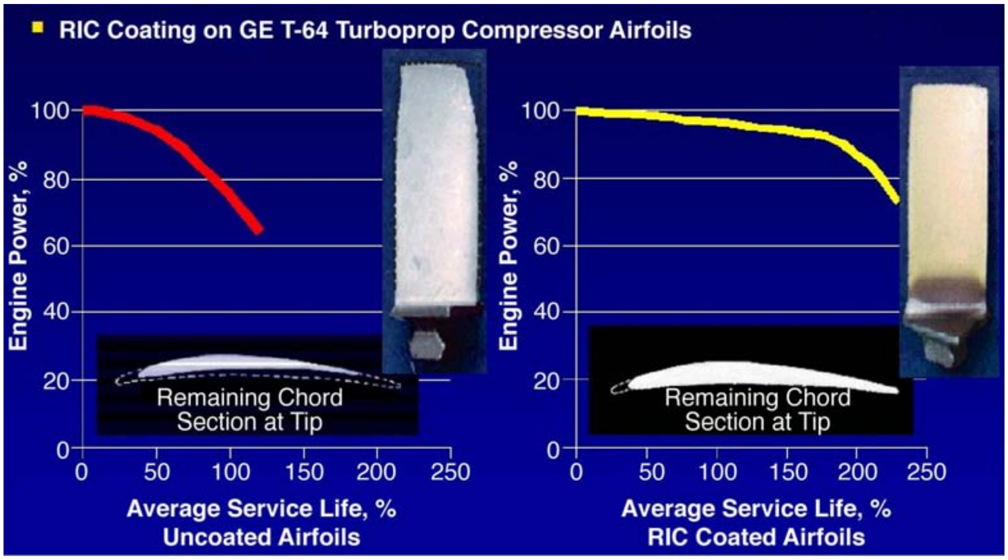

Figure 2-5
Relative erosion performance of T64 turboshaft engines uncoated and Liburdi RIC TiN coated blades in service. The coated airfoils maintained engine power and stall margin ~2.5 times longer than the uncoated airfoils.

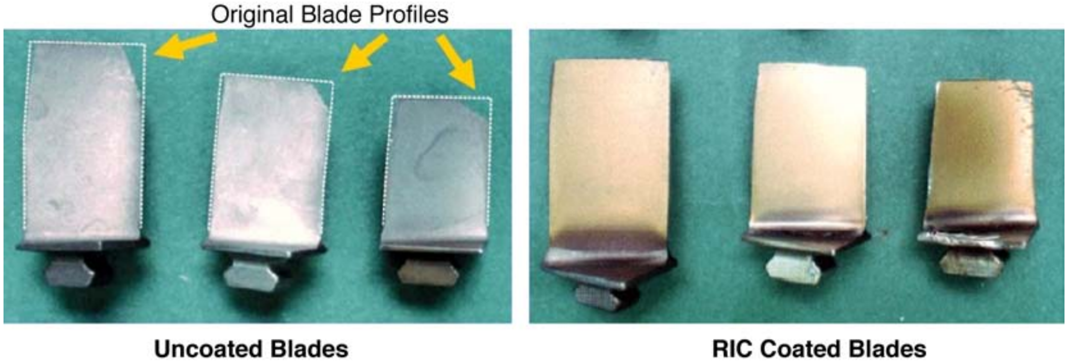

Figure 2-6
Comparison of Liburdi RIC TiN coated and uncoated blade profiles following field service. The uncoated blades show trailing edge thinning and chord loss while the coated blades have maintained their profile.

Liburdi has also reported favorable erosion testing results in recent engine competitions, but is not able to provide the test conditions or test data since they are proprietary to the OEMs conducting the evaluations. It has been reported that in a recent evaluation at Rolls-Royce of eight different erosion coatings, monolayer RIC TiN coating was ranked in the top two. In a recent test conducted by Honeywell for the AGT 1500 engine, Liburdi's Multilayer RIC TiN coating performed well for erosion and fatigue performance (**Note:** No test data were made available for this report).

Fatigue Testing: Fatigue testing was conducted on three test specimens each of 17-4 PH and Ti-6-4 in the early phases of the TiN RIC coating development at the National Research Council of Canada [56]. No debit was seen in the 17-4 PH, but the Ti-6Al-4V tested at the lower edge of the band of S-N curves for the uncoated alloy.

Component fatigue testing has been conducted by the Naval Aviation Depot on coated and uncoated T58 blades Stages 3 and 7 (A286 alloy). No difference was noted between the coated or uncoated components. See Figure 2-7.

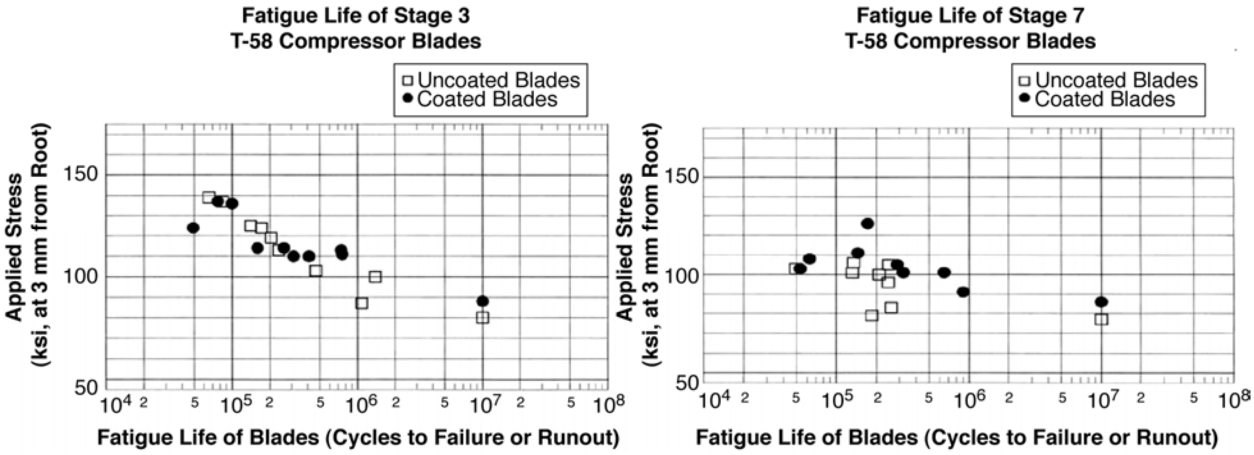

Figure 2-7
Component fatigue test data for Liburdi RIC TiN on coated and uncoated T58 stages 3 and 7 compressor blades [53]

Other fatigue testing evaluations complete for engine qualification have not been published and are considered proprietary to the OEM.

2.2.1.3 Land-Based Gas Turbine Applications

RIC coatings were also applied to Frame 7EA VGV compressor inlet vanes as a demonstration of coating capability. They have coated a set of GE Frame 7FA Row-0 blades and are processing Row 1 blades (see Figure 2-8). These parts are currently scheduled for service evaluation of effectiveness in reducing water droplet erosion of these components. No field experience data are available at the time of this report.

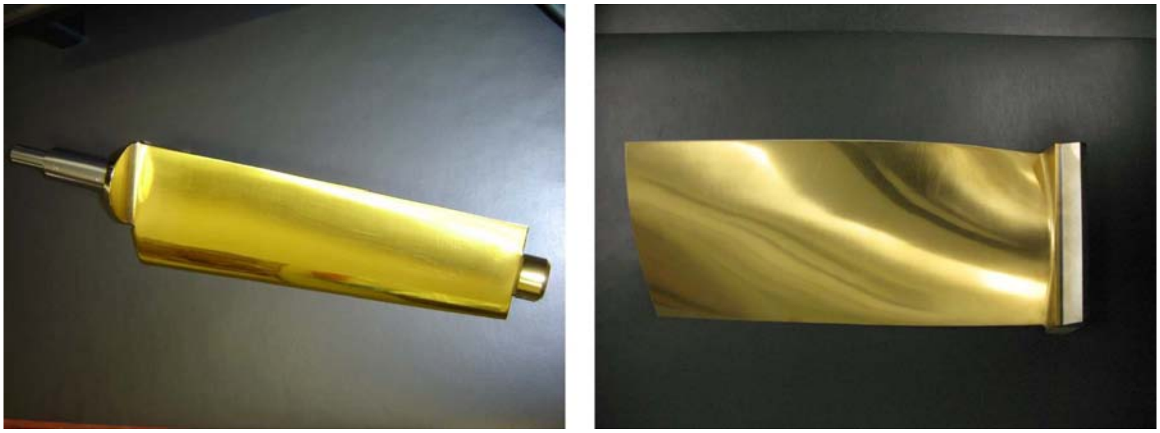

Figure 2-8
Frame 7EA VGV compressor inlet vane and Fr 7FA Row 0 compressor blade coated with Liburdi RIC erosion-resistant coating [53]

2.2.2 Praxair Surface Technologies

2.2.2.1 Background

Praxair Surface Technologies (PST) headquartered in Indianapolis, Indiana, [59] is one of the leaders in providing unique, customized coating and surface enhancement services with over 50 years of application expertise. Praxair's technological capabilities range from thermal spray, vapor deposition, electro-deposition, and diffusion coatings. In addition to their broad range of surface treatments, they offer many services such as a variety of finishing and machining, inspection and testing, heat treatment, and other service operations that enhance products and processes.

Praxair has production capability for all thermal spray coatings with flame spray, wire spray, shrouded plasma spray (SPS), air plasma spray (APS), low-pressure plasma spray (LPPS), high-velocity oxygen fuel (HVOF), and detonation gun (D-Gun) processes. They also apply weld overlays and laser cladding applicable to steam-turbine water-droplet-erosion mitigation. Praxair is NADCAP certified for coating processes.

In the mid-1980s Praxair began development of a new series of coatings with the cathodic arc PVD process for the gas turbine compressor airfoil erosion-resistant-coating market. They have conducted and published an extensive amount of research into the characterization of the deposition process, the coating microstructure, the composition effects, and the influence on physical properties with a focus on optimizing erosion performance. Initial erosion testing revealed a substantial improvement in erosion performance compared to their D-Gun coatings under similar test conditions.

In the late 1980s they began the marketing of their Praxair 24K coating based on a monolithic TiN structure. In 1991 they introduced their multilayer TiN-based erosion-resistant coating designated 24K Type II that offered even better erosion resistance than the monolithic 24K.

Erosion performance of Praxair's multilayer TiN_x 24K Type II has demonstrated superior erosion resistance on a variety of compressor airfoils. Praxair holds seven patents covering their CA-PVD coatings and processes (see the patent summary table in the appendix).

In 2004 Praxair expanded their CA-PVD production capacity to meet the increased demand in erosion coatings for desert environment turbine operations. Praxair has established a mass production facility to cost effectively apply their multilayer coating (24K Type II) to helicopter engine compressor blades and vanes. To date, Praxair has coated more than half a million blades and vanes with their CA-PVD erosion-resistant coatings.

D-Gun Coatings: Erosion-resistant coatings for gas and steam turbines have traditionally been applied by D-gun or HVOF processes for depositing tungsten carbide or chrome carbide hard facing (PST coating designations: LW-2A, LW1N30, SDG 2002, and LC-1H among others). Typical thicknesses for these coatings are in the range of 6–20 mils (0.15–0.51 mm), but they may be applied to a lower thickness range on thin section components such as compressor blades for flight engines. Table 2-2 lists erosion properties for several of the thermal sprayed coatings produced by PST.

Table 2-2
Relative erosion performance at 30 and 90 degrees for several D-Gun carbide-based coatings compared to CA-PVD TiN and ZrN coatings [60, 62]

Coating	Room Temp. (RT) Erosion Rate 30 Degrees (Microns/Gram)	RT Erosion Rate 90 Degrees (Microns/Gram)	500°C (932°F) Erosion Rate 30 Degrees (Microns/Gram)	500°C (932°F) Erosion Rate 90 Degrees (Microns/Gram)
WT-1 tungsten carbide-nickel	55	150	80	220
LC-1H chromium carbide nickel-chromium	50	100	80	190
LC-1C chromium carbide nickel-chromium	75	225	115	325
CA-PVD TiN 24K Type I	5	16	18	80
CA-PVD ZrN	7	12	18	40

Sue and Tucker [60] reported on the erosion performance of tungsten carbide nickel (WT-1) and chromium carbide nickel-chromium-based D-Gun coatings. The coatings were evaluated with 27 micron alumina at 120 m/s (394 ft/s) particle velocity at 30 and 90 degrees. Testing was conducted from room temperature to 700°C (1292°F) on 250 micron thick coatings. It was noted that the WT-1 was being applied to aircraft compressor blades. This and other thermal spray coatings have been used on certain versions of the CFM-56 flight engine [61]. No comparative data were provided for substrate materials under these test conditions. At 30 degrees, the erosion proceeded by plowing and cutting actions, while at 90 degrees brittle fracture of the carbides and indentations of the binder phase was evident. Of significance was a second paper by Sue and Troue [62] that reported erosion performance for several of Praxair's newer PVD coatings that are produced by their proprietary CA-PVD process. Both the CA-PVD TiN and ZrN coatings outperformed the D-Gun coatings by substantial margins. A more complete comparison for the thermal spray coatings and arc coatings is presented later (see Figure 2-17).

2.2.2.2 Praxair 24K Coating Structure and Coating Process

Coating Characterization – Beginning in the mid-1980s, Praxair applied substantial resources to the development of CA-PVD erosion-resistant coatings. Sue evaluated TiN, ZrN, and CrN coatings with the cathodic arc process [66]. PST's monolithic TiN 24K coating was developed and evaluated for a number of turbine applications. Lab erosion data demonstrated a significant improvement over the thermal spray coatings. Sue published a series of articles describing the coating microstructure, grain size, crystallographic texture, residual strain, hardness, and erosion resistance of these initial coatings and obtained patents for the deposition process and coating structures [63, 64, 65].

Further work demonstrated that there was a preferred nitrogen content range that improved the coatings' erosion performance. Sue describes the preferred composition range for sub-stoichiometric TiN coatings as being between 36 and 44 atomic percent nitrogen [66]. The effect of varying the nitrogen content on the microhardness, residual compressive stress, crystallographic texture, and grain size for the titanium nitride coatings is shown below in Figure 2-9. The effect on relative erosion resistance is demonstrated in Figure 2-10. It should be noted that the coating grain size measured perpendicular to the (111) diffraction plane was in the nano-scale range and was found to vary from ~ 20 nm at 32.5 at% nitrogen to ~ 75 nm at 50 at% nitrogen.

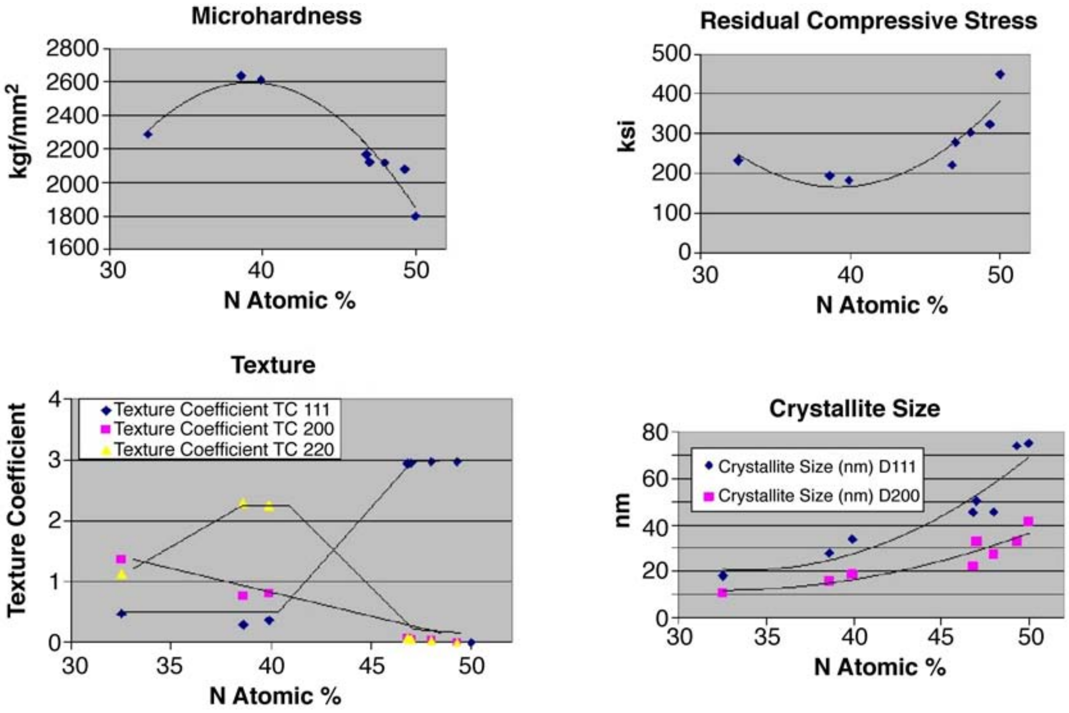

Figure 2-9
Effect of TiNx coating nitrogen content on microhardness, residual compressive stress, crystallographic texture, and crystallite size [59, 66]

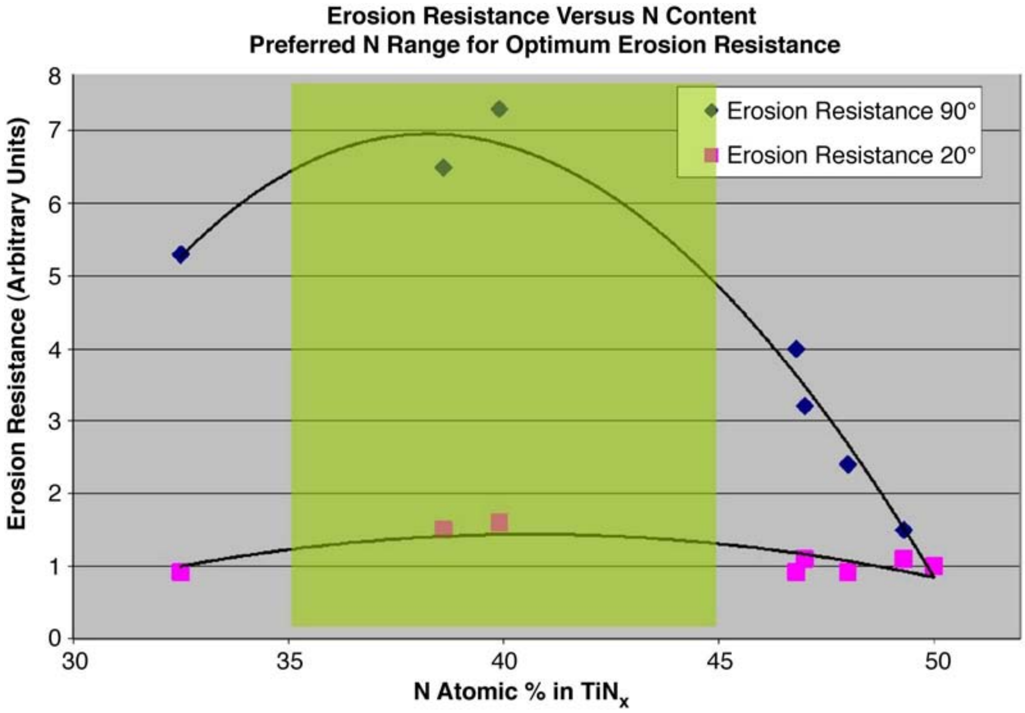

Figure 2-10
Erosion resistance as a function of TiNx nitrogen content at 30 and 90 degrees with 50 micron alumina at 80–120 m/s. The shaded area shows the region for optimum erosion performance. [59, 66]

In 1991 Praxair Surface Technologies, Inc., first introduced their 24K Type II coating. It is a multilayered coating system based on sub-stoichiometric TiNx with much improved erosion resistance compared to conventional TiN coatings. Sue and Troue [67] started the development of the TiN multilayer coating system for compressor airfoils based on several factors:

- By using a multilayer architecture, the coating thickness could be significantly increased without increasing the residual compressive stress too much.
- The multilayer concept further improves the erosion resistance, minimizing crack propagation by compliance layers improving coating toughness.
- Sub-stoichiometric TiNx was identified as a promising candidate material for improved erosion resistance, increased hardness, and toughness compared to the stoichiometric TiN.
- The multilayer approach resulted in significantly smaller grain size than the monolayer. Sue 1991 found that by interrupting the growing crystal columns with a layer of a different nitrogen content, the grain size was reduced by about a factor of two from the monolayer, further improving the erosion characteristics [67].

The multilayer coating consists of a thick starter layer of stoichiometric TiN, followed by up to 30 alternating thick sub-stoichiometric layers (B) and thin fully stoichiometric layers (A) that are designed to optimize coating toughness and erosion resistance. A typical coating thickness is 5–25 microns. Figure 2-11 shows a photomicrograph and schematic of PST's 24K Type II TiN production coating architecture. The coating is described in detail by Sue and Troue [67].

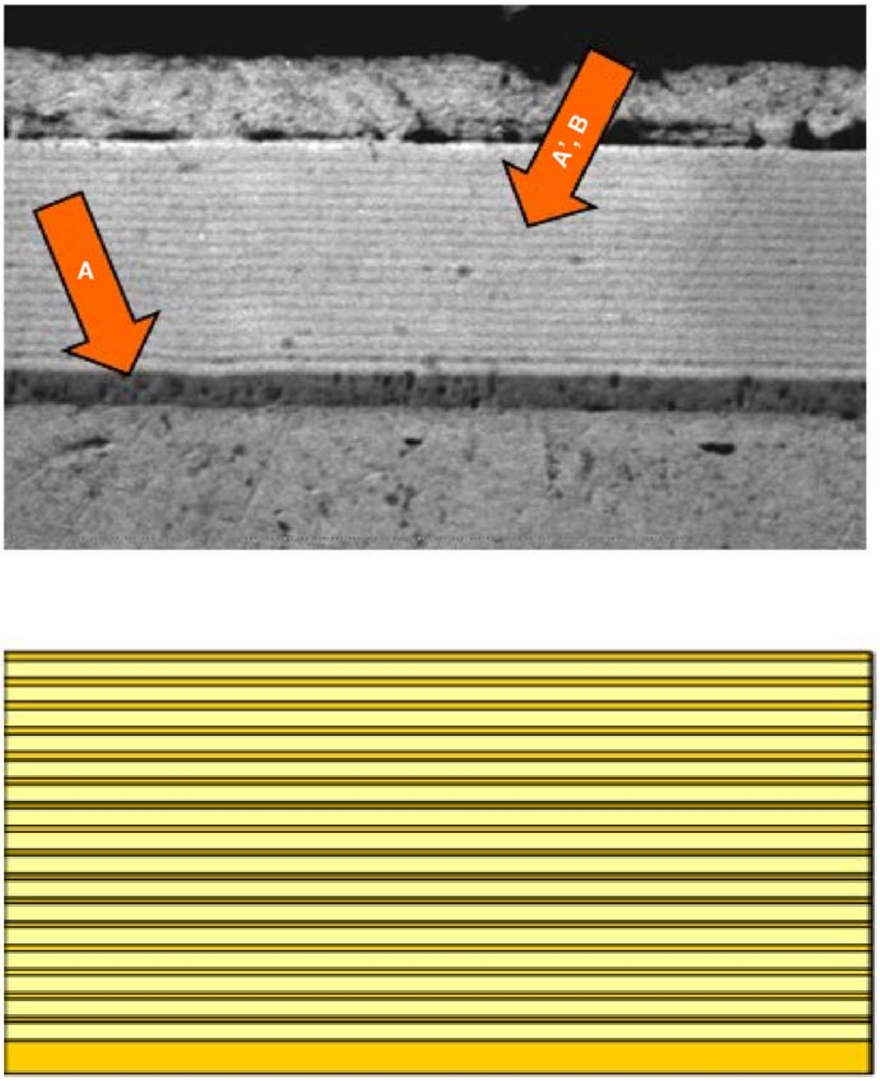

Figure 2-11
Photomicrograph and schematic of PST 24K Type II TiN erosion-resistant coating architecture [67]

2.2.2.3 Coating Equipment and Process

Praxair has four CA-PVD coaters in operation. Units 1 and 2 are single cathode systems with 20 inch (51 cm) diameter x 22 inch (56 cm) high coating zones. Unit 3 is the largest and has a coating zone of 30 inches (76 cm) in diameter x 36 inches (91 cm) in height and is shown in Figure 2-12. Unit 4 is the newest with up to six cathodes in operation; it is designed for very high volume coating production of compressor airfoils. Figure 2-13 shows the multiple cathode Unit 4. Praxair has a great depth of expertise in the CA-PVD process and can quickly scale their proprietary process to much larger components based on customer interest.

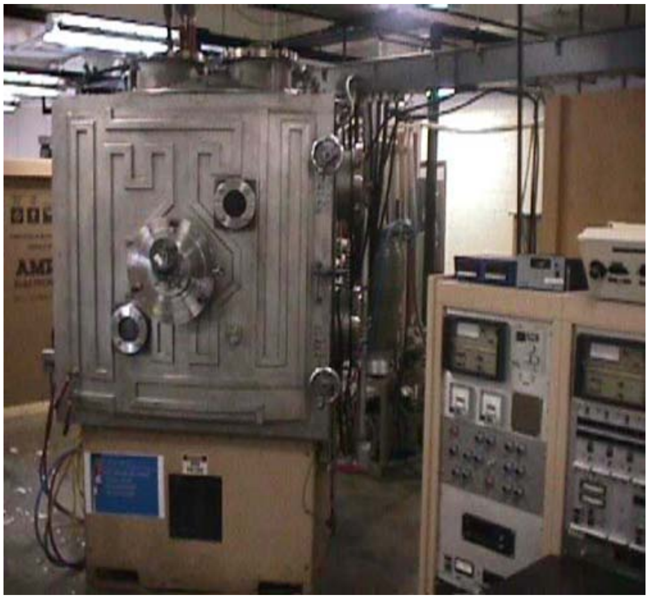

Figure 2-12
Praxair CA-PVD coater # 3 with multiple arc cathodes, a load capacity of 400 lbs (181 kg) (rotation mode), and a coating zone 30 inches (76 cm) in diameter and 36 inches (91 cm) in height

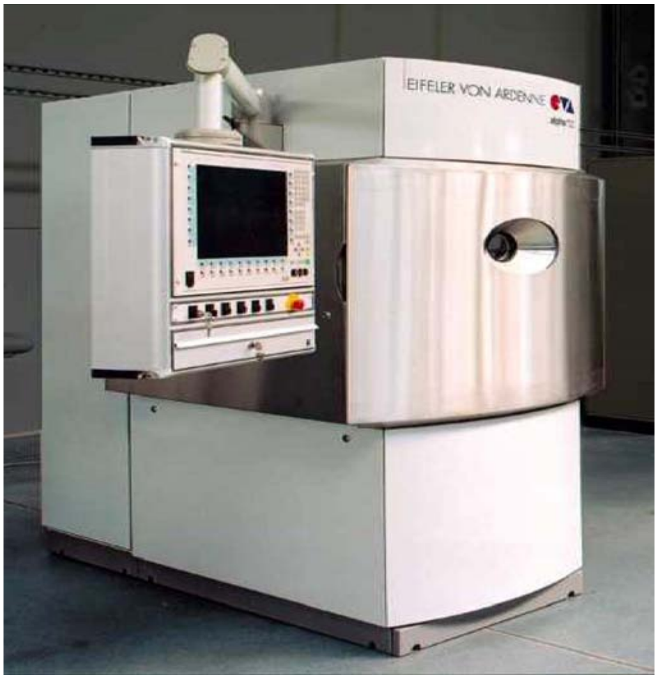

Figure 2-13
Praxair chamber #4 multiple cathodes coating

They use a proprietary 4 inch diameter cathode design that is based on their extensive development experience; it is described in U.S. patent 4,929,322 [68]. Typical operating conditions are 150–300 amps arc current per cathode to evaporate the Ti. Flexible tooling has been designed to be able to coat a variety of rotor blades and stator vanes, accommodating variety in dovetail design and masking requirements Parts are mounted into masking fixtures and loaded onto the part turntable. The system is pumped down and partially backfilled with Argon. The parts are sputter and or glow discharge cleaned *in situ* and preheated to the coating deposition temperature. Nitrogen is introduced into the chamber as the deposition process is initiated. The partial pressure of the nitrogen determines the nitrogen content of the nitride layers. Deposition temperature ranges from 450–600°C (842–1112°F), depending on the application. This is typically monitored by either an optical pyrometer or a thermocouple (TC) mounted on a rotary feed through the inside of the chamber to control substrate temperature within pre-established limits for the alloy. A bias voltage of 100–200 volts is used to create dense coating structure and properties while maintaining a low deposition temperature. Coating thickness is typically 5–25 microns with up to 30 nitride layers. The multilayer structure is created by modulating the nitrogen partial pressure within the coating chamber to create the stoichiometric and sub-stoichiometric TiN_x multilayer coating. The nitrogen pressure is changed on a programmed schedule to create roughly 30 layers in the coating. A coating repair process has been developed in the event of any run deviations.

2.2.2.4 QC Metrics

Coating quality control is based on coating lots (each coating run). Review of electronic run data for conformance to process control limits for gas flow, pressure, temperature, evaporator data, bias data, and other key process metrics is performed for lot certification. Metallographic evaluation is conducted on one sample per coating run, and it is evaluated for thickness, thickness distribution around the airfoil, microstructure, and coating imperfections. Parts are inspected for visual appearance and conformance to color and other visual standards (see Figure 2-14). Additional test samples are evaluated for coating adhesion using the American Society for Testing and Materials (ASTM) scratch test standard, and Knoop hardness is verified to be within control limits. Erosion performance is verified in conformance with customer specification requirements.

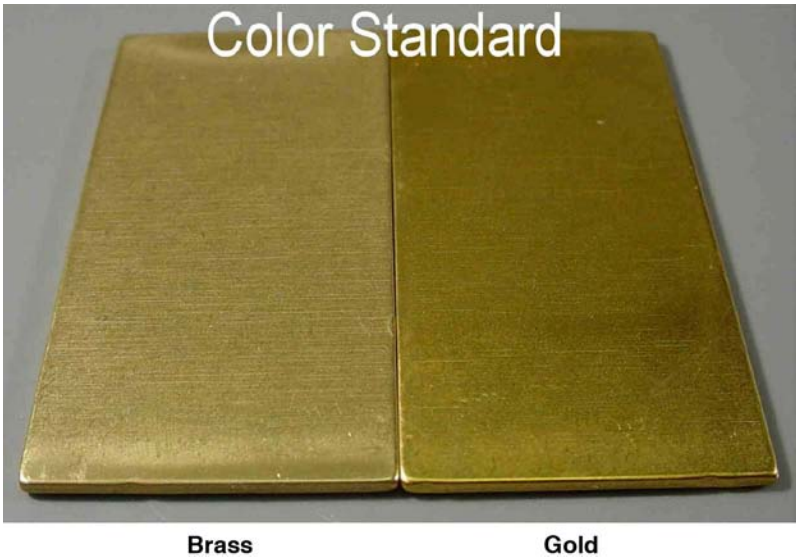

Figure 2-14
Praxair 24K color comparison between sub-stoichiometric (left) and fully stoichiometric TiN (right). The coating color is used as a quality control metric.

2.2.2.5 Performance Testing and Field Service

Erosion Testing: PST uses modified ASTM G76 parameters to screen the performance of their PVD erosion-resistant coating. They use a 0.1875 inch (4.76 mm) orifice , 2 inch (50 mm) length; 4 inch (100 mm) stand off , 50 micron angular alumina, typically at 40 psi (276 kPa) for 20 degrees and 45 psi (310 kPa) for 90 degrees . Particle velocity is in the 80–120 m/s (262–394 ft/s) range. The erosion rate is specified as mg of sample weight loss per gram of erodent.

Figure 2-15 shows the excellent performance of the PST 24K Type II coating under these test conditions at 20 degrees and 90 degrees compared to uncoated Ti 6-4 and Inconel (IN) 718. These results are replotted in Figure 2-16 to show the relative percent improvement compared to the bare alloys. The multilayer structure affords similar erosion performance at 90 degrees and 20 degrees under these test conditions. Most TiN-based erosion coatings perform substantially better at the low angles and exhibit higher erosion rates at the high angles. On a relative basis, the 24K Type II coating gave a 20 times improvement for both alloys at 20 degrees and 7 and 11 times, respectively, for Ti-6-4 and IN 718 at 90 degrees.

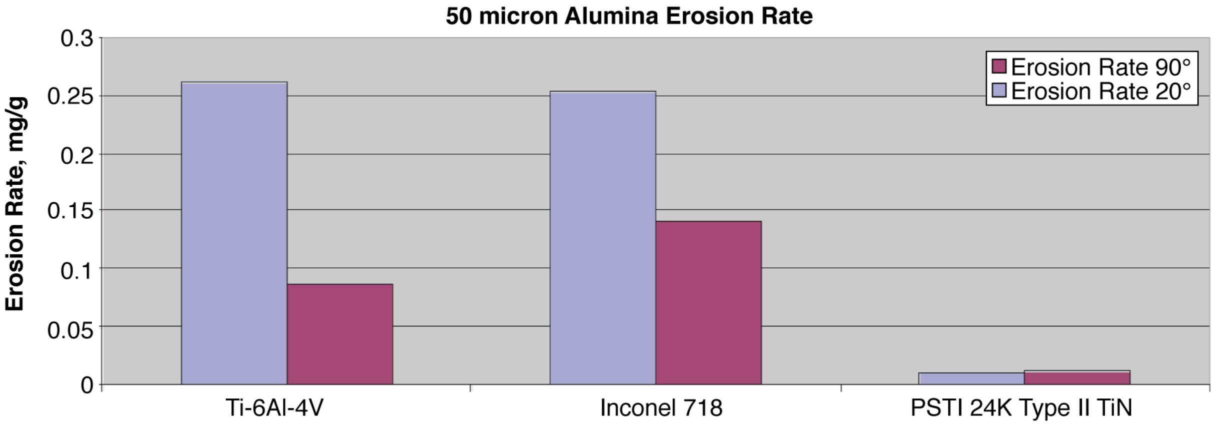

Figure 2-15
PST 24K Type II erosion test results compared to Ti 6-4 and IN 718 uncoated alloys at 20 and 90 degree impingement angles. 50 micron alumina at 80–120 m/s (262–394 ft/s). [59]

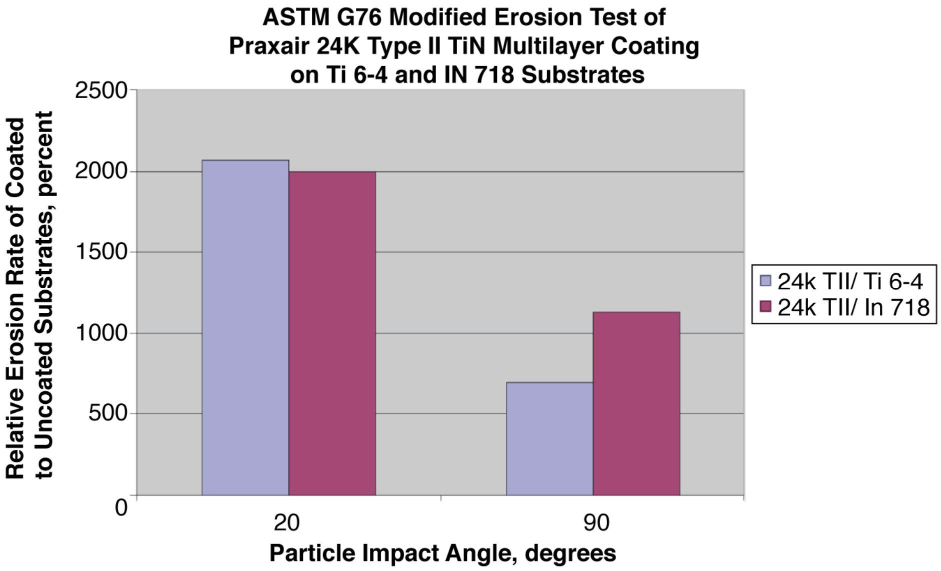

Figure 2-16
ASTM G76 modified erosion test of Praxair 24K Type II TiN multilayer coating data replotted to show relative improvement compared to uncoated Ti 6-4 and IN 718 alloys at 20 and 90 degree particle impact angles.

This improved high-angle performance of the Praxair multilayer structure is excellent and may be of significant importance for water droplet erosion resistance in IGT and steam turbine applications. Figure 2-17 compares the room temperature erosion resistance of Ti-6-4, PST's CA-PVD coatings (TiN Type I, TiN Type II, and ZrN Type II), and five of PST's D-Gun and Super D-Gun coatings. The tests were done with 50 micron alumina at the parameters listed above. It further demonstrates the excellent performance of the TiN 24K Type II coating architecture.

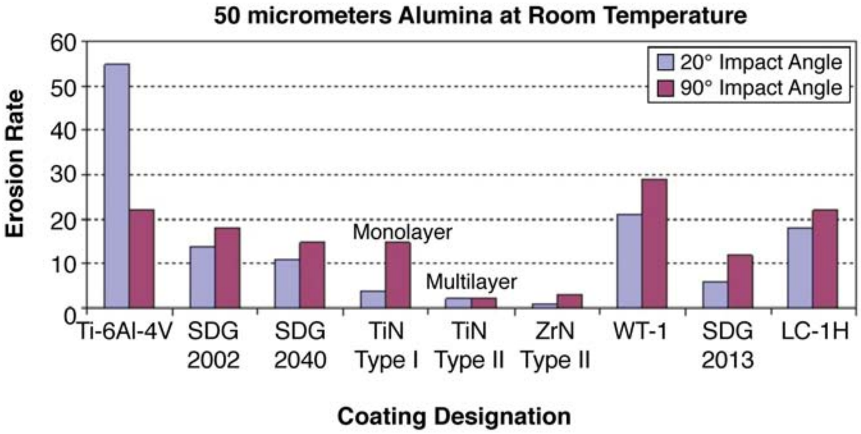

Figure 2-17
Comparison of various Praxair thermal spray and CA-PVD coatings in relative erosion resistance at 20 and 90 degrees [69]

Another modified erosion test is shown below in Figure 2-18, using Arizona Road Dust as the erodent in place of the 50 micron alumina. Testing is carried out on coated and uncoated Ti 6-4 airfoils at a 20 degree impact angle. After 2500 grams (5.5 lb) of erodent, the uncoated airfoil is eroded completely through the thickness of the blade, while the PST 24K type II coating is not breached. Close examination of the coated airfoil shows an elliptical erosion pattern caused by the low-angle particle stream.

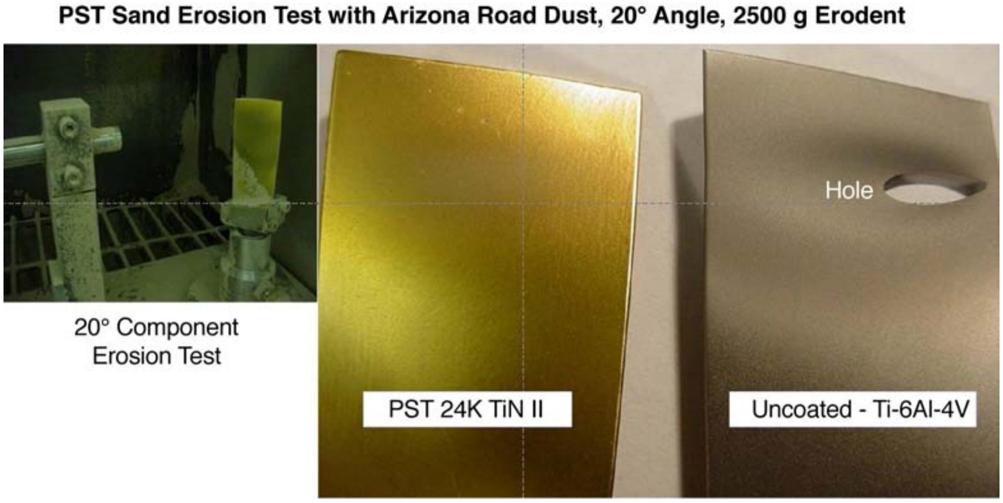
PST Sand Erosion Test with Arizona Road Dust, 20° Angle, 2500 g Erodent
20° Component Erosion Test
PST 24K TiN II
Hole
Uncoated - Ti-6Al-4V

Figure 2-18
Compressor blade 20 degree erosion test comparing PST 24K Type II coating to uncoated blade after 2500 grams (5.5 lb) of Arizona Road Dust. The uncoated blade is completely eroded through the thickness (hole), but the coated blade is intact.

In elevated temperature erosion rig testing at 620°F (327°C), 950 ft/s (290 m/s) particle speed, with 20 micron and 200 micron alumina at 24 and 28 degree impact angles, the time for coating removal was 1 hour for the Type I coating and 5 hours for the Type II TiN coating, that is, a factor of 5 times life improvement for Type II under these test conditions.

2.2.2.6 Rain Erosion Testing

Praxair is the only supplier of the PVD erosion coatings to provide water droplet erosion test data. The testing was carried out at the AFML/UDRI Rain Erosion Test Facility. The test facility and test method are described later in this report. The test conditions were 90 degrees, 1 inch (2.54 cm) per hour rain, 1.8–2 mm (71–79 mils) droplet size, and 223 m/s (732 ft/s) velocity. The sample reportedly showed no signs of failure after more than 3 hours of testing under these conditions, and this was considered a successful test of the coating. Figure 2-19 shows a specimen after such a test.

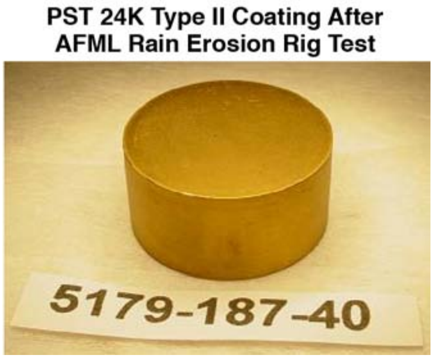

PST 24K Type II Coating After
AFML Rain Erosion Rig Test

Figure 2-19
Praxair 24K+ Type 2 TiN coating rain erosion test sample after 450 minutes [70]

Fatigue Data: Praxair has not published or supplied fatigue test data on their coatings. They report that the coatings have passed OEM fatigue testing on test bars and components as part of their coating qualification process. Such data are apparently proprietary to each OEM.

Field Service data: Praxair has not provided any field service data. They hold production qualifications on several aeroengine platforms. However, the field data are considered proprietary to the OEMs. Praxair has not applied their erosion-resistant coatings to large land-based gas turbines or steam turbines.

2.2.3 MDS-PRAD Technologies

2.2.3.1 Background

MDS-PRAD Technologies Corporation (MPT) based in Prince Edward Island (PEI) [71] is a Canadian-Russian joint venture with the Ural Works of Civil Aviation (PRAD) formed in 1997 to commercialize PRAD’s proprietary erosion-resistant coating (ER-7) and establish production capabilities in North America. ER-7 was developed in the early 1990s by PRAD to protect compressor components in Russian helicopter engines, which experienced extreme erosion wear during Afghan desert operations. The coating was deployed on the TV2-117 (MI-8 helicopter) and the TV3-117 (MI-24 & MI 28 helicopters) among other engines. MDS-PRAD holds an exclusive license to commercialize this coating for non-Russian turbine engines worldwide.

The coating was extensively evaluated as part of a five-year U.S. government Foreign Comparative Test (FCT) program (Russian erosion-resistant coatings for U.S. Navy GTE compressors). This program focused on qualification testing of ER-7 for the U.S. Navy T64 turbine engine including erosion and fatigue testing materials representing all 16 stages of the compressor. Based on the successful results of the FCT program, MDS-PRAD received production erosion coating approval for the GE T64 engine (Stage 1–14 blades and Stage 1–13 vanes) and began commercial production in 2003 in PEI. In addition to the T64 engine, MDS-PRAD has qualified their coating on the T58 engines with GE and the GEM and Gnome engines with Rolls-Royce. In June 2006 they shipped their one millionth coated compressor airfoil. They are a NADCAP-approved coating supplier.

2.2.3.2 ER-7 Coating Structure and Coating Process

The ER-7 coating consists of a proprietary multi-layered nano-structured metal and ceramic matrix applied by a special process using CA-PVD and is comprised of titanium and titanium nitride and other elements according to Simpson [72]. The coating is made up of both hard nitride protection layers and soft metallic layers. The alternating layers are produced by modulating the nitrogen partial pressure in the coating chamber. Simpson characterized the coating as being 5-20 microns thick with a Vickers hardness of 2800–3200.

The coating structure is shown in Figure 2-20 below. The actual details of the coating microstructure, composition, and processing details have been kept confidential and not been published to date.

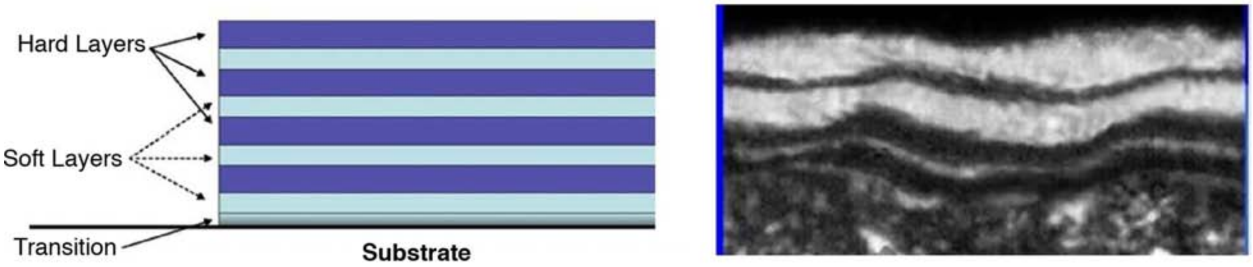

Figure 2-20
Multilayer coating architecture of MDS-PRAD's ER-7 erosion coating

Left: The schematic depicts an eight layer system with a transition layer at the coating substrate interface. Right: Micrograph of ER-7 etched structure – Bright phases are nitride layers. [72, 74]

The multilayered system provides a better defense against crack propagation under fatigue conditions than typical single layer systems. The same is also true under erosion conditions where multiple impacts from particulate occur. Additional coatings are currently under development at MDS-PRAD to further extend erosion resistance. MDS-PRAD has coated components up to 22 inches (56 cm) in length. New equipment being designed will allow coating of larger parts. Figure 2-21 shows their coating facility in PEI.

Figure 2-21
MDS-PRAD production facility in Prince Edward Island

2.2.3.3 Performance Testing and Field Service

During Operation Desert Storm in the 1990s, it was recognized that gas turbine operation in a desert environment significantly impacted turbine engine durability due to severe particulate erosion of the compressor section of the engines. Time on wing (TOW) less than 100 hours was reported.

The U.S. Navy extensively evaluated the ER-7 erosion coating in the FCT program. The initial program goal was to demonstrate a greater than 2 times improvement in TOW (from 100 to 200 hours) with coated components. The results of lab, engine test, and field service experience are reported below for the T64 FCT program and for the T58 CIP program.

2.2.3.3.1 FCT Test Program

Klein and Simpson [73] reported on the results of ASTM G76 erosion testing of ER-7 coated and uncoated coupons of the four compressor alloys (17-4 PH, Custom 450, IN 718, and Ti 6-4) found in the T64 engine. Testing was conducted at 15, 45, 75, and 90 degree impingement angles and is plotted as milligrams of weight loss per minute of test time as shown in Figure 2-22. These data are re-plotted in Figure 2-23 to show the relative erosion performance improvement of the ER-7 coating compared to the substrate alloys.

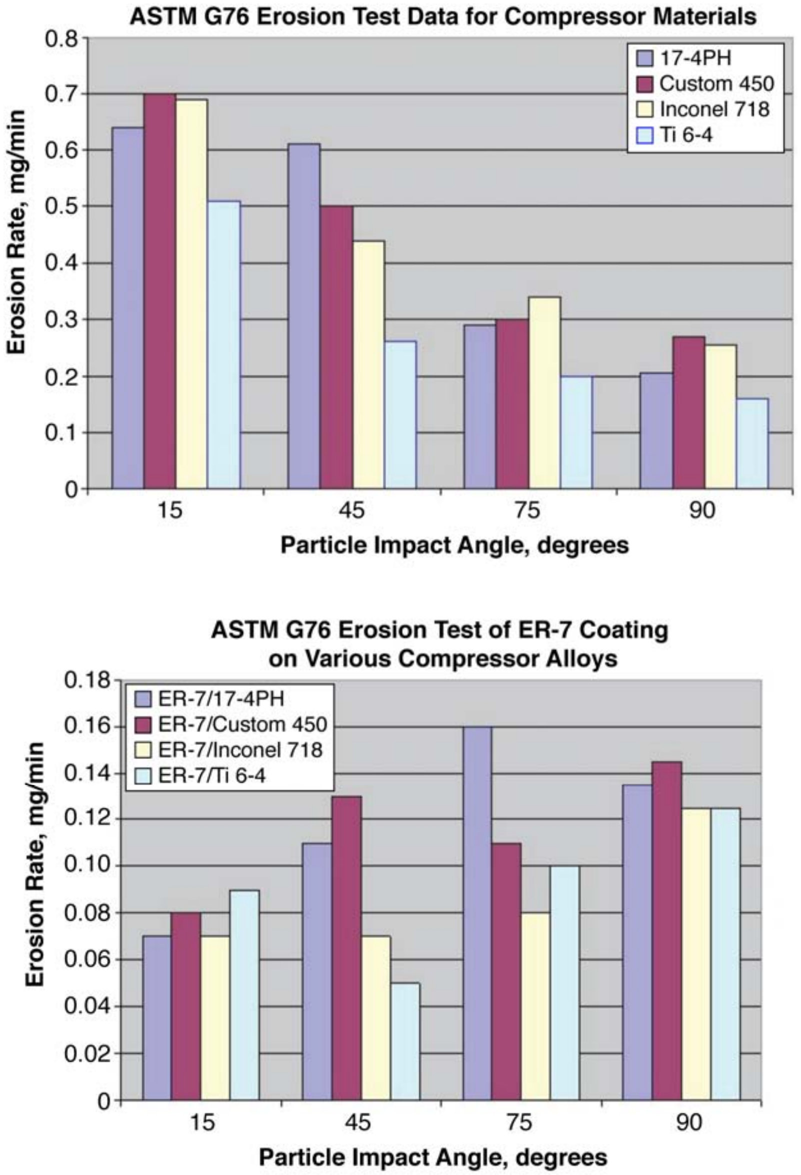

Figure 2-22
Erosion performance of ER-7 coating compared to uncoated 17-4 PH, Custom 450, IN 718, and Ti 6-4 as a function of erosion angle. ASTM G76 50 micron alumina erosion testing. [73]

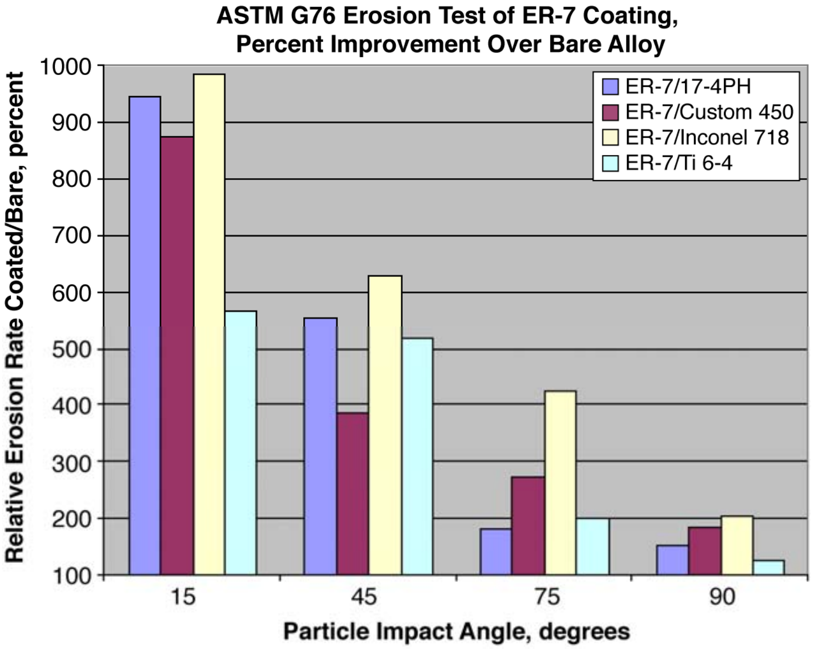

Figure 2-23
Relative improvement in erosion performance of ER-7 coating compared to uncoated 17-4 PH, Custom 450, IN 718, and Ti 6-4 as a function of erosion angle. ASTM G76 50 micron alumina erosion testing. [73]

The ER-7 coating is shown to be strongly affected by particle impact angle and is consistent with more “brittle” material behavior compared to the “ductile” response of the uncoated alloys. It does comparatively well at low particle impact angles (~5.5–10 times at 15 degrees) and (~ 4–6 times at 45 degrees) when compared to any of the common compressor alloys evaluated (for example, 17-4 PH, Custom 450, IN 718, and Ti 6-4). At high angles the coating still provided some protection over the substrate (1.2–2 times), but it is not nearly as effective as it is at the lower angles. Since the erosion pattern seen on the T64 compressor blade is predominately believed to be low-angle erosion of the blade trailing edge (TE) pressure face resulting in chord loss, the coating evaluations were moved forward to component rig testing.

2.2.3.3.2 T64 Stage 1 Blade Erosion Wind Tunnel Testing – University of Cincinnati

This test erosion testing of ER-7 coated and uncoated T64 Stage 1 (Ti 6-4) compressor blades was conducted in the room-temperature erosion wind tunnel at the University of Cincinnati. Four blades were fixtured as shown in Figure 2-24 (left). One coated blade and one uncoated blade were used for the erosion measurements; the outside blades were used to direct airflow and simulate the conditions in the engine. The tests were conducted at a 20 degree impact angle as defined by a line from the blade’s leading edge to the trailing edge on the pressure side. To simulate service conditions, silica sand with a nominal 10 micron size (with particles up to 100 microns) was used. The particle velocity was 700 ft/sec (215 m/s) and was based on the T64 Stage 1 blade tip speed at full military power. The sand was metered into the wind tunnel in 0.5 kg (17.6 oz) increments for the first several test intervals and then in 1 kg (35.3 oz) amounts for the balance of the test. The results of this testing are plotted in Figure 2-24 (right). The ER-7 coating provided approximately a 3 times improvement in expected component life based on effective chord loss criteria.

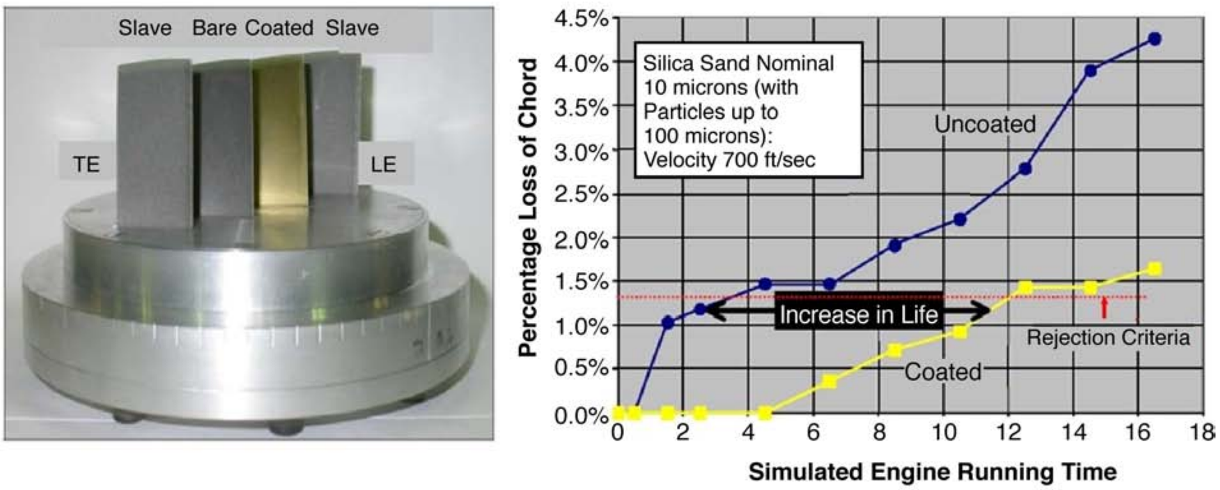

Figure 2-24
Particle erosion testing on T64 Stage 1, Ti 6-4 compressor blades in the University of Cincinnati erosion wind tunnel

Left) Wind tunnel erosion fixture with four blades – The outside blades are used to direct airflow and simulate engine conditions and are not measured. Right) Plot of the erosion results for bare and ER-7 coated airfoils at a 20 degree impact angle with 10 micron silica at 700 ft/sec (215 m/s). [73, 74]

2.2.3.3.3 T64 Engine Qualification Testing

Shell et al. [74] reports on the results of T64 coating qualification testing funded as part of the Navy ER-7 FCT program.

Fatigue Testing: One of the concerns with introducing coated hardware into the engine was the impact on the component fatigue performance. Axial-axial strain-controlled high-cycle fatigue (HCF) testing was conducted on round test bars of Ti 6-4, A286, and IN 718 at A ratios of infinity (mean stress of 0) and 1 (The mean stress is half of the maximum stress.). The coating had no adverse effect on IN 718 or A286, regardless of the A ratio. With the Ti 6-4, a 10 % debit was found in the absence of a mean stress; a significant debit of 45% was noted under mean stress conditions (see Figure 2-25). Component fatigue testing verified the round bar results for all three materials. Based on these findings, it was decided to partially coat the outer half of the Ti 6-4 alloy blades, masking the lower half. Following coating, the masked portion of the airfoils was peened to restore the fatigue performance on the fatigue-sensitive lower half of the airfoil.

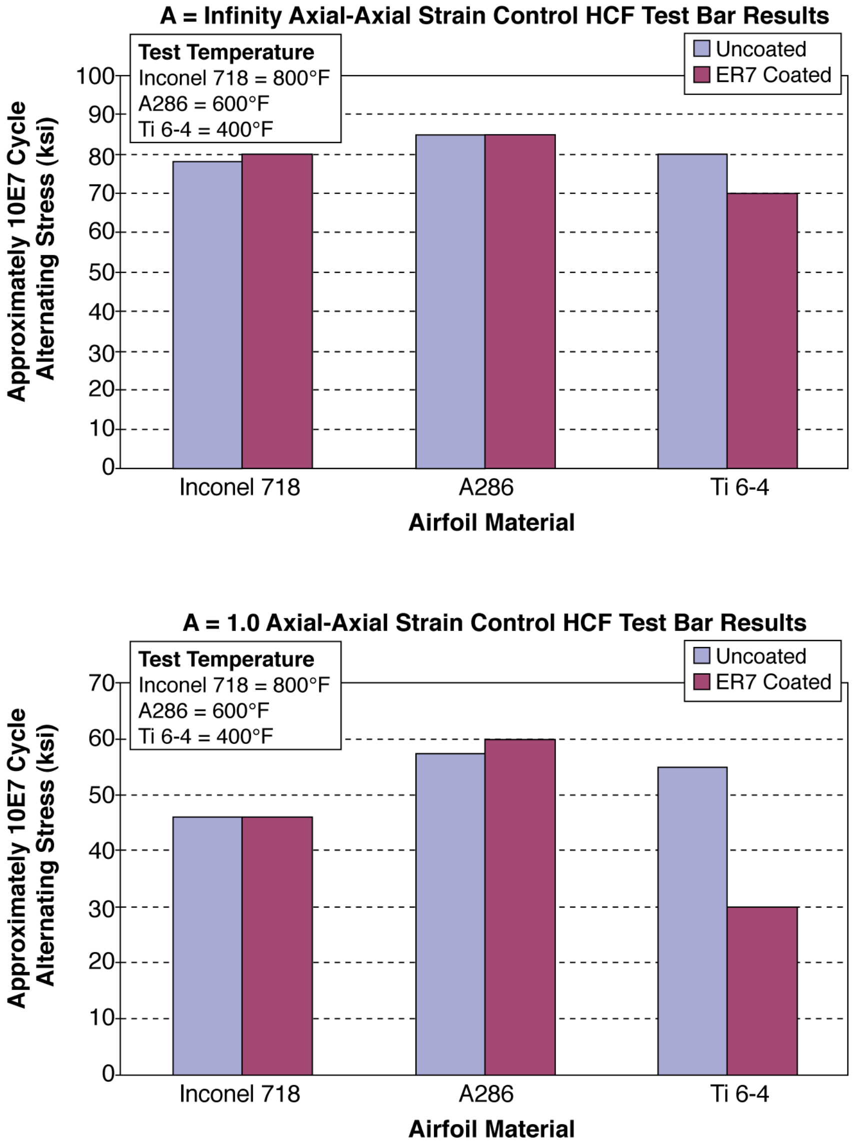

Figure 2-25
HCF test results for ER-7 coated and uncoated IN 718, A286, and Ti 6-4 cylindrical test bars [74]

Sand Ingestion Test: A T64 sand ingestion test was conducted with a mix of coated and uncoated airfoils to obtain a direct comparison of the effectiveness of the ER-7 coating. The sand used for the engine test was 100–200 micron silica and was coarser than that used in lab testing in order to accelerate the test and mitigate downstream damage to the hot section of the engine with the finer media. This would allow a direct assessment of engine power loss attributable to compressor erosion. The test engine was run until a predetermined power loss (estimated at 25%) was attained, and the engine began to stall and surge. The engine had ingested 16.1 pounds (7.3 kg) of sand when the test was terminated.

Figure 2-26 shows the rotor after teardown. The coated blades have suffered much less chord loss than the uncoated airfoils. Figure 2-27 summarizes the chord loss by stage. The middle stages suffered the greatest chord loss. The photos in the right of the figure are of a Stage 5 blade and show the profile retention of the coated blade versus an eroded uncoated airfoil. The chord loss at the trailing edge is due to TE thinning. The average improvement in the performance retention due to the use of the ER-7 coating was estimated at 2.5 to 4 times better than uncoated blades and vanes, based on the chord and trailing edge thickness measurements on a representative sampling of airfoils.

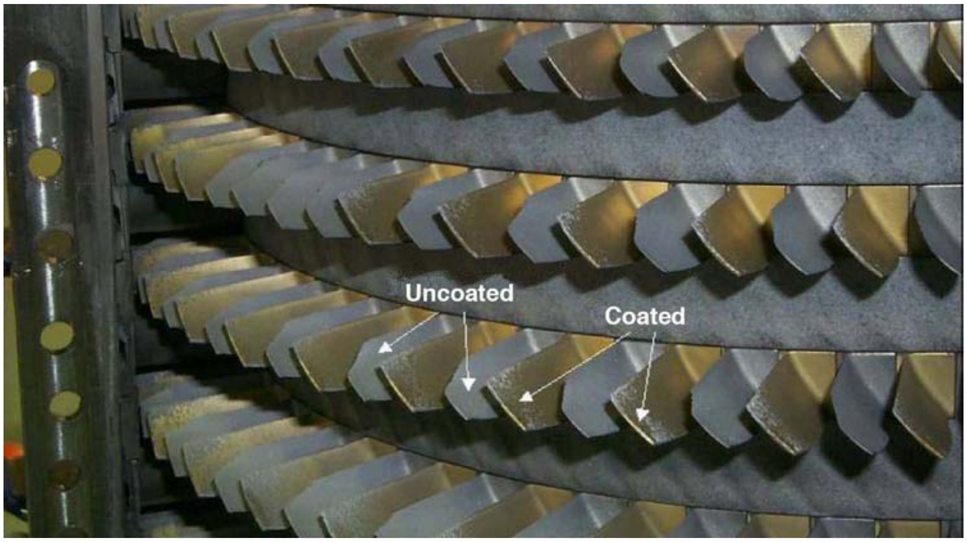

Figure 2-26
T64 compressor rotor at teardown following sand ingestion testing at Kirtland Air Force Base. ER-7 coated and uncoated blades were used in the rainbow rotor. Severe erosion of the uncoated airfoil trailing edge is particularly apparent. [74]

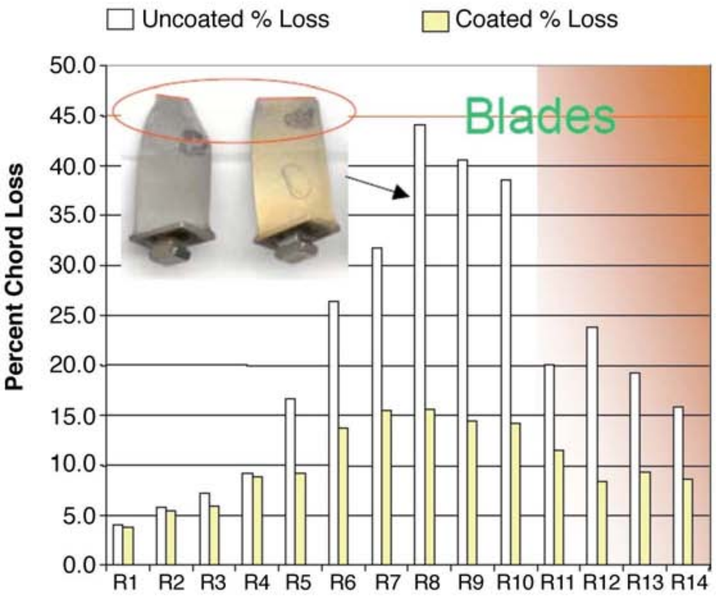

Stage 5 Blades

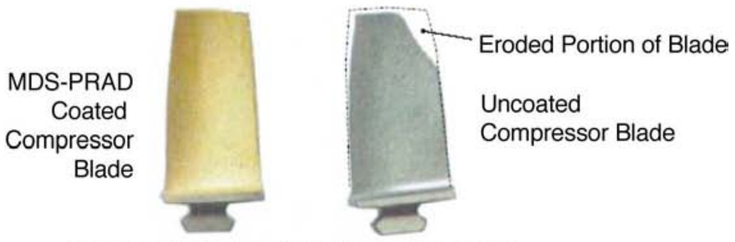
MDS-PRAD
Coated
Compressor
Blade
Eroded Portion of Blade
Uncoated
Compressor Blade

Results of T64 Engine Sand Ingestion Test
Conducted by GE and U.S. Navy

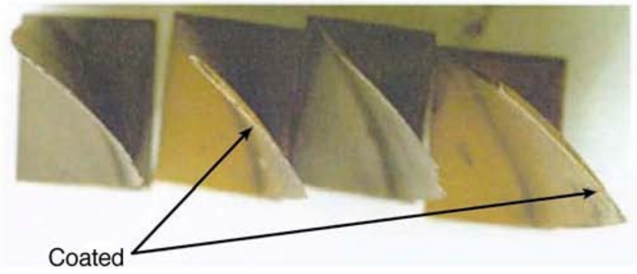

Figure 2-27
Improved chord and trailing edge thickness retention seen for ER-7 coated compressor blades and vanes compared to uncoated parts following teardown of the T64 sand ingestion test engine. [74]

2.2.3.3.4 Field Service Experience

Lead the Fleet Engine: In order to establish the operational effectiveness of the ER-7 coating, a lead the fleet (aero)engine (LTFE) was assembled with fully coated rotor and stator airfoils. Typical experience for the T64 fleet operating in a heavy sand environment is 110–120 hours before the engine needs to be removed for low power. This was confirmed in Operation Enduring Freedom and Operation Iraqi Freedom, where the average T64 TOW was 113 hours.

After 374 hours the LTFE was removed for evaluation of the coating performance due to loss of power in the engine hot section module. A detailed inspection of the airfoils revealed that the coating was intact on the pressure and suction side of the airfoils with the exception of the first blade where the coating had been eroded by high-angle attack across the span to the mid-chord. The coating at the leading edge of all of the airfoils was eroded by high-angle attack on all of the airfoils down to the parent metal, resulting in some chord loss. A 3.3 times improvement was demonstrated in the LTFE compared to the desert operations baseline. Additional service life remained in the compressor module at the time of removal even though some coating loss was noted.

Operational Experience: T64 field experience on the CH-53 helicopter in Operation Iraqi Freedom demonstrated increased engine TOW from approximately 120 hrs (uncoated compressor) to over 1400 hrs for compressors with the ER-7 coating, resulting in a life extension of nearly 12 times [75]. This is substantially better than the 3 times improvement predicted in testing done at the University of Cincinnati [73], the ~ 2.5–4 times performance improvement observed in the T64 sand ingestion testing conducted by Navair under the FCT program [74], or the > 3.3 times improvement noted in the LTFE field service evaluation. These differences are likely due to different evaluation criteria. In field service, the engines are removed from service based on power loss (typically 25%) rather than the chord loss measurement standards used in the lab testing and in engine test conditions (mixed engine set of coated and uncoated hardware and coarse particle size).

Further understanding of these issues is important in the development of better screening metrics. The final arbiter of any coating is always field service, and in this case, erosion coatings have provided a substantial benefit.

2.2.3.3.5 T58 Sand Ingestion Testing

Following the successful introduction of ER-7 in the T64 fleet, evaluations were conducted on the T58 engine [76]. The GE T58 engine is installed on the CH-46E helicopter. Like the T64 engine, the T58 has experienced significant reductions of TOW when operating in dusty desert environments. While the design life of the compressor is 3000 hours, T58 engines have been driven off wing in as little as 100 hours of desert operations for erosion-related performance loss.

In order to assess erosion performance in the T58, two back-to-back sand ingestion tests were conducted with the goal of demonstrating a 2 times increase in performance retention with the ER-7 coating. The test parameters were based on the previous T64 sand ingestion test: 100–200 micron silica sand was used, and the engines were run until they had zero stall margin. The first engine, which was used as a baseline, had uncoated airfoils and ingested 8.5 lbs (3.9 kg) of sand when stall occurred. In the second engine, the ER-7 coating was applied to all blades, variable vanes, and vane segments. One uncoated blade per stage was included for comparison purposes. The coated engine was able to ingest 17 lbs (7.7 kg) of sand before it stalled. This demonstrated a 2 times increase in engine operation and met the program goal.

Analysis of the coated and uncoated components following teardown revealed minimal difference in erosion on the ER-7 coated and uncoated variable vanes and fixed vane segments. Field experience has shown that these components show less erosion than the blades and are routinely returned to the field following engine overhaul. It was also noted that the coating was rapidly removed from the vane segments, which was attributed to much thinner coating being deposited due to geometry factors limiting line-of-sight coating.

Figure 2-28 depicts the coated and uncoated first stage blades following the test. The T58 first stage blades are subject to leading edge erosion and—more important—leading edge curl. Leading edge curl is seen in a number of engines (T700 and AGT 1500 among others) and is the result of a burr formation from repeated high-angle ballistic impact of sand particles, resulting in a local yielding of the blade material. No solution has been found to date to eliminate leading edge curl. The ER-7 coating was found to minimize burr formation even in the presence of leading edge erosion.

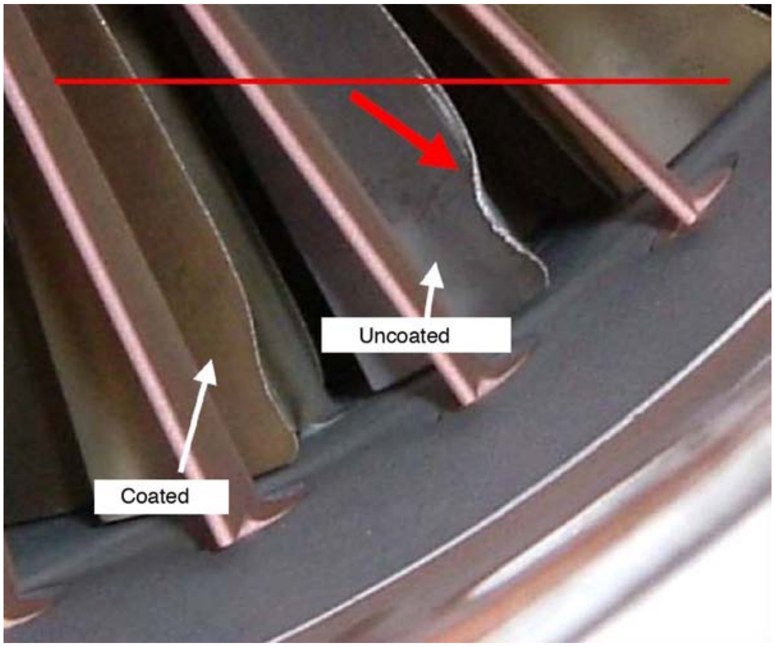

Figure 2-28
T58 ER-7 coated and uncoated first stage blades showing differences in degree of leading edge curl

The erosion patterns on the entire rotor are depicted in Figure 2-29. The photo on the left is the pressure side and the suction side is shown on the right.

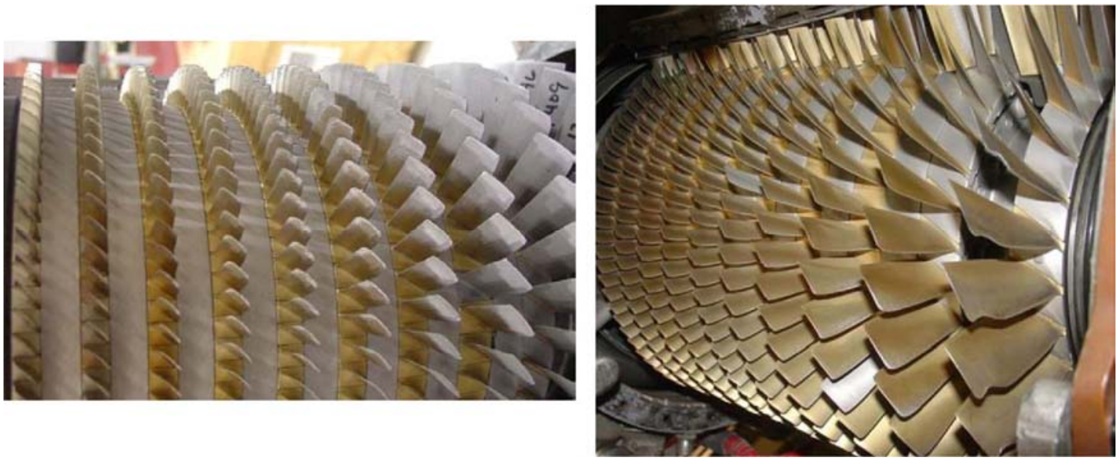

Figure 2-29
T58 ER-7 coated rotor showing erosion patterns following sand ingestion testing

Left: Pressure side showing pattern of coating loss (silver). Right: suction side with coating intact. Note the leading edge erosion on first stage blade due to high-angle particle impact.

Based on the increase in engine performance noted in the sand ingestion test ER-7 coating has been introduced into the fleet on the blades. Field results are not yet available. It will be interesting to see if the T58 field experience is similar to the T64.

2.2.4 Performance Turbine Components

The headquarters for Performance Turbine Components (PTC) is located in Jupiter, Florida. They have developed a TiN-based coating targeted for application in the Frame 7FA compressor blades. They have provided the following information about their coating process and experience [77].

PTC is the industry leader in erosion coating applications for the land-based (gas) turbine industry. PTC's T-Armor coating was developed to address the root cause of compressor airfoil failures caused by erosion, allowing the user to have increased operating flexibility and to be less hampered by continued inspections and airfoil replacement due to erosion and corrosion. PTC has been coating land-based compressor parts for over four years at their facilities in Florida. The T-Armor coating is claimed to lead the industry in erosion and corrosion prevention. They have several sets of land-based compressor blades and vanes in operation. PTC's T-Armor coating has been applied to GE 7FA+E engine R0 compressor blades and inlet guide vanes (IGVs) in Siemens Westinghouse units for erosion and corrosion prevention.

2.2.4.1 Coating Process

T-Armor is applied with a reactive ion/CA-PVD process. It is reported by PTC that the T-Armor coating process is “patent pending” and has been validated by over 18,000 hours of operation and over 1300 hours of wetted operation in the 7FA operating environment. They have conducted rigorous validation testing to ensure the quality of their process. Validation testing included material tests for high-cycle fatigue, corrosion and crevice corrosion concerns, and erosion tests in a laboratory environment. The results of these tests showed that the T-Armor process provided both high resistance to water erosion and also greatly reduced the concern for corrosion, corrosion-assisted fatigue, and crevice corrosion, a known problem area in coating compressor airfoils made from stainless steels. The validation program proved the T-Armor process provided positive benefits to the base blade or vane.

PTC reported that the T-Armor coating process has been developed to provide the optimum coating thickness in the areas of most concern. For example, the 7FA+E R0 blades are coated with the greatest coating thickness on the airfoil leading edge just above the platform, providing optimum benefit for leading edge cavitation erosion. T-Armor can be applied from thicknesses of 8–20 microns, depending upon the need and application. The T-Armor coating can be applied in either a monolithic or multilayer coating. The type of erosion environment determines the coating application.

2.2.4.2 Field Experience

T-Armor has been applied to new and used/run parts on Frame 7FA R0 blades (see Figure 2-30). All new and used parts are processed and inspected to aeroengine (Federal Aviation Administration) standards. They have accumulated over 18,000 hours of operation with over 1300 hours of fogging (wet) operation. Minor deterioration of the coating was observed on the blade leading edge, as shown in Figure 2-31 PTC has been coating several rows of blades for field engine service.

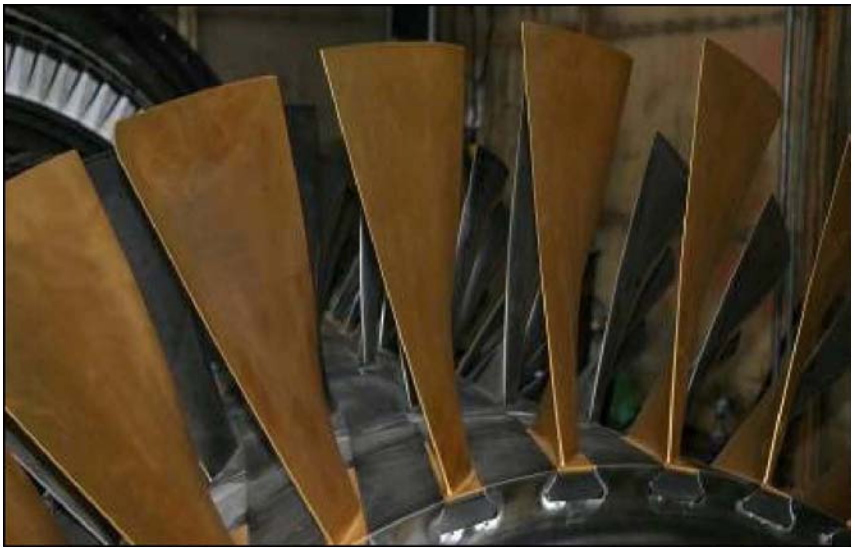

Figure 2-30
T-Armor coated Frame7 FA R0 compressor blade row

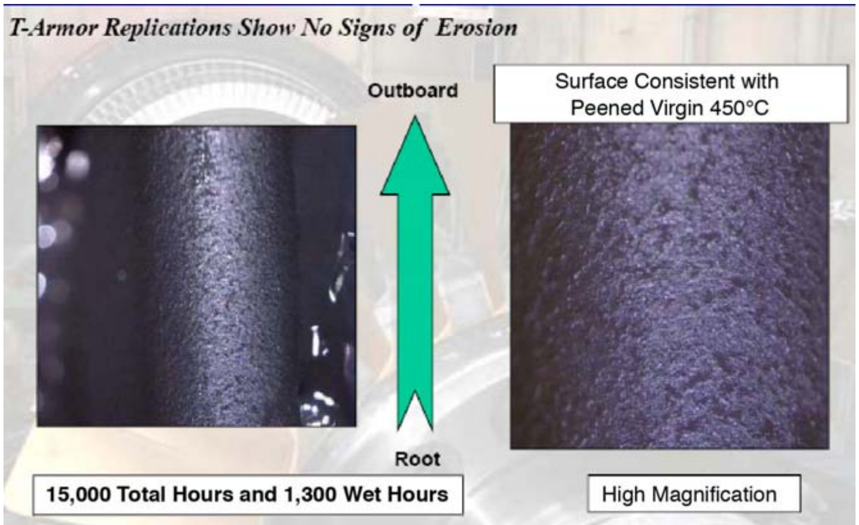
T-Armor Replications Show No Signs of Erosion
Outboard
Surface Consistent with Peened Virgin 450°C
Root
15,000 Total Hours and 1,300 Wet Hours
High Magnification

Figure 2-31
Condition of the leading edge of R0 blade from Frame 7FA engine coated with T-Armor coating after 15,000 hours of operation. 1300 hours with fogging (wet) operation.

2.2.5 BryCoat, Inc.

BryCoat, Inc. is located in Oldsmar, Florida. The following information on the coating processes and their capabilities and experience was provided as a response to the EPRI coating vendor survey on erosion coatings.

BryCoat was founded in 1989 and incorporated in 1990. BryCoat is an AS9100 B registered company, has ISO 9001:2000 certification, and received in 2007 NADCAP accreditation in the following areas:

- PVD coating
- Thermal spray coating
- Dry film lubricant coating (tungsten disulfide)
- Stripping of coatings

They are a supplier of TiN coatings for several products such as tool and die, engine parts, marine parts, and others. In addition to the traditional thermal spray processes, BryCoat also uses an advanced PVD process in a vacuum chamber to deposit TiN coatings. An HVOF process is used to apply tungsten and chrome carbides. After the initial inspection and cleaning, the parts are loaded onto fixtures and loaded into the coating chamber. The air in the chamber is removed, leaving a high vacuum environment. Substrates are preheated to process temperature and ion cleaned to remove the final atomic contaminants from the surface. A flow of ionized nitrogen and argon is introduced into the chamber. Titanium is flash evaporated and ionized by a vacuum arc. The plasma cloud is accelerated to the substrates. A voltage is applied to the substrates to accelerate the ions in the plasma cloud. The titanium and nitrogen combine on the surface of the substrate, forming a dense, hard coating of TiN. The coating bonds to the surface of the substrate and even penetrates the surface slightly. The coating cycle lasts several hours. All process variables are carefully controlled to ensure a high-quality coating. Each coating batch is inspected for coverage, adhesion, thickness, uniformity, and hardness.

Additional information about the types of coating and application received from BryCoat is listed below.

1. Titanium nitride (TiN) PVD coating
   a. Excellent for cavitation erosion resistance, wear resistance, galling prevention, sliding wear, adhesive wear.
   b. Thin film usually 3 microns typical thickness. Thicknesses up to 12 microns monolithic TiN have been done successfully.
   c. Applied by CA-PVD coating vacuum deposition process.
   d. Service temperatures up to 1100°F (593°C) in normal atmosphere.
   e. Coat steels, stainless steels, titanium, nickel alloys, etc.
   f. Follows surface finish of substrate material.
   g. Sizes up to 4 foot (122 cm) length. (Multiple chambers available for that size.)
   h. Coating test results for thickness, hardness, and scratch adhesion will be provided upon request. Witness samples are coated with each chamber run, tested, and stored long term.
   i. BryCoat has successful applications of TiN for land-based turbine compressor blade applications to minimize cavitation erosion.

2. Titanium nitride multilayer (TiN) PVD coating
   a. Excellent for erosion protection from fine particulates.
   b. Thin film usually 10–30 microns thickness.
   c. Applied by CA-PVD coating vacuum deposition process.
   d. Service temperatures up to 1100°F (593°C) in normal atmosphere.
   e. Coat steels, stainless steels, titanium, nickel alloys, etc.
   f. Follows surface finish of substrate material.
   g. Sizes up to 4 foot (122 cm) length. (Multiple chambers available for that size.)
   h. Used for sand erosion applications in aerospace and defense turbine applications.
3. Chromium nitride (CrN)
   a. Excellent corrosion protection (chrome plating replacement) and wear resistance of precision components.
   b. Similar properties with higher temperature tolerance than TiN coating.
   c. Can be applied 2–18 microns thickness.
   d. Typically has a lower (coefficient of friction) COF than titanium nitride.
   e. Applied by CA-PVD coating vacuum deposition process.
   f. Service temperature up to ~1400°F (~ 760°C).
   g. Coat steels, stainless steels, titanium, nickel alloys, etc.
   h. Follows surface finish of substrate material.
   i. Sizes up to 4 foot (122 cm) length. (Multiple chambers available for that size.)
4. Tungsten and chrome carbide HVOF thermal spray coatings
   a. Excellent for erosion protection, corrosion protection, and wear resistance.
   b. Usually 0.005–0.010 in. (0.127–0.254 mm) thickness (Greater thicknesses are available).
   c. Applied by HVOF thermal spray process.
   d. Service temperatures to 1500°F (833°C).
   e. Coat steels, stainless steels, titanium, nickel alloys, aluminum, etc.
   f. As-coated surface finish of 64–128 micro-inches (1.6–3.3 micrometers).
   g. Sizes up to 8 foot (2.4 m) length.

2.2.6 Sputtek, Inc.

The headquarters and coating facilities of Sputtek, Inc., are located in Toronto, Canada. Information from Sputtek in response to the EPRI coating vendor survey is provided in this section.

2.2.6.1 Coating Process

Sputtek has ISO 9001:2000 certification and is also a NADCAP approved coating supplier. Sputtek's coating method is based on CA-PVD. The originality of their technology is based on the use of a high level of ionization and the control of the ion bombardment energy to specific values (through several methods) in the vacuum-arc process. They obtained thick (> 20 µm) coatings with a lower level of stress. It is claimed that their coatings have a dense, nano-scale structure, with good adhesion, cohesion, and ductility. The mechanical properties combine a relatively high hardness (1800–2200 HV) with good ductility and the capability to withstand large deformations, thermal shock, and intensive erosion.

Sputtek's CA-PVD coating deposition facility is shown in Figure 2-32.

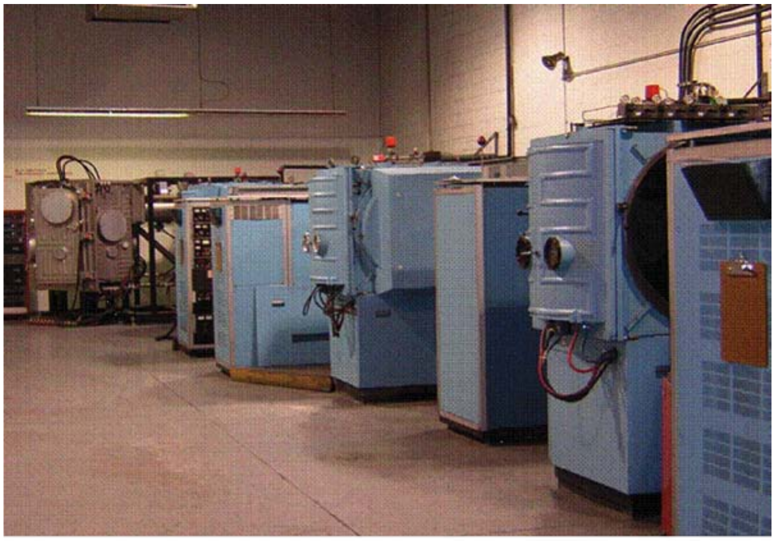

Toronto Coating Facility
Four Deposition Systems SP-1000 (1.0 m^3 - 35 ft^3 Capacity)
and Prototype SP-2000 (2.0 m^3 - 70 ft^3 Capacity)

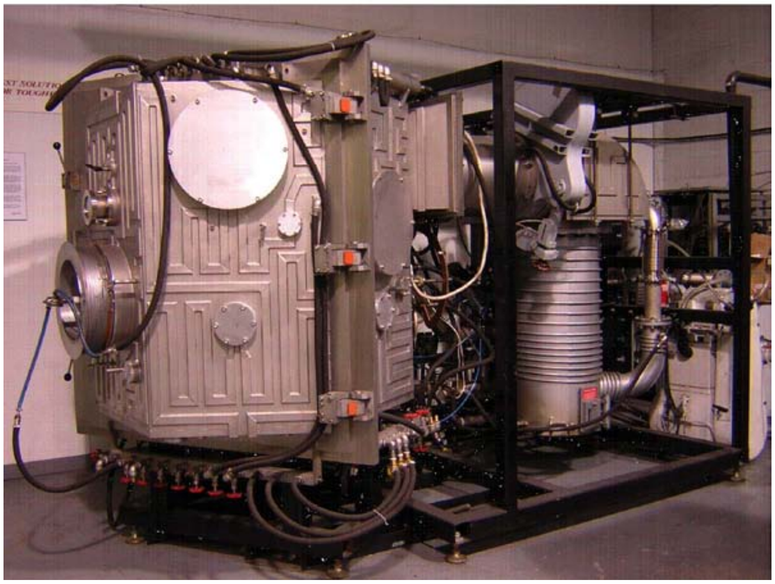

Figure 2-32
Sputtek's CA-PVD coating deposition systems located in Toronto, Canada. Bottom photo shows a close-up of the new system.

In order to further enhance the capacity to withstand high surface loads, they have developed a "duplex" process by introducing an ion nitriding stage at the beginning of the deposition process. The two steps of the process are taking place in the same machine cycle, and the possible oxidation of the part between operations is avoided. Charged particles (plasma) are magnetically accelerated toward the parts to coat, with energies 100–1,000 times higher than in the electron beam machines that are currently available. The very high energy bombardment results in high-density coatings with excellent adhesion to the part. The coatings currently available from Sputtek are listed here:

- Titanium aluminum nitride – TiAlN (ERCOTEC)
- Chromium nitride – CrN
- Titanium carbonitride – TiCN
- Titanium nitride – TiN
- Zirconium nitride – ZrN

Sputtek has developed various coatings for heavy-duty, large tools for stamping, rolling, hot and cold forging, punching, die-casting, wear mechanism parts, etc. They reported that based on the data provided by their customers, the coatings demonstrate 2–20 times increase in life vs. uncoated parts. The new duplex coatings (ion nitriding plus CrN or TiAlN) are used in extreme pressure applications such as tooling for heavy stamping of high-strength low-alloy steels (up to 80–120 ksi (552–827 MPa) yield strength), for cold and hot forging, as well as for die casting. In such applications, the duplex CrN/C has proven its efficiency due to the same combination between high hardness, oxidation resistance, and corrosion inertness. The data provided by Sputtek's customers has indicated that the life of both pins and cavities increased 5–14 times.

During the past four years, Sputtek has developed a proprietary sand erosion-resistant coating. This coating is targeted for application in the compressor stages of the turbo engines used in sand-contaminated environments. Sputtek's coatings provide good adhesion and a high capability to accommodate a significant mismatch of the coefficient of thermal expansion between the substrate material (Ti6Al4V, A286, AM 350, 17-7 PH, Inconel 718, etc.) and the coating. At the same time, the coating accommodates the conflicting requirements of hardness, thickness, and ductility by reducing the residual compressive stresses in the coating. As a result, Sputtek has produced reliable coatings up to 20–25 µm thick that are able to resist severe erosion without cracking and spalling.

2.2.6.2 Testing and Validation

The coating has been tested by several specialized laboratories such as the Natural Research Council-Canada and University of Cincinnati (Prof. W. Tabakov) as well as the major gas turbine manufacturers (GEAE, Honeywell-United States, TURBOMECA-France, and MTU-Germany). The tests have been successful, and they triggered the validation processes for this coating as a second step toward its use in production. The erosion-protection coating is already in production for the land-based gas turbine engines manufactured and refurbished by Magellan-Orenda Aerospace, Canada.

The ERCOTEC coating has been also tested for the complex validation AGT1500/Tiger program. All the tests revealed a substantial erosion protection when compared with the uncoated blades, and ERCOTEC performed better than some of the coatings from other coating vendors.

Sputtek has supplied ERCOTEC coated test coupons to EPRI for further independent evaluation and testing (by TurboMet International), which is in progress.

2.2.6.2.1 Microstructure of the Coating

An example of metallurgical cross section of an AM350 steel sample coated with TiAlN monolayer coating is shown in Figure 2-33. The ion nitrided sublayer is also shown in this figure. Figure 2-34 shows the microhardness test results on the ion-nitrided sublayer.

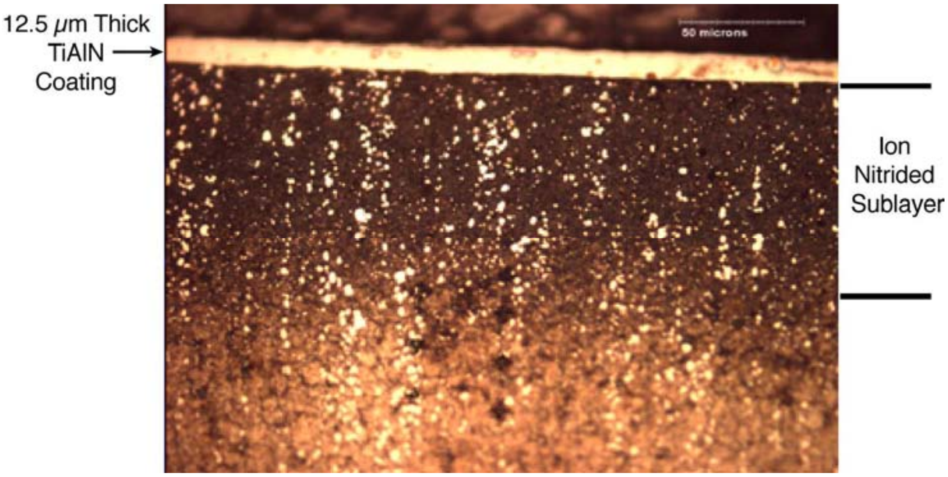

Figure 2-33
Metallurgical cross section of Sputtek's TiAIN coating

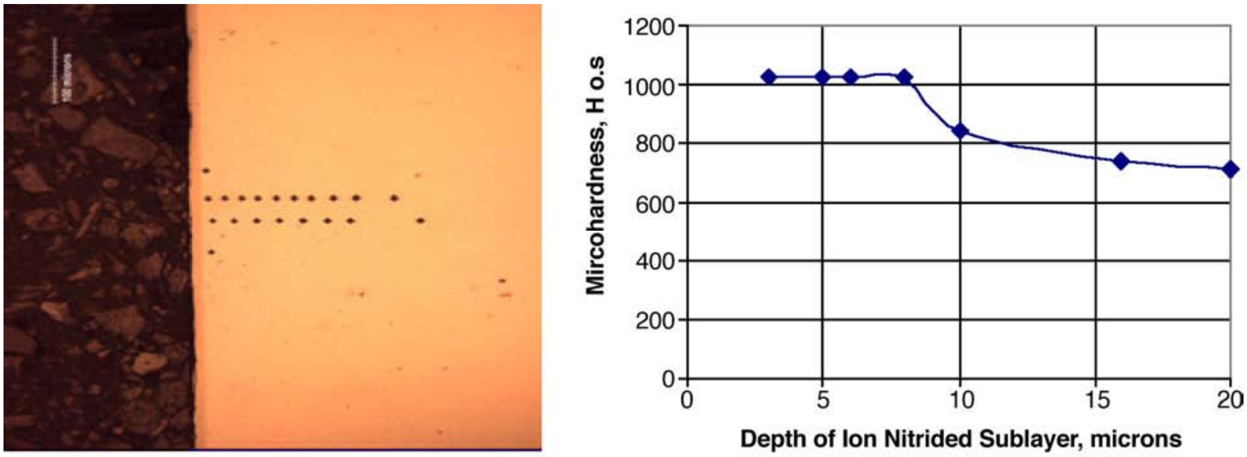

Figure 2-34
Microhardness indentations (left) and hardness profile (right) of the ion nitrided sublayer (0.5N load) in the duplex coating (TiAIN + ion nitriding)

2.2.6.2.2 Adhesion Scratch Tests

Sputtek conducted tests to determine the adhesion strength of the TiAlN coating according to ASTM C1624-05 specifications. This test is conducted by scratching the coating surface with a diamond-tipped stylus under gradually increasing loads. At a critical stress, the coating will start to crack. As the load is increased, the depth of the scratch increases, and the coating will start to spall. The load at which the first cracking appears is taken as an approximate indication of adhesion strength. An example of such a scratch is shown in Figure 2-35.

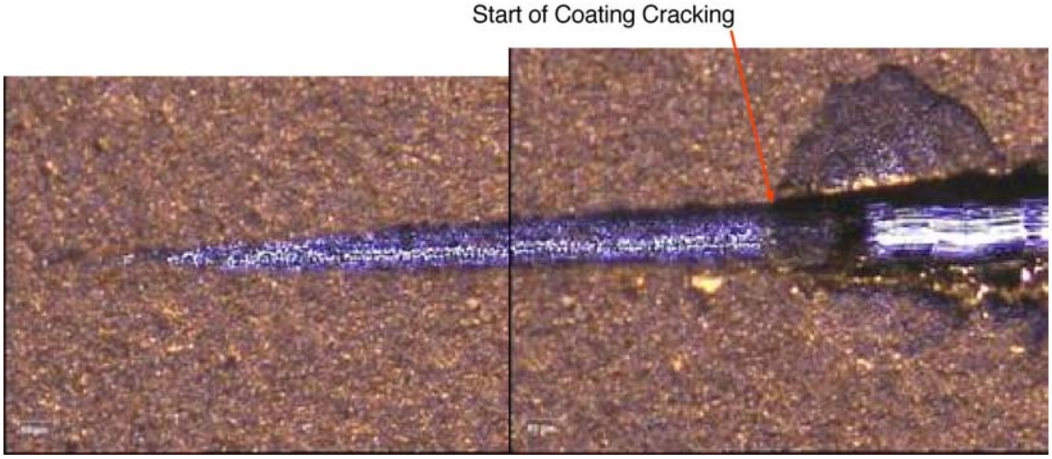

Figure 2-35
Adhesion scratch test of TiAlN coating on AM350 steel; coating thickness is 15 microns; average microhardness is 2720 HV50; critical load for coating crack is 60N.

These results indicate that the coating has good adhesion strength to the substrate alloy.

2.2.6.2.3 Sand Erosion Test Results

Sand erosion tests were performed by the Turbomachinery Erosion Laboratory at the University of Cincinnati. Test conditions used in these rainbow tests were reported as follows:

- Coating: TiAlN; abrasive: Al_2O_3; size: 50 micron grit; amount: 20 g (0.7 oz); temperature: 21^{o}C (70°F)
- Substrate: Ti alloy; particle velocity: 152 m/s (499 ft/s)

The test results are shown in Figure 2-36. These results show that the coating provides very good erosion protection at both low- and high-angle impingement conditions.

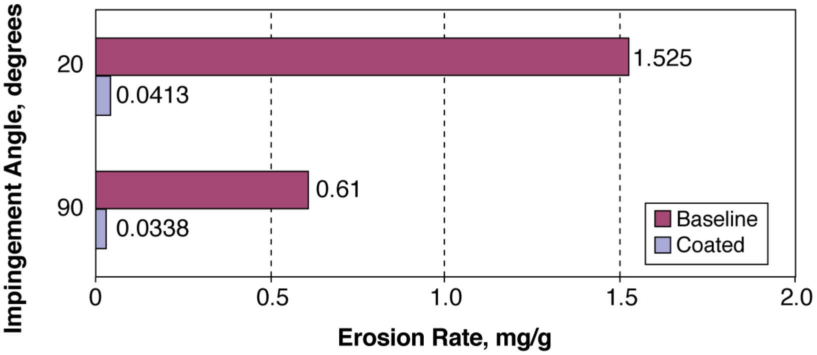

Figure 2-36
Sand erosion test results of TiAlN coating by the University of Cincinnati showing 37 times improvement at 20 degree impingement and 18 times improvement at 90 degree impingement

After a recent (2007) rainbow test conducted by one of the major gas turbine engine manufacturers, Sputtek reported that their TiAlN coating was one of the best performing coatings. The actual engine test conditions and results are provided below (see Figure 2-37).

Test conditions

Substrate: AM350 stainless steel

Duration: 180 min. at max. engine power + 60 min. at approximately 65% max. power

Abrasive: 120 micron sand

Total amount: 1.3 lbs. (590 g)

Ingestion rate: 0.08–0.4 lb./min (36–181 g/min)

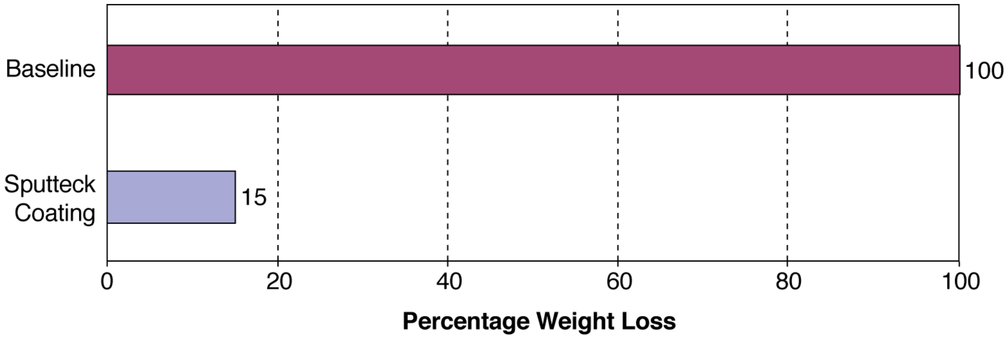

Figure 2-37
Results of rainbow tests on aeroengine compressor blades showing a factor of 7 times improvement in erosion resistance over uncoated substrate

Sputtek reported that they have large enough chambers to accommodate parts up to 22 in. (55.9 cm) long, but this size can be increased even further. They stated that they will be able to coat the Frame FA R0 blades or larger in their chambers without any problem.

2.2.7 American Surface Modification, LLC (AMS)

American Surface Modifications (AMS) is located in Houston, Texas. They provide corrosion- and erosion-resistant thick coatings by air plasma spray, HVOF, wire arc, and flame spray. Currently, they do not have CA-PVD or other vapor or sputter deposition processes. However, they can provide diffusion coatings (aluminides and borides).

Current coatings for erosion and/or corrosion resistance for commercial use are listed in Table 2-3.

Table 2-3
Coating chemistries, thickness, and temperature limits

Coating Type	Composition	Thickness Limits	Temperature, °F Limit
CrC-NiCr	75% Cr_2C_3+ 25% (80%Ni-20Cr)	0.020" (0.51 mm) max.	1800 (982°C)
WC-Co-Cr	88WC-12Co 90WC-10Co 86WC-10Co-4Cr	0.050" (1.27 mm) max	1200 (649°C)
Stellite 6	Co-28Cr-4W-1.2C-1Si	0.050" (1.27 mm)	1200 (649°C)
Tribaloy	T-400: Co-28Mo-8Cr-2Si T-800: Co-28Mo-17Cr-3Si	0.015" (0.38 mm)	1600 (871°C)
17-4PH Steel	Fe-16Cr-4Ni-3Cu-0.3Nb	0.250" (6.35 mm)	800 (427°C)
Ni-Cr	Ni-20Cr	0.100" (2.54 mm)	1800 (982°C)
Inco 713	Ni-14Cr-2(Nb+Ta)-1Ti-6Al-0.01B-0.1Zr-0.15C	0.100" (2.54 mm)	1650 (899°C)
Superalloys	Various, Inco 625, Inco 718	0.100" (2.54 mm)	1650 (899°C)
MCrAlY Coatings	Various: NiCoCrAlY CoNiCrAlY NiCrAlY High Cr, NiCrAlY CoCrAlY	0.050" (1.27 mm)	2200 (1204°C)
Diffusion coatings	NiAl and Al-Si type coatings	0.003" (0.076 mm) max	2000 (1093°C)

Due to the process used by ASM, the surface finish obtained is “rougher” than the other vapor phase deposition methods. Most carbides have a finish of less than 150 μin R_a, although an as-sprayed finish of less than 80 μin R_a can also be achieved.

ASM has supplied industrial gas turbine coatings since its beginning in February of 2006. To date, all coatings have been accepted by customers as meeting their expectations.

ASM has applied coatings to hot section blades and nozzles but has not applied erosion-resistant coatings to compressor blades on gas turbines.

2.2.8 Analytical Services and Materials

Analytical Services and Materials, Inc**., (AS&M)** is a small research and engineering firm specializing in advanced technologies. They have been providing services for over 20 years. They are based in Hampton, Virginia, near the NASA Langley Research Center, and in Edwards, California, close to the NASA Dryden Flight Research Center.

AS&M has a specialty coating division that has developed innovative nano-composite and sol-gel coatings, Aerocoat K and Wearcoat, to mitigate erosion, corrosion, cavitation, weathering, and wear. Earlier versions of the Aerocoat K coating were evaluated as part of a Small Business Industrial Research (SBIR) program for mitigating erosion on the V-22 Osprey impeller and were found promising in erosion testing at the University of Cincinnati wind tunnel with 9.5 micron silica particles at a particle velocity of 183 m/s (600 ft/s) [79, 80].

The Aerocoat K coating system is ambient curing, and it comprises an adhesion-enhancing epoxy based primer and an erosion-resistant nano-composite siloxane topcoat (see Figure 2-38 for a schematic of the coating architecture). Light abrasive treatment is recommended prior to application of the primer. The abrasive treatment can be grit blasting with 120 mesh alumina sand or scuffing with 120 grit abrasive sanding disc or emery cloth, followed by cleaning with dry air or solvent wash. The primer is applied by brush or high-pressure low-volume (HPLV) spraying to a thickness of 1–2 mils and then cured for 24 hours at room temperature or for 2 hours at 230°F (110°C). A minimum top coating thickness of 6–8 mils (150–200 microns) is recommended for most industrial applications. Higher thickness provides more protection and coatings of up to 40 mils have been deposited successfully. The topcoat is applied with an airless spray on the Aerocoat K primed surface. A mist coat of 1–3 mils thickness is applied, followed by curing for 3 hours around 70°F (21°C); The second overcoat of 4–6 mils and subsequent overcoats of 4–6 mils higher thicknesses are applied at 2-hour intervals. Curing of the coating is obtained in 1–3 days at room temperature, depending on the total coating thickness [81]. There are no limitations to the size of component that can be coated; the coating thickness and uniformity are checked with ultrasonic, eddy current, or magnetic probes, depending on the substrate material.

Particle erosion testing of the Aerocoat K coating with 100 micron (120 grit) alumina at 30 and 90 degrees is shown in Figure 2-39 comparing performance under these test conditions to several different materials. At 30 degrees a 20 times improvement is demonstrated for Aerocoat K compared to Ti 6-4. At 90 degrees a 13 times improvement is obtained under the same conditions. Given the larger particle size used in this testing, these results are considered significant relative to potential IGT applications where coating thickness and weight are as critical as they are in aero thin-section compressor blade applications. Although no results for water droplet erosion have been reported, the coating has been tested for cavitation resistance in accordance with ASTM G32. Figure 2-40 plots the performance of the Aerocoat K coating versus various substrate materials.

AS&M reports that they have coated several sets of IGT compressor blades with Aerocoat K and the components are now undergoing engine testing.

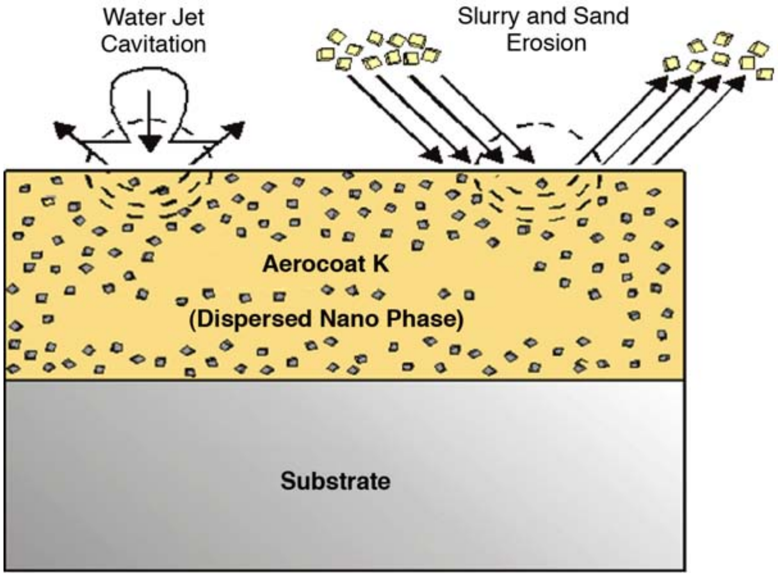

Figure 2-38
Aerocoat K coating has a tough nano-composite polymeric matrix, designed to absorb and dissipate the impact energy without tearing or debonding.

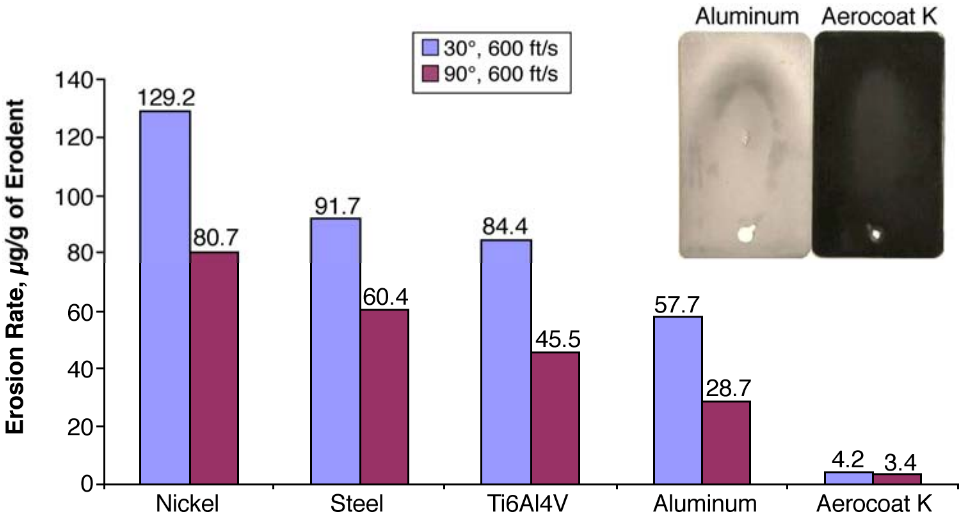

Figure 2-39
Erosion test results for AS&M's Aerocoat K polymeric coating with 120 grit alumina at 600 ft/s (183 m/s) in ASTM G 76 test

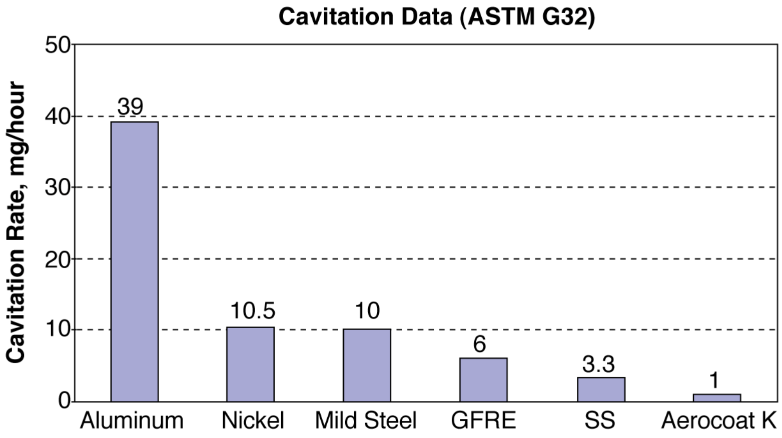

Figure 2-40
ASTM G 32 cavitation test results for Aerocoat K compared to various substrate materials. Testing was performed at 20 kHz, at 500 watts in de-ionized water with a pulsed cycle of 4 s on/1 s off for times ranging from 2–20 hours. [82]

2.2.9 Chromalloy Nevada

Currently, Chromalloy Nevada supplies various coatings for high-temperature oxidation and corrosion resistance. They use various application methods, such as pack coating, slurry, vapor phase, air plasma spray (APS), low-pressure plasma spray (LPPS), EB-PVD, and HVOF. However, for the erosion protection of steam turbine components, they are using chrome carbide and boride coatings. They have no erosion-resistant coatings currently targeted for gas turbine components.

3

LIQUID DROPLET EROSION TEST FACILITIES

3.1 Background

The main intended application of the erosion-resistant coatings is in large frame land-based gas turbine engines and steam turbines to mitigate both solid particle and liquid droplet erosion (SPE and LDE) during service. In addition to the SPE tests conducted routinely by the coating vendors and OEMs, it is essential to evaluate the coatings for LDE resistance. Such test systems, which will simulate the conditions in the gas turbine compressor inlets and steam turbine inlet and exhaust locations, are not readily available. Some of the OEMs have their own test systems to verify their component designs, but these systems are not readily available to outside organizations.

The cause of LDE is primarily water droplets—either from gas turbine fogging operation (land-based turbines), rain and marine environment for flight engines, or steam condensation in steam turbines. The droplet velocities could ranges from subsonic 200 m/s (656 ft/s) to supersonic velocities of 370 m/s (1214 ft/s) at Frame 7FA R0 compressor blades. The size of the water droplets varies depending on various conditions as described below.

Water droplet sizes (from Sherwood Pumps) [83] are usually expressed in microns (micrometers or µm). (One micron equals one thousandth of a millimeter.) A graphic illustration of relative water droplet sizes under various conditions is provided in Figure 3-1. Other than the effects of the specific material being sprayed, the four major factors in a mechanical spray system affecting droplet size are: a) nozzle tip style, b) capacity, c) spraying pressure, and d) spray pattern type. Lower spraying pressures provide larger droplet sizes, and higher spraying pressures yield smaller droplet sizes. The smallest droplet sizes are achieved by air atomizing tips. Generally speaking, the largest spray droplets are produced by wide-angle, flat, hydraulic spray tips. In the hydraulic spray tip series, the smallest droplet sizes are produced by hollow-cone spray tips.

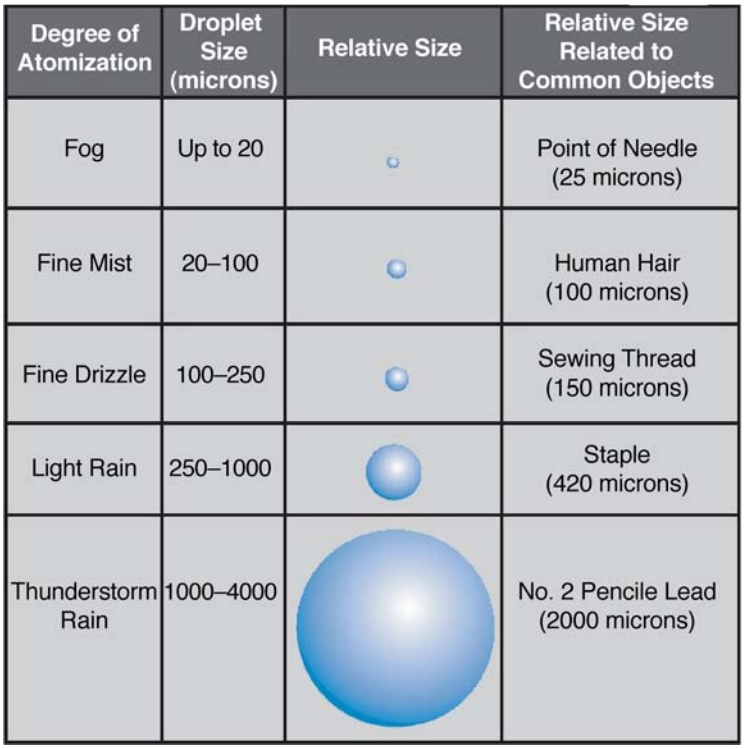

Degree of Atomization	Droplet Size (microns)	Relative Size	Relative Size Related to Common Objects
Fog	Up to 20	●	Point of Needle (25 microns)
Fine Mist	20–100	●	Human Hair (100 microns)
Fine Drizzle	100–250	●	Sewing Thread (150 microns)
Light Rain	250–1000	●	Staple (420 microns)
Thunderstorm Rain	1000–4000	●	No. 2 Pencile Lead (2000 microns)

Figure 3-1
Graphic of relative water droplet sizes [83]

There are several methods of conducting these erosion tests. The process for conducting SPE tests are somewhat standardized and specifications (such as ASTM G76 for SPE and ASTM G73 for LDE) are available. However, there are wide variations among the coating vendors, OEMs, test labs, and universities in the way that SPE tests are conducted. Erodent materials, angles of impingement, gas pressure, nozzles, velocity of particles, and so on vary among the test facilities. This makes direct comparisons of the results difficult.

For LDE tests, there are even more variations in the testing methods, depending on the final use of the data. Tests range from large drops simulating rain fall to small particles simulating fogging environment.

The following sections summarize the available information from an EPRI survey on the test facilities and methods available for liquid and solid particle erosion tests.

3.2 AFRL/UDRI Rain Erosion Testing

(Excerpted from the Air Force Research Laboratory, Materials and Manufacturing, *Rain Erosion Test Apparatus User Guide* [84])

> The phenomenon known as rain erosion, or the damage to materials caused by the impingement of raindrops at high speed, has long been a concern to the United States Air Force. The Air Force Research Laboratory (AFRL) at Wright-Patterson Air Force Base, Ohio, has conducted and sponsored research on rain erosion-resistant materials since 1947. In the course of rain erosion research over the years, the rotating arm apparatus has provided the best laboratory simulation of the environment for evaluating materials and investigating rain erosion mechanisms. Typically, in a rotating arm apparatus, test specimens are attached to the tip of a knife-edge propeller-like blade which is rotated horizontally at a specific velocity through a simulated rainfall. The results of rotating arm investigations have been correlated with actual flight test results, taking into consideration the relative ranking of the erosion resistance of materials and the mode of failure of these materials under the influence of raindrop impingement.
>
> The University of Dayton Research Institute (UDRI) has been involved in rain erosion research and erosion-resistant material development since 1964. UDRI participated in the design, development, construction, and calibration of the present Rain Erosion Test Apparatus. Over the years, UDRI has conducted more than 60,000 evaluations, representing practically all rain erosion-resistant aerospace systems developed over the last 40 years.
>
> The AFRL Rain Erosion Test Apparatus is capable of attaining constant velocities between 100 and 900 miles per hour, although current operations are limited to a maximum of 650 mph. The test specimens are exposed to a calibrated one inch per hour simulated rainfall. Raindrop impact is randomly distributed over the exposed surfaces of the test specimens. The test duration can be designated specific increments (i.e., seconds, minutes or hours) or terminated at the operator’s discretion when erosion damage is observed.

3.2.1 UDRI Rain Erosion Test Apparatus

The rotating arm apparatus consists of an 8 foot (2.4 m) diameter, double-arm blade designed to produce high tip velocities with zero lift and low drag coefficient. Duplicate test specimens are mounted at the leading edge tip sections of the double rotating arm. The specimens can be rotated at variable velocities between 100 and 650 mph (45 and 290 m/s). The double arm blade is mounted horizontally on a vertical drive shaft (see Figure 3-2). The simulated rainfall is produced by four curved manifold quadrants. Each manifold has 24 equally-spaced capillaries. De-ionized water is delivered to the four manifold quadrants simultaneously from a water storage tank. Temperature controlled water then fills the capillaries to produce raindrops. Drop size and drop rate are controlled by the water temperature, capillary orifice diameter, and head pressure of the water storage tank. Raindrops from the simulation apparatus impact the test specimens throughout their entire annular path. Drop size and drop rate are approximately 1.8–2.0 mm (71–79 mils) and 6 to 7 drops per second, respectively. Calibration of the water supply system is scheduled on a regular basis.

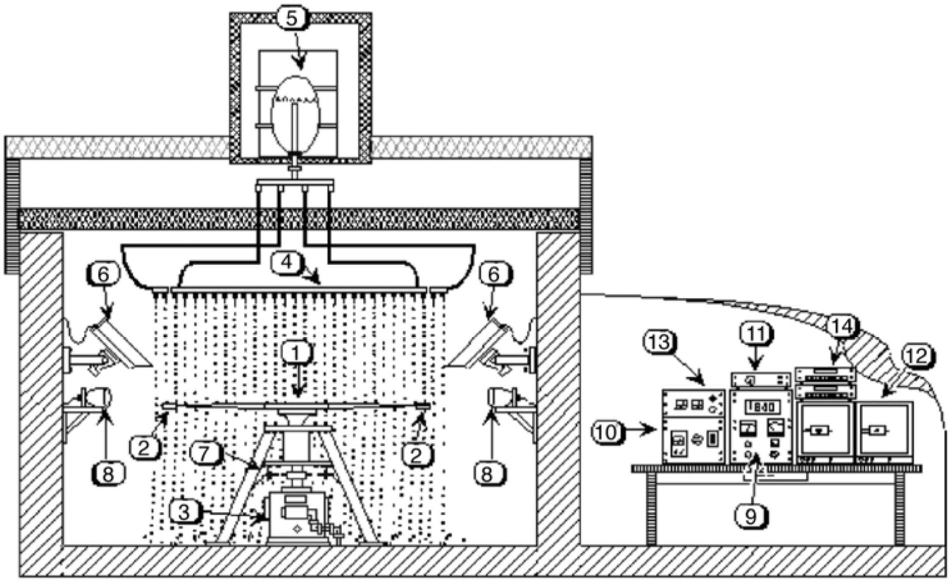

1. Double-Arm Blade
2. Mated Test Specimens
3. Verticle Drive Gearbox and Shaft
4. Curved-Manifold Quadrant
5. Water Storage Tank for Rain Simulation
6. Remote-Controlled Cameras
7. Magnetic Pickups for Firing Strobe Lights
8. High-Intensity Stobe Light for Stop-Motion Veiwing
9. Variable Speed Readout and Control
10. Strobe Control
11. Remote Color Camera Controls
12. Color Montitors for Specimen Viewing
13. Rain Simulation Control
14. VCRs for Videotaping Tests

Figure 3-2
AFRL/UDRI rain erosion test facility schematic [84]

All functions of the apparatus are controlled and monitored from the remote control room. Instantaneous velocity readout is monitored by an integrating digital voltmeter. Variable speed operation is possible through the operator’s manual control. Magnetic pickups and high intensity strobe lights provide stop motion viewing of the test specimens under actual test conditions. Closed-circuit television cameras and monitors allow the operator to visually observe the test specimens undergoing rain field exposure. Tests can also be videotaped for later study.

3.3 ALSTOM Materials LDE Test System

ALSTOM Materials has built up, over many years, comprehensive knowledge in the field of water droplet erosion (WDE) of materials and components. Located in Switzerland, their test facilities conduct comparative material tests on their self-developed WDE test rig. The materials' failure mechanisms and the behavior under erosive water droplet impacts are investigated using the test rig shown in Figure 3-3. The actual turbine blades are assembled on a rotor. Droplet characteristics include:

- Droplet impact speeds of 50–500 m/s (164–1641 ft/s)
- Droplet size is definable between 0.2 and 1.2 mm (7.9 and 47.2 mils).

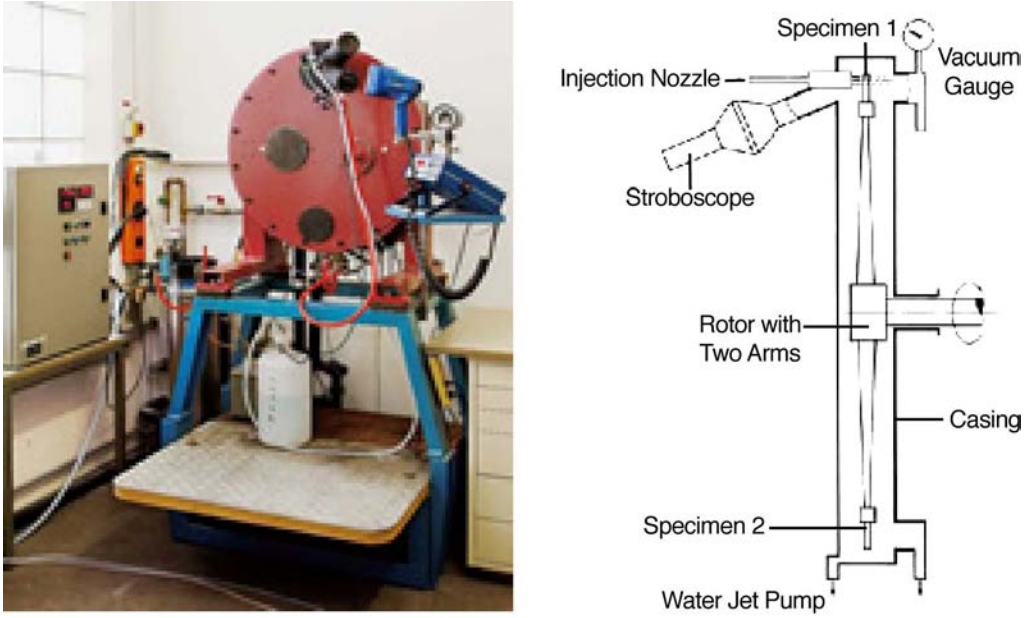

Figure 3-3
Water droplet erosion test rig at ALSTOM in Switzerland

3.4 Dynaflow, Inc., Test System

Dynaflow is located near the Baltimore suburb of Jessup, Maryland. They are a highly specialized research and development laboratory that provides testing analytical services in fluid mechanics, flow visualization, computational fluid mechanics, fluid-structure interactions, water jet testing, cavitation erosion testing, and water droplet erosion testing [85]. The test rigs are shown in Figure 3-4. They have rotating-disk liquid impact (water jet) test systems to conduct ASTM G-73 specification and similar tests with speeds up to 750 ft/s (229 m/s). They also conduct custom-designed experiments in water droplet erosion testing using high-pressure water pumps and specially designed nozzles to create the impact conditions desired. The speed of the water jet and droplets can be varied from subsonic (200 m/s [656 ft/s]) to supersonic speeds (> 700 m/s [> 2297 ft/s]) to represent conditions encountered in gas and steam turbines. They can test standard and nonstandard size specimens.

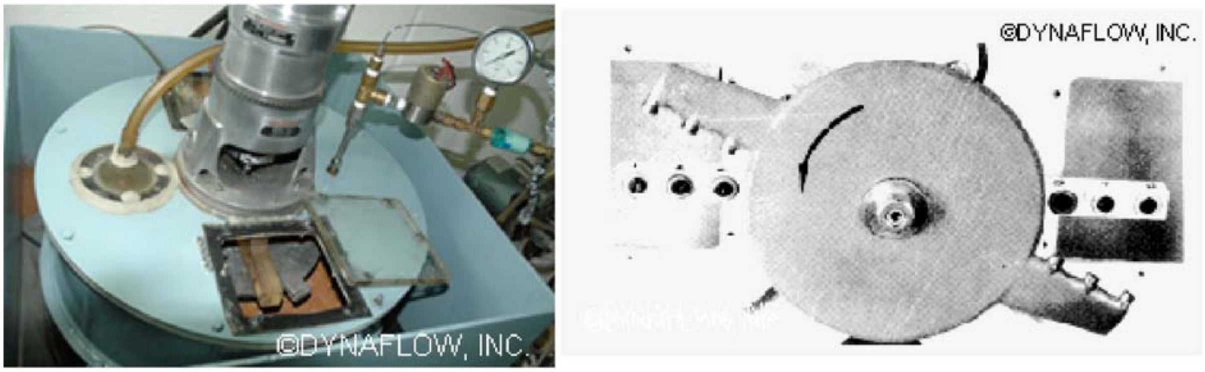

a) ASTM G-73 Test Rig at Dynaflow

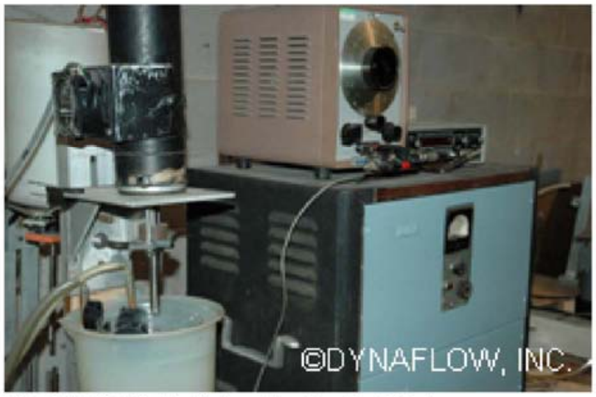

b) ASTM G-32 Cavitation Erosion Test System

Figure 3-4
Test systems used at Dynaflow for water droplet erosion and cavitation erosion testing

3.5 Skoda Turbine Blade Water Erosion Test Facility

Skoda is a major steam turbine manufacturer in Czechoslovakia. The turbine division of Skoda Concern Plzen has LDE test facilities. The following information was provided by Skoda for the EPRI survey [86]. They started experimental work on erosion testing on turbine blades in 1972. The equipment permits testing at high speeds. The test system is shown in Figure 3-5.

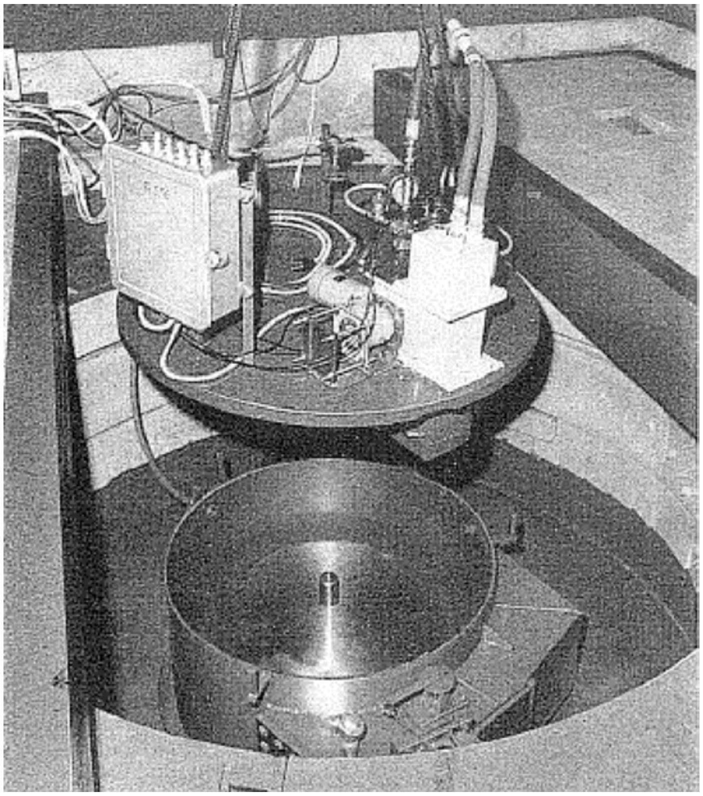

Figure 3-5
Erosion test stand at Skoda

Test specimens in the shape of circular discs 15 mm (0.59 in.) in diameter are secured to the circumference of a carrier disk or a constant strength. Two or four specimens at a time can be tested in this system. The test chamber is evacuated to a pressure of 1.5–3 kPa. The water jet runs through one or more nozzles at a speed of 15–17 m/s (49–56 ft/s). The volume of water entering the nozzles is excited by ultrasonic frequency of 16–40 kHz. This caused disintegration of the water jet into droplets ranging in diameter from 150 to 420 microns. Special shields and protection mechanisms are in place to protect the specimens from water jet impacts during startups and coast-down cycles.

Skoda ran tests up to 14,000 rpm, which correspond to tip velocity of 600 m/s (1969 ft/s). Their calculations of the droplet velocities in steam turbines range from 110 to 550 m/s (361 to 1805 ft/s) with the droplet diameters of 30–450 microns. Thus, the design conditions of the test system meet the actual simulation of the conditions encountered by steam turbine blades in operation.

4

SOLID PARTICLE EROSION TESTING

4.1 Overview of the Types of SPE Tests

A variety of test methods have been developed to characterize solid particle erosion (SPE) of materials. This section will highlight several of the methods referenced for characterization of the erosion performance of compressor materials and coatings. In all cases, a screening test is no substitute for field testing under actual turbine operating conditions. It is difficult to simulate engine conditions in laboratory testing. The goal of any of these screening tests is to have fidelity with the type of degradation observed in the field and to rank the relative erosion resistance of the materials and coatings consistent with that.

Among the key factors to take into consideration are the type of erodent (for example, alumina, silica, Arizona Road Dust), particle size range (10–200 microns or larger), particle velocity (30–215 m/s [98–705 ft/s] or higher), and angle of impingement (15–90 degrees). In reporting erosion test results, it is important for these parameters to be specified. The ASTM G76 test method for conducting solid particle erosion via gas jets is often referenced for erosion test studies. It was developed for erosion characterization of structural materials and is not completely suited for conducting studies of compressor blades or coatings. This has resulted in a number of different approaches being taken for testing these materials.

Initial screening of coatings is generally carried out with some form of a modified G76 test since it is the simplest to set up. Typically, researchers will modify the test conditions to be: 1) more representative of field conditions and 2) better at monitoring erosion of coatings that are in the 10–20 micron thickness range. Typical modifications are using silica instead of alumina, using higher particle velocities to better simulate turbine conditions, using a larger diameter nozzle to increase the area tested, and evaluating weight loss instead of volume loss.

Erosion results are influenced by the harness, friability, and angularity of the particles. Silica provides results that are closer to conditions in the field than alumina does; the appropriate particle size to use is often debated. The larger test area helps to screen for coating defects that might be present and to improve the resolution of the test. Erosion rates are usually defined as the number of grams of material or coating eroded per gram of erodent impacting the sample (mg/g) rather than a volume loss (mm^3/g) as specified in G76. For coatings, it is difficult to establish a reliable density to calculate volume loss from the weight loss.

A critical feature in all erosion testing is the use of a witness coupon for comparison of erosion results taken at different times. Often, the coupon will be the substrate material being coated (for example, Ti 6-4, IN 718, or 17-4 PH) rather than 1020 steel called for in G76. This also provides some measure of erosion performance (compared of the substrate) to guide coating development. It is difficult to make comparisons of coating data generated in different labs because there are often differences in the actual conduct of the test that lead to different erosion rates.

Two keys areas of variation are the actual particle velocity and geometry factors with the amount of erodent hitting the coupon. It is difficult to measure particle velocity accurately without specialized equipment (for example, a laser Doppler velocimeter). The double rotating disk method is cumbersome in actual practice. Often the particle velocity that is reported is an estimate based on an aerodynamic calculation of particle speed. The second factor is the amount of erodent actually hitting the sample. At low angles, this can be especially significant because the erosion “footprint” may be larger than the coupon being tested. When doing component testing, low-angle results need to be carefully evaluated. For example, if variations in setup result in even a small amount of the erosion stream impacting the blade’s leading edge (in a low-angle test of the airfoil), misleading weight loss results can be generated.

More sophisticated test methods with better instrumentation are used as part of a typical development path prior to an engine test. This often includes doing elevated temperature erosion testing of the coating. Gas turbine compressor temperatures range from ambient at the inlet to a compressor discharge temperature of 600°C + (1112°F +) in some cases. The greatest erosion loss is typically observed in the middle stages of the compressor where the particles have been concentrated toward the outer third of the airfoil, so conducting some tests at higher temperature seems justified.

4.2 ASTM G76, Standard Method for Conducting Erosion Tests by Solid Particle Impingement Using Gas Jets

This information is excerpted from ASTM G76-04 [87].

> This test method covers the determination of material loss by gas-entrained solid particle impingement erosion with jet nozzle type erosion equipment. This test method may be used in the laboratory to measure the solid particle erosion of different materials and has been used as a screening test for ranking solid particle erosion rates of materials in simulated service environments**.** Actual erosion service involves particle sizes, velocities, attack angles, environments, and so forth, that will vary over a wide range. Hence, any single laboratory test may not be sufficient to evaluate expected service performance. This test method describes one well characterized procedure for solid particle impingement erosion measurement for which inter-laboratory test results are available.

4.2.1 Apparatus

> The apparatus is capable of eroding material from a test specimen under well controlled exposure conditions. A schematic drawing of the exit nozzle and the particle-gas supply system is shown in Figure 4-1. A test system used at SwRI for SPE testing is shown in Figure 4-2. Deviations from this design are permitted; however, adequate system characterization and control of critical parameters are required. Deviations in nozzle design and dimensions must be documented. Nozzle length to diameter ratio should be

25:1 or greater in order to achieve an acceptable particle velocity distribution in the stream. The recommended nozzle consists of a tube about 1.5 mm (0.060 inch) inner diameter, 50 mm long, manufactured from an erosion-resistant material such as WC, A12O3, and so forth. Erosion of the nozzle during service shall be monitored and shall not exceed 10 % increase in the initial diameter.

Necessary features of the apparatus shall include a means of controlling and adjusting the particle impact velocity, particle flux, and the specimen location and orientation relative to the impinging stream.

Various means can be provided for introducing particles into the gas stream, including a vibrator-controlled hopper or a screw-feed system. It is required that the system provide a uniform particle feed and that it be adjustable to accommodate desired particle flow values.

A method to measure the particle velocity shall be available for use with the erosion equipment. Examples of accepted methods are high-speed photography, rotating double-disk, and laser velocimeter. Particle velocity shall be measured at the location to be occupied by the specimen and under the conditions of the test.

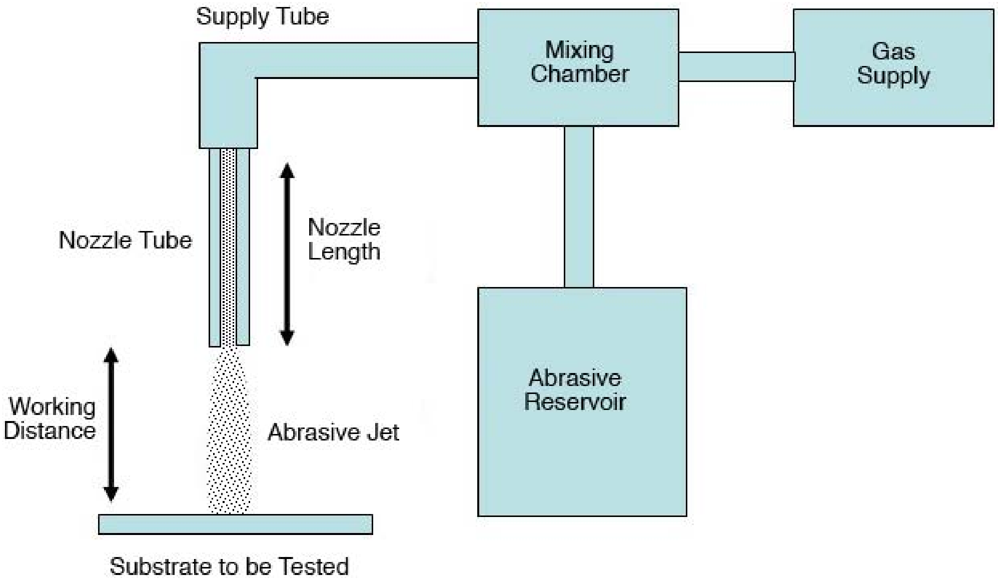

Figure 4-1
ASTM G76 solid particle erosion test rig schematic

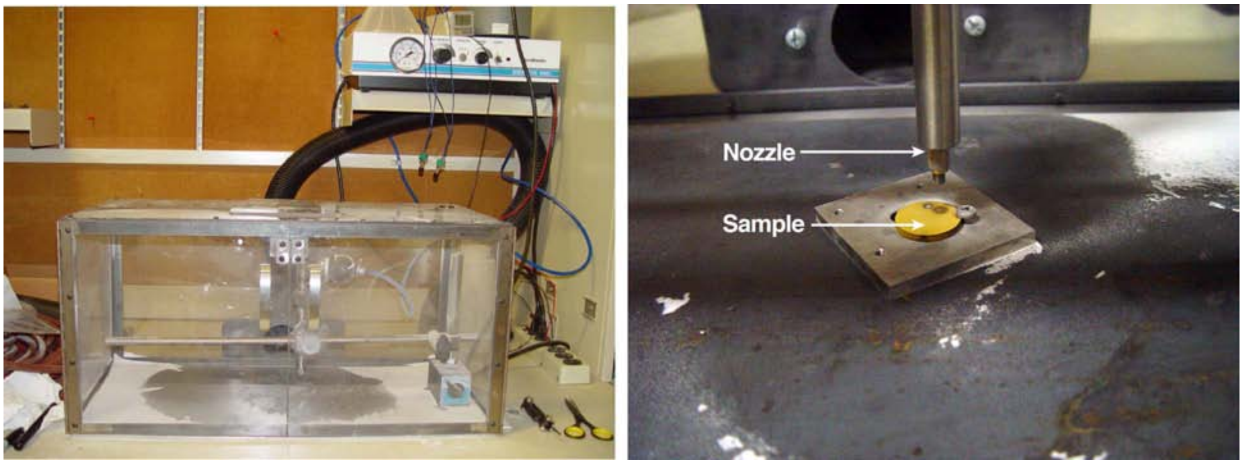

Figure 4-2
ASTM A76 solid particle erosion test rig at SwRI. Photo at right shows a coated disc sample and the nozzle aimed at 90 degree impact angle

4.2.2 Test Materials and Sampling

This test method can be used over a range of specimen sizes and configurations. One convenient specimen configuration is a rectangular strip approximately 10 by 30 by 2 mm thick. Larger specimens and other shapes can be used where necessary, but must be documented.

The abrasive material to be used shall be uniform in essential characteristics such as particle size, moisture, chemical composition, and so forth.

Sampling of material for the purpose of obtaining representative test specimens shall be done in accordance with acceptable statistical practice. Practice E 122 shall be consulted.

4.2.3 Calibration of Apparatus

Specimens fabricated from Type 1020 steel equivalent to that used in the interlaboratory test series shall be tested periodically using specified 50 µm A12O3 particles to verify the satisfactory performance of the apparatus. It is recommended that performance be verified using this reference material every 50 tests during a measurement series, and also at the beginning of each new test series whenever the apparatus has been idle for some time. The recommended composition, heat treatment, and hardness range for this steel are listed in the specification. The use of a steel of different composition may lead to different erosion results. A photomicrograph of the specified A12O3 particles is shown in the specifications.

Calibration at standard test conditions is recommended even if the apparatus is operated at other test conditions.

In any test program the particle velocity and particle feed rate shall be measured at frequent intervals, typically every ten tests, to ensure constancy of conditions.

4.2.4 Standard Test Conditions

This test method defines the following standard conditions.

The nozzle tube shall be 1.5 mm +/- 0.075 mm inner diameter at least 50 mm long.

The test gas shall be dry air, −50°C dew point or lower.

The abrasive particles shall be nominal 50 µm angular A12O3, equivalent to those used in the interlaboratory test series (see Fig. 3). Abrasive shall be used only once.

The abrasive particle velocity shall be 30 +/- 2 m·s−1, measured at the specimen location. At this velocity the gas flow rate will be approximately 8 L·min−1 and the system pressure will be approximately 140 kPa (20 psig) although the pressure will depend on the specific system design.

The test time shall be 10 min to achieve steady state conditions. Longer times are permissible so long as the final erosion crater is no deeper than 1 mm.

The angle between the nozzle axis and the specimen surface shall be 90 +/- 2°.

The test temperature shall be the normal ambient value (typically between 18°C to 28°C).

The particle feed rate shall be 2.0 +/- 0.5 g·min−1. This corresponds to a particle flux at the specimen surface of about 2 mg·mm−2·s−1 under standard conditions. Particle flux determination requires measurement of the eroded area on the specimen and is subject to considerable error. A measured width and depth profile of an erosion crater produced using stated conditions is shown in Fig. 4 and indicates a typical eroded width/depth relation.

The distance from specimen surface to nozzle end shall be 10 +/- 1 mm.

4.2.5 Optional Test Conditions and Test Procedure

When test conditions or materials other than those given in the specifications are used, reference to this test method shall clearly specify all test conditions and materials. It should be noted that other conditions, for example, larger particle velocities, may adversely affect measurement precision.

Establish and measure the particle velocity and particle flow specified. Adjust equipment controls to obtain proper velocity and flow conditions before inserting test specimens. Particle flow rate values are determined by collecting and subsequently weighing the abrasive exiting from the nozzle for a measured time period.

Prepare the specimen surface if required to achieve uniformity and adequate finish. Grinding through a series of abrasive papers to 400 grit is usually adequate so long as all surface scale is removed. A surface roughness of 1 µm (40 µin.) rms or smaller is recommended. Clean the specimen surface carefully.9 Weigh on an analytical balance to +/- 0.01 mg.

Mount the specimen in proper location and orientation in the apparatus. Subject the specimen to particle impingement for a selected time interval, measured to an accuracy of 5 s. Remove the specimen, clean carefully,9 reweigh and calculate the mass loss.

Repeat this process to determine at least four points for a total time of at least 10 min and plot those values as mass loss versus elapsed time. Suitable times would be 2, 4, 8, and 16 min for a material such as Type 1020 steel. Steady state erosion should result after 1 to 2 min, depending on the material. Two examples of measured erosion versus time curves are shown in Fig. 5.

The steady state erosion rate (see Terminology G 40) is determined from the slope of the mass loss versus time plot. The average erosion value is calculated by dividing erosion rate (mg·min−1) by the abrasive flow rate (g·min−1) and then dividing by the specimen density (g·cm−3). Report the average erosion value as (mm3·g−1).

4.3 SPE Test Facilities

4.3.1 Metcut Research, Inc.

Metcut Research, Inc., based in Cincinnati, Ohio, is one of the leading independent materials engineering and testing laboratories. They offer expertise and laboratory facilities in the broad field of materials evaluation, including both metallic and nonmetallic structural materials. Their metallurgical laboratory focuses on metallurgical evaluation, failure analysis, quality assurance of materials, and thermal spray coatings. They perform a wide variety of tests that measure the static and dynamic mechanical properties of specimens, components, and assemblies. Metcut has been utilized for ASTM G76 and other customer-specification-based particle erosion tests of compressor blade alloys and coatings. They have established in-house modifications to the G76 standard based on their testing experience. They are also relied upon for component fatigue testing of coated and uncoated compressor blades.

4.3.2 University of Dayton Research Institute Facility

Following is a description excerpted from the University of Dayton Research Institute (UDRI) Facility User Guide [88].

Apparatus Description

Dust particles are accelerated in a small diameter (approximately 0.25-inch) high-speed gas jet and directed onto a test specimen. Since the diameter of the dust jet is smaller than the test specimen area, the specimen holder and jet are articulated so that the test specimen is moved through the dust jet in a uniform manner. This articulation provides a uniform particle loading (dust mass intercepted per unit surface area) over a square area of approximately 316 cm2 (i.e., 7.0-inch square). The test chamber containing the nozzle and articulating stage is shown in Figure 4-3.

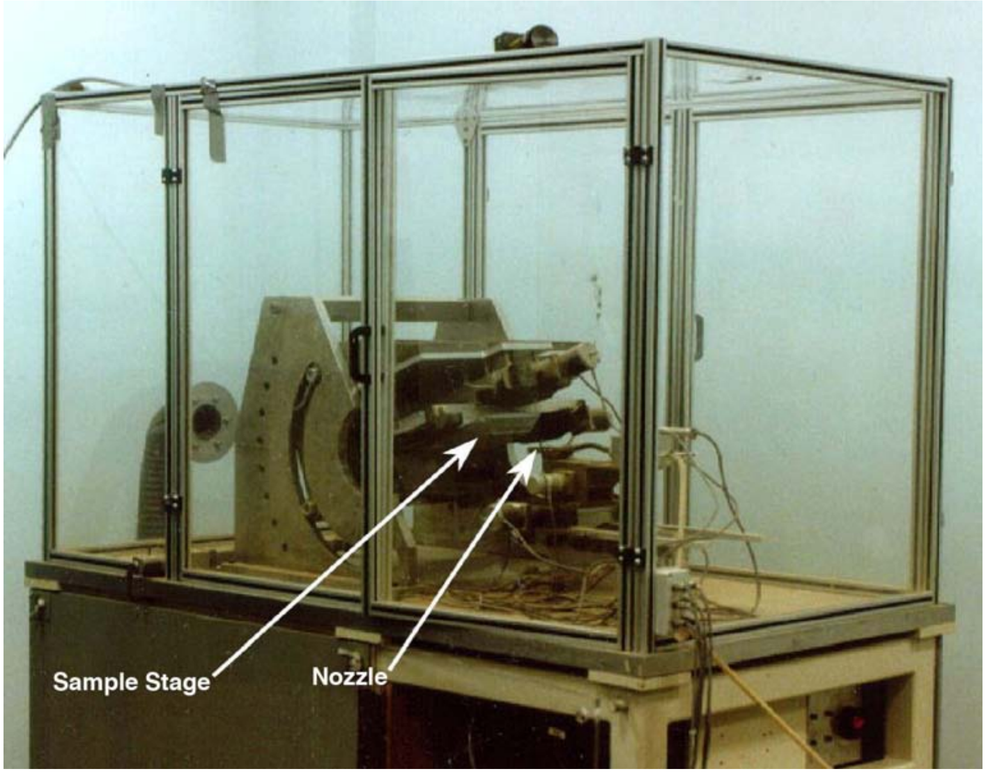

Figure 4-3
UDRI particle erosion rig (From UDRI Facility Description) [88]

Compressed air provides the transport gas stream with regulators and pressure transducers to measure and control the pressure at the nozzle inlet. Dust particles are metered into the transport gas stream from a pressurized screw feeder system. Since the screw feeder provides a very accurate and uniform dust flow, the particle mass applied to the specimen is determined by the run time based on prior calibration of the screw feeder. Consistent flow rates as low as 0.3 g/min can be achieved with this system.

Dust velocity is determined as a function of the nozzle inlet pressure and the particle size by prior calibration. Thus, for a given test with a specified particle size, a specific test velocity can be selected from this velocity versus pressure calibration. Particle size, velocity and impact angle can be controlled independently. This provides an excellent capability to parametrically evaluate the response of critical materials and coatings to solid particle impact effects. Materials from such components as leading edges, windscreens, radomes, paints, and any special coatings can be evaluated in a well-controlled laboratory environment under realistic particle impact conditions.

Test Conditions

A “Test Condition” consists of four independently variable parameters that define the exposure environment for the sample. These parameters are:

1. Particle Size – Standard particles consist of dry silica dust that have been sieved to ~ ten narrowly defined size ranges from less than 38 microns to greater than 250 microns. Particle sizes are uniformly distributed within each of these ranges. Combinations of these ranges may also be used to create a custom range and particle distribution.

2. Velocity – Mean particle stream velocity can be specified at any value in the range 30 m/s to 330 m/s. Mean velocity is determined by sampling the velocity at 20 points across the stream.

3. Impact Angle – Impact angle can be specified at any value in the range 90 degrees (normal incidence) to 20 degrees, as measured from a line lying within the plane of the sample. See Figure 4-4.

4. Mass Loading – The mass of impinging particles, given in g/cm2 of sample area, can be specified to almost any value. Small mass loading results in short exposure duration, while larger mass loading simply requires a longer exposure time. Typical values of mass loading vary widely and are in the range 0.0001 g/cm2 (extremely light) to 1.0 g/cm2 (extremely heavy). Mass loading can also be specified in increments, with damage evaluation conducted between each increment A Test Condition consists of these four parameters specified for each sample to be tested. Note that for a specific Test Condition, mass loading may be specified in increments, with evaluations (mass loss, IR transmission, etc.) conducted between each increment.

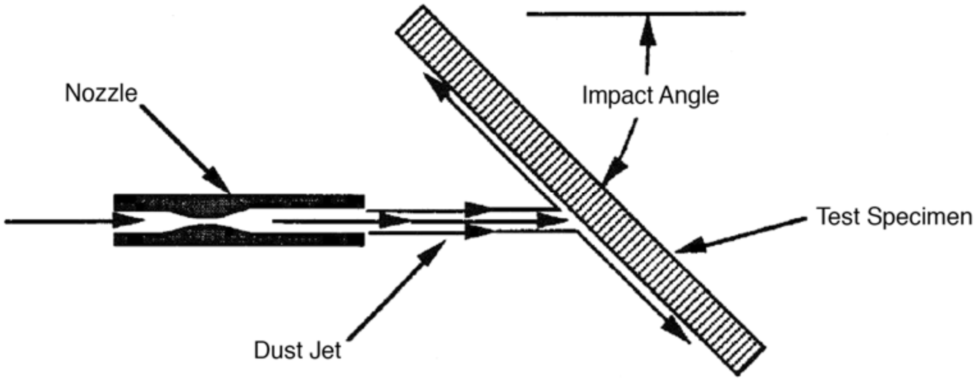

Figure 4-4
Schematic of gas jet particle erosion test showing particle impact angle (From UDRI Facility Description)

4.3.3 University of Cincinnati Erosion Facility Description

The University of Cincinnati's (UC's) high-temperature erosion tunnel rig simulates particle surface interactions at operating conditions in compressors and turbines

- Temperatures (ambient–2000°F)
- Impact velocities 60–1800 ft/sec (18–550 m/s)
- Impingement angles (0–90 degrees)
- Particles and target materials (various)
- Particle loading (various)

The UC erosion wind tunnel facility is shown schematically in Figure 4-5. Abrasive particles of a given constituency and measured weight are placed into the particle feeder. The particles are fed into a secondary air source and blown into the particle preheater and then to the injector, where they mix with the primary air supply, which is heated by the combustor. The particles are then accelerated via high velocity air in a constant-area steam-cooled duct, and they impact the specimen in the test section. The particulate flow is then mixed with coolant and directed to the exhaust tank.

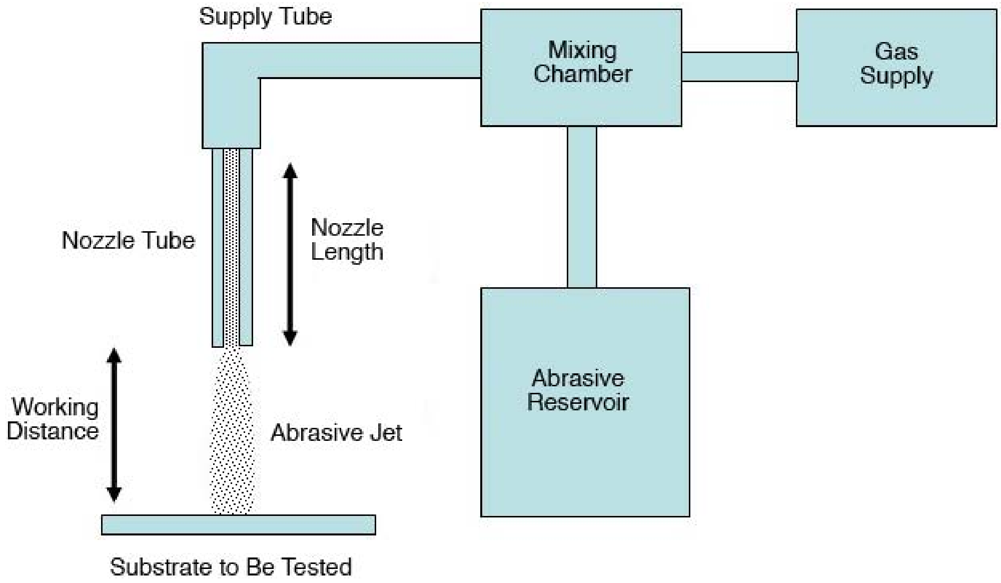

Figure 4-5
University of Cincinnati high-velocity erosion test facility schematic

Varying the tunnel airflow controls particle velocity; the particle impingement angle is controlled through the target sample rotation relative to the airflow. Heating the flow stream, which, in turn, heats the erosive media and sample(s), varies the temperature. As can be seen from Figure 4-5, the tunnel geometry is uninterrupted from the acceleration tunnel throughout the test section in order to preserve the aerodynamics of the flow passing over the sample(s) [90].

4.3.4 National Research Council of Canada SPE Test Facility

The National Research Council (NRC) of Canada, located in Ottawa, Canada has SPE test facilities and has extensive experience in conducting such tests.

ASTM G76-02, Standard Test Method for Conducting Erosion Tests by Solid Particle Impingement Using Gas Jets, is used as the reference for the erosion test. The test conditions recommended by this ASTM specification are shown in Table 4-1. An S. S. White Industrial Airbrasive unit shown in Figure 4-6 is used to perform the erosion tests. The velocity of abrasive particles is controlled by adjusting the pressure of the carrier gas, and the particle flux (feed rate) is controlled by changing the amplitude of the vibrating hopper. A silicon carbide nozzle with an inner diameter of 1.14 mm (0.045 inch) is used for particle injection. During testing, the coupon to nozzle tip distance is maintained constant at 38 ± 1 mm (1.5 ± 0.04 inch).

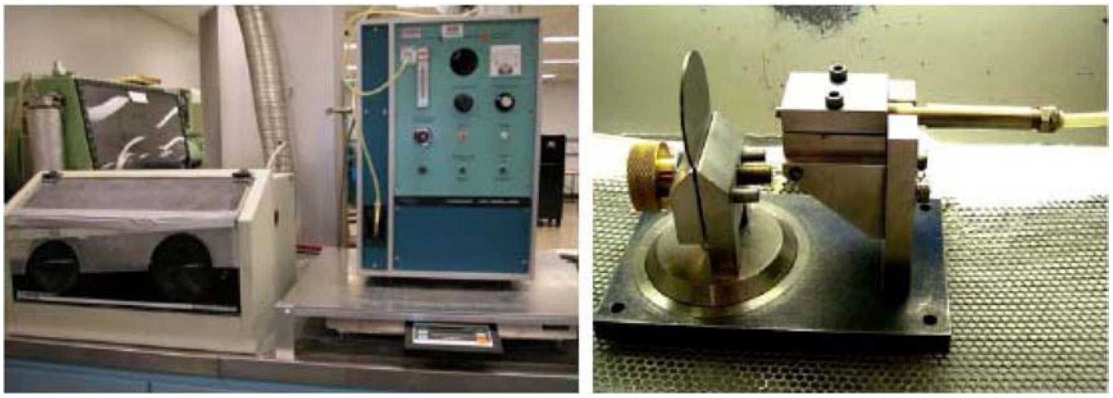

Figure 4-6
S.S. White Industrial Airbrasive unit for erosion tests at NRC Canada

Details of the test conditions used are listed below:

- Impingement angle: 90°
- Erodent: angular Al_2O_3 powders with an average particle size of 50 μm
- Particle velocity: 84 m/s (275 ft/s)
- Particle feed rate: 0.7 ± 0.1 g/min

- Distance between test coupon and nozzle tip: 38 ± 1 mm
- Carrier gas: argon
- Test temperature: room temperature

A Sartorius R160P precision balance is used to measure the weight loss of the tested coupons. Accuracy of the measurement was ± 0.01 mg for weights less than 30 g, ± 0.02 mg for weights in the range of 30–80 g, and ± 0.05 mg for weights in the range of 80–162 g. Before erosion testing, the balance was externally calibrated using a Troemner ultra class 100 g calibration weight block (99.99989 g) traceable to NIST.

Table 4-1
ASTM G76 particle erosion standard test conditions

Erosion Test Key Variables	ASTM G76-04 Standard Parameters
Standard Test Conditions	
Nozzle ID	1.5 ± 0.075 mm (0.059 ± 0.003 inch)
Test gas	Dry air - 50°C dew point or lower
Abrasive particles	50 micron angular alumina
Particle velocity	30 ± 2 m/s
Gas flow	~ 8 L/min
System pressure	140 kPa (20 psig)
Test time	10 min or longer – erosion scar less than 1 mm depth
Test angle	90 ± 2 degrees
Test temperature	18–28 C
Particle feedrate	2.0 ± 0.5 g/min
Particle flux	~ 2 mg/mm^2 - sec
Nozzle to specimen distance	10 ± 1 mm
Sample weight loss	Record ± 0.01 mg
Erosion rate	mm^3/g of alumina based on wt. loss/material density

5
REFERENCES

---

1. *Turbine Steam Path Damage: Theory and Practice, Volume 2 – Damage Mechanisms.* EPRI, Palo Alto, CA: 1999. TR-108943-V2.
2. V. P. Swaminathan, "Investigation of High-Pressure Compressor Blade Failures in LM6000 Sprint Engines," Unpublished results presented at the Western Turbine Users and Combustion Turbine Operators Task Force Conferences (March 2004 and August 2006).
3. V. P. Swaminathan, "Development of Erosion-Resistant Nano-Technology Coatings for Steam and Gas Turbines," EPRI Project update presented at the EPRI Sponsor Meeting, Charlotte, NC, 2007.
4. W. Tabakoff, "Investigation of Coatings at High Temperature for Use in Turbomachinery," *Surface and Coatings Technology*, Volume 39/40, pp. 97–115 (1989).
5. J. Y. DeMasi-Marcin and D. K. Gupta, "Protective Coatings in the Gas Turbine Engine," *Surface and Coatings Technology*, Volume 68/69, pp. 1–9 (1994).
6. I. G. Wright, "Is there any reason to continue research efforts in erosion-corrosion?" *Proceedings of the John Stringer Symposium on High Temperature Corrosion*, ASM International, 2001.
7. I. Finnie, "Some Reflections on the Past and Future of Erosion." *Wear*, Vol. 186–187, pp. 1–10 (1989).
8. S. J. Matthews, *Erosion-Corrosion of Cr3C2-NiCr High Velocity Thermal Spray Coatings.* PhD thesis, The University of Auckland, 2004.
9. G. D'Alessio and D. Nagy; "Performance of Erosion Resistant Coatings for Compressor Airfoils," *Journal of the Canadian Ceramic Society*, Vol. 63, No. 1, pp. 59–63 (February 1994).
10. S. S. Balasubramaniyam, *Computational Modeling of Brittle Impact Erosion Mechanism*. MS Thesis, West Virginia University, December 1998.
11. A. Sue and H. Troue, U.S. Patent 5,185,211, "Non-Stoichiometric Titanium Nitride Coating," Issued Feb. 9, 1993.
12. J. Liburdi, D. Nagy, and V. Parameswaran, "Erosion Resistant Titanium Nitride Coating for Turbine Compressor Applications," Paper No. 92-GT-417, presented at the ASME IGTI Gas Turbine Conference, Cologne, Germany (June 1992).
13. F. J. Heyman, "Liquid Impingement Erosion," in *ASM Handbook Volume 18, Friction, Lubrication and Wear Technology.* ASM International, Metals Park, OH 1992.

14. J. H. Brunton and M. C. Rochester, “Erosion of Solid Surfaces by the Impact of Liquid Drops,” in *Treatise on Materials Science and Technology, Volume 16, Erosion,* Ed. Carolyn M. Preece, Academic Press, 1979, pp.186-248.
15. M. K. Lee, W. W. Kim, C. K. Rhee, and W. J. Lee, “Liquid Impact Erosion Mechanisms and Theoretical Impact Stress Analysis in TiN-Coated Steam Turbine Blades,” *Metallurgical and Materials Transactions A.* Vol. 30A, pp. 961–968 (1999).
16. R. Bunshah. *Deposition Technologies for Films and Coatings.* Noyes Publications, Park Ridge, NJ 1982, pp. 1–18.
17. D. Mattox. *The Foundations of Vacuum Coating Technology.* Noyes Publications/William Andrews Publishing, Norwich, NY 2003.
18. R. Bunshah, “Evaporation,” in *Deposition Technologies for Films and Coatings.* Noyes Publications, Park Ridge, NJ 1982, pp. 83–169.
19. Liburdi Engineering Presentation, “Erosion Solutions for Industrial Turbine Engines,” January 2007.
20. Not used.
21. D. Mattox, “Ion Plating Technology,” in *Deposition Technologies for Films and Coatings.* Noyes Publications, Park Ridge, NJ 1982, pp. 244–287.
22. P. Lowden, D. Nagy, S. Holliday, and A. Aguero, “Development of Erosion Resistant Coatings for Compressor Application,” *Canadian Aeronautics and Space Journal.* Vol. 36, p. 24 (1990).
23. V. Parameswaran, J. Immarigeon, and D. Nagy; “Titanium Nitride Coating for Aero Engine Compressor Gas Path Components,” *Surface Coatings and Technology*. Vol. 52, pp. 251–260 (1992).
24. D. Nagy, V. Parameswaran, J. MacLeod, and J. Immarigeon; “Protective Coatings for Compressor Gas Path Components,” *NATO Advisory Group for Aerospace R&D* (*AGARD) Conference Proceedings,* AGARD-CP-558, 1994, pp. 27-1–27-10.
25. Not used.
26. B. Rother, “Cathodic Arc Evaporation as a Coating Technique,” *Surface Engineering*, Vol. 4, No. 4 (1988).
27. A. Snapper, U.S. Patent 3,625,848, “Arc Deposition Process and Apparatus,” Issued December 7, 1971.
28. L. Sablev, U.S. Patent 3,793,179, “Apparatus for Metal Evaporation Coatings,” Issued February 19, 1974.
29. I. Brown, “Cathodic Arc Deposition of Films,” *Annual Review of Materials Science*. Vol. 28, pp. 243–69 (1998).
30. J. A. Sue and H. Troue, U.S. Patent 5,071,693, “Multilayer Coating of a Nitride Containing Compound and Method for Producing It,” Issued December 10, 1991.
31. Eifeler Von Ardenne, Alpha 900T CA-PVD System Brochure.

32. A. Rogozin and R. Fontana, "Reactive Gas Control of the Arc," *IEEE Transactions on Plasma Science*. Volume 25**,** pp. 680–684 (1997).

33. A. Sue and H. Troue, U.S. Patent 4,929,322, "Apparatus and Process for Arc Vapor Depositing a Coating in an Evacuated Chamber," Issued May 29, 1990.

34. G. Vergason, U.S. Patent 5,037,522, "Electric Arc Vapor Deposition Device," Issued August 6, 1991.

35. R. Welty, U.S. Patent 5,269,898, "Apparatus and Method for Coating a Substrate Using Vacuum Arc Evaporation," December 14, 1993.

36. P. Holubar and T. Cselle, **"**Driving Forces Of Today's Manufacturing Technology" presented at the Third International Conference for Milling, VUT, Brno, Czech Republic (2003).

37. I. Brown, "Cathodic Arc Deposition of Films," *Annual Review of Materials Science,* Vol. 28, pp. 243–69 (1998).

38. J. DeMasi-Marcin and D. Gupta, "Protective Coatings in Gas Turbine Engines," *Surface Coatings and Technology*. Vol. 68/69, pp. 1–9 (1994).

39. Not used.

40. R. Wei, E. Langa, C. Rincon, and J. Arps, "Solid Particle Erosion Protection of Turbine Blades with Thick Nitrides and Carbonitride Coatings from Magnetron Sputter Deposition," presented at the ASM International Surface Engineering Conference (ISEC), Seattle, WA (May 2006).

41. V. P. Swaminathan, R. Wei, and D. Gandy, "Erosion Resistant Nanotechnology Coatings for Gas Turbine Applications," Paper No. GT2007-27027, presented at the ASME Turbo Expo 2007, Montreal, Canada (May 2007).

42. J. Thornton, "Coating Deposition by Sputtering," in *Deposition Technologies for Films and Coatings.* Noyes Publications, Park Ridge, NJ 1982, pp. 170–243.

43. D. Mattox, "Growth and Growth-Related Properties of Films Formed by Physical Vapor Deposition," *ASM Metals Handbook, Tenth Edition, Vol. 5* (2002).

44. B. Movchan and A. Demschishin, *Phys. Met. Metallogr.* Vol. 28, p. 83 (1969).

45. J. Thornton, *Journal of Vacuum Technology*. Vol. 11, p. 666 (1974).

46. R. Messier, A. Giri, and R. Roy, "Revised Structure Zone Model for Thin Film Physical Structure," *Journal of Vacuum Science and Technology A.* Vol. 2, No. 2, pp. 500–503 (Apr–June 1984).

47. U. Schulz, K. Fritscher, C. Levens, M. Peters, and W. A. Kaysser, "The Thermocyclic Behavior of Differently Stabilized and Structured EB-PVD TBCs," *Journal of the Minerals, Metals, and Materials Society.* Vol. 49, No. 10 (October 1997).

48. A. Sue and H. Troue, U.S. Patent 5,185,211; "Non-Stoichiometric Titanium Nitride Coating," Issued February 9, 1993.

49. D. Gupta and M. Freiling, U.S. Patent 4,904,528, "Coated Gas Turbine Compressor Components," Issued February 27, 1990.

50. P. LeClair, “Titanium Nitride Thin Films by the Electron Shower Process.” MS Thesis, Massachusetts Institute of Technology, 1998.
51. T. B. Massalski, ed., *Binary Alloy Phase Diagrams, Vol. 3.* ASM International, Materials Park, OH 1990, pp. 2705–2707.
52. R. Tollett, “RIC Tin Coatings for Compressor Life Extension of Hardware in Erosive Environments,” Liburdi Engineering Limited, Internal Report. May 5, 2006.
53. Liburdi Engineering Presentation, “Erosion Solutions for Industrial Turbine Engines,” January 2007.
54. P. Lowden, D. Nagy, S. Holiday, and A. Aguero, “Development of Erosion Resistant Coatings for Compressor Airfoils,” *Canadian Aeronautics and Space Journal*. Vol. 36, p. 24 (1990).
55. J. Liburdi, D. Nagy, and V. Parameswaran, “ Erosion Resistant Titanium Nitride Coating for Turbine Compressor Applications” Paper No. 92-GT-417, presented at the ASME IGTI Gas Turbine Conference, Cologne, Germany (June 1992).
56. V. Parameswaran, J. Immarigeon, and D. Nagy, “Titanium Nitride Coating for Aero Engine Compressor Gas Path Components,” *Surface Coatings and Technology.* Vol. 52, pp. 251–260 (1992).
57. G. D’Alessio and D. Nagy, “Performance of Erosion Resistant Coatings for Compressor Airfoils,” *Journal of the Canadian Ceramic Society*. Vol. 63, No. 1, pp. 59–63 (February 1994).
58. Not used.
59. Praxair’s Response (from Albert Feuerstein) to EPRI Coating Vendor Survey, January 2007.
60. J. A. Sue and R. C. Tucker Jr., “High Temperature Erosion Behaviour Tungsten and Chromium Carbide Based Coatings,” *Surface and Coatings Technology.* Vol. 32, pp. 237–248 (1987).
61. R. Hillery, “Coatings for Performance Retention,” *Journal of Vacuum Science and Technology A.* Vol. 4, No. 6, pp. 2624–2632 (1986).
62. J. A. Sue, and H. H. Troue, “High Temperature Erosion Behavior of Titanium Nitride and Zirconium Nitride Coatings,” *Surface and Coatings Technology.* Vol. 49, pp. 31–39 (1991).
63. J. A. Sue and H. H. Troue, “Effect of Crystallographic Orientation on Erosion Characteristics of Arc Evaporation of Titanium Nitride Coating,” *Surface and Coatings Technology.* Vol. 33, pp. 169–181 (1987).
64. J. A. Sue and H. H. Troue, “Influence of Residual Compressive Stress on Erosion Behavior of Arc Evaporation Titanium Nitride Coating,” *Surface and Coatings Technology.* Vol. 36, pp. 766–780 (1988).
65. J. A. Sue and H. H. Troue, “Influence of Crystallographic Orientation, Residual Strains, Crystallite Size and Microhardness on Erosion in ZrN Coatings,” *Surface and Coatings Technology.* Vol. 39/40, pp. 421–434 (1989).
66. J. A. Sue and H. H. Troue, U.S. Patent 5,185,211, “Non-Stoichiometric Titanium Nitride Coating,” Issued February 9, 1993.

67. J. A. Sue and H. H. Troue, U.S. Patent 5,071,693, “Multilayer Coating of a Nitride Containing Compound and Method for Producing It,” Issued December 10, 1991.
68. J. A. Sue and H. H. Troue, U.S. Patent 4,929,322, “Apparatus and Process for Arc Vapor Depositing a Coating in an Evacuated Chamber,” Issued May 29, 1990.
69. M. Brennan, Praxair Follow-on Response to EPRI Vendor Survey, 2007.
70. Praxair Report of WPAFB Rainfall Erosion Test Results on 24k Type 2 Coatings, November 2005.
71. MDS-PRAD Technologies Corporation, Technology Summary Document, October 6, 2006.
72. G. Simpson, “Foreign Comparative Test Program on Russian Erosion Resistant Coatings for Navy GTE Compressors,” Presentation at U.S. Department of Defense Joint Technology Exchange Group (JTEG) Meeting, Lima OH (July 24–26, 2001).
73. M. Klein and G. Simpson, “The Development of Innovative Methods for Erosion Testing a Russian Coating on GE T64 Gas Turbine Engine Compressor Blades,” Paper GT2004-54336, presented at the ASME Turbo Expo 2004, Vienna, Austria (June 14–17, 2004).
74. J. Schell, W. Thorn, M. Lasconde, G. Hein, M. Klein, and M. Mendez, “Erosion Durability Improvement of the T64 Engine for Military Helicopters,” presented at the American Helicopter Society 60th Annual Forum, Baltimore, MD (June 7–10, 2004).
75. MDS-PRAD Technologies Corporation, Coating Brochure, 2006.
76. B. Fischer, M. Klein, and V. Montes Cintron, “Erosion Durability Improvement of the T58 Engine for Military Helicopters,” presented at the American Helicopter Society 61st Annual Forum, Grapevine, TX (June 1–3, 2005).
77. G. Prus, Response to EPRI Coating Vendor Survey and Brochure, Performance Turbine Components, dated Oct. 2006.
78. A. Gongescu, Response to EPRI Coating Vendor Survey, 2007.
79. G. Y. Richardson, C. S. Lei, and W. Tabakoff, “Erosion Testing of Coatings for V-22 Aircraft Applications,” presented at the International Conference on Metallurgical Coatings and Thin Films (ICMCTF 2001) (May 2, 2001).
80. G. Y. Richardson, C. S. Lei, and W. Tabakoff, “Erosion Testing of Coatings for V-22 Aircraft Applications,” *International Journal of Turbomachinery*. Vol. 9, No. 1, pp. 35–40, (2003).
81. Aerocoat K Technical Data Sheet, May 2006.
82. R. Sivakumar, AS&M Presentation, “Aerocoat K Erosion, Corrosion and Cavitation Resistant Coating,” January 2007.
83. http://www.sherwoodpumps.com/FileAttachments/Spray/en-us/Spray%20Tip%20Classification%20by%20Droplet%20Size.pdf
84. Air Force Research Laboratory, Materials and Manufacturing, *Rain Erosion Test Apparatus User Guide*, July 2006.
85. Dynaflow, Inc., brochure on Research & Development in Applied Sciences.

86. L. Prchlik, SKODA brochures/publications on Research on Erosion of Steam Turbine Blades.
87. ASTM G76-04, Standard Test Method for Conducting Erosion Tests by Solid Particle Impingement Using Gas Jets.
88. Particle Erosion Test Apparatus, Air Force Research Lab, Utilization Policy, Operating Procedures, and Specimen Configurations, July 1999.
89. Not used.
90. A. Hamed W. Tabakoff, R. Riva, K. Das, and P. Arora “Turbine Blade Surface Deterioration by Erosion,” Paper GT2004-54328, Proceedings of ASME Turbo Expo 2004, Vienna, Austria (June 14–17, 2004).

A
APPENDIX

Table A-1
Listing of erosion coating patents (1979 to 2007)

Inventor(s)	Assignee	Patent Number	Issue Date	Coating Concept
R. Holzl	Chemetal Corp.	4,147,820	4/3/79	LT-CVD tungsten-tungsten carbide.
S. Naik	AVCO Corp	4,761,346	8/2/88	Layer system of ductile inner layer – outer carbide, boride or nitride hard layer.
M. Hakim	Liburdi Engineering Ltd	4,803,127	3/27/89	Low temperature CVD of TiN.
A. Sue and H. Troue	Union Carbide (Now Praxair)	4,839,245	6/13/89	CA-PVD zirconium nitride average grain size < 0.3 nm.
D. Garg et al.	Air Products and Chemicals Inc	4,855,188	8/8/89	LT CVD tungsten-tungsten carbide with ductile Ni and W inner layers.
A. Sue and H. Troue	Union Carbide (Now Praxair)	4,895,765	1/23/90	CA-PVD titanium nitride and zirconium nitride coatings and method of manufacture.
D. Gupta and M. Freling	United Technologies	4,904,528	2/27/90	Hyperstoichiometric TiN by CA-PVD. Claim excess nitrogen in TiN with N:Ti ratios of 1.05 to 1.15 generate significant residual compressive stress in canceling fatigue debit in titanium compressor alloys.
D. Garg et al.	Air Products and Chemicals Inc	4,927,713	5/22/90	LT CVD tungsten-tungsten carbide with ductile W inner layers.
D. Garg et al.	Air Products and Chemicals Inc	5,006,371	4/9/91	LT CVD tungsten-tungsten carbide with ductile W inner layers. Method patent.

Table A-1 (continued)
Listing of Erosion Coating Patents (1979 to 2007)

Inventor(s)	Assignee	Patent Number	Issue Date	Coating Concept
A. Sue and H. Troue	Union Carbide (Now Praxair)	5,071,693	12/10/91	The invention relates to a *multilayer coating* of at least two layers of a nitride-containing compound, such as titanium nitride, in which at least one layer contains at least 2 atomic percent of nitrogen different than the nitrogen contained in an adjacent layer. The invention also relates to a method for producing the *multilayer coating*.
A. Sue and H. Troue	Praxair S.T. Technology	5,185,211	2/9/93	A wear and erosion-resistant coating for substrates having a non-nitrogen titanium-containing outer surface onto which a non-stoichiometric titanium nitride coating is deposited in which the nitrogen content in the titanium nitride coating is from 32.5 to 47 atomic weight percent.
A. Sue and H. Troue	Praxair S.T. Technology	5,242,753	9/7/93	A wear and erosion-resistant coating for substrates which comprises a sub-stoichiometric zirconium nitride coating having a nitrogen content in the zirconium nitride coating from 41 to 48 atomic weight percent.
S. Paidassi, et al.	Commissariat A L'Energie Atomique	5,547,767	8/20/96	Tungsten-solid solution carbon or nitrogen tungsten enriched multilayers.
Rickerby , et al.	Rolls-Royce , Turbomeca, Etat Francais-Delegation Generale Pour L'Armement	5,656,364	8/12/97	A multiple layer erosion-resistant coating on a substrate comprises alternate layers of tungsten and titanium diboride. All of the layers have the same thickness and preferably have thicknesses of between 0.3 and 1 micrometer to give improved ***erosion resistance***. The layers are produced by sputtering.
S. Paidassi, et al.	Turbomeca & Commissariat A L'Energie Atomique	5,702,829	12/30/97	Tungsten-solid solution carbon or nitrogen tungsten enriched multilayers.

Table A-1 (continued)
Listing of Erosion Coating Patents (1979 to 2007)

Inventor(s)	Assignee	Patent Number	Issue Date	Coating Concept
Rickerby , et al.	Rolls-Royce , Turbomeca, Etat Francais-Delegation Generale Pour L'Armement	5,876,572	3/2/99	A multiple layer erosion-resistant coating on a substrate comprises alternate layers of tungsten and titanium diboride. All of the layers have the same thickness and preferably have thicknesses of between 0.3 and 1 micrometer to give improved ***erosion resistance***. The layers are produced by sputtering. Method patent.
Rickerby , et al.	Rolls-Royce , Turbomeca, Etat Francais-Delegation Generale Pour L'Armement	5,952,085	9/14/99	A multiple layer erosion-resistant coating on a substrate comprises alternate layers of tungsten and titanium diboride. All of the layers have the same thickness and preferably have thicknesses of between 0.3 and 1 micrometer to give improved ***erosion resistance***. The layers are produced by spattering.
A. Sue	Praxair S.T. Technology	6,025,021	2/15/2000	Multilayered coating where the first layered zone deposited on a substrate which comprises at least one layer of a titanium nitrogen-containing layer with a nitrogen content varying from 0 to 35 atomic percent, a second layered zone deposited on the first layered zone and which comprises at least two layers of a titanium nitrogen-containing compound with a nitrogen content varying from 38 atomic percent to 54 atomic percent of nitrogen.
B. Sanders et al.	Analytical Services and Materials (AS&M)	6,706,405	3/16/04	Erosion-resistant composite coating based on siloxane polymeric compounds applied at room temperature.
A. Paderov et al.	None	6,797,335	9/28/04	Multilayer coating with alternating stacks of metal and metal nitrides, carbides, borides or combinations with ion implantation to improve properties.

Table A-1 (continued)
Listing of Erosion Coating Patents (1979 to 2007)

Inventor(s)	Assignee	Patent Number	Issue Date	Coating Concept
K. Wiedemann et al.	Analytical Services and Materials (AS&M)	7,033,673	4/25/06	Erosion-resistant silicone coating applied at room temperature.
C. Leyens et al.	Sheffield Hallam Univ.	7,160,635	1/9/07	TiAlCr nitride erosion-resistant coatings and method of manufacture. CA-PVD and MS-PVD.

Export Control Restrictions
Access to and use of EPRI Intellectual Property is granted with the specific understanding and requirement that responsibility for ensuring full compliance with all applicable U.S. and foreign export laws and regulations is being undertaken by you and your company. This includes an obligation to ensure that any individual receiving access hereunder who is not a U.S. citizen or permanent U.S. resident is permitted access under applicable U.S. and foreign export laws and regulations. In the event you are uncertain whether you or your company may lawfully obtain access to this EPRI Intellectual Property, you acknowledge that it is your obligation to consult with your company's legal counsel to determine whether this access is lawful. Although EPRI may make available on a case-by-case basis an informal assessment of the applicable U.S. export classification for specific EPRI Intellectual Property, you and your company acknowledge that this assessment is solely for informational purposes and not for reliance purposes. You and your company acknowledge that it is still the obligation of you and your company to make your own assessment of the applicable U.S. export classification and ensure compliance accordingly. You and your company understand and acknowledge your obligations to make a prompt report to EPRI and the appropriate authorities regarding any access to or use of EPRI Intellectual Property hereunder that may be in violation of applicable U.S. or foreign export laws or regulations.

The Electric Power Research Institute (EPRI), with major locations in Palo Alto, California; Charlotte, North Carolina; and Knoxville, Tennessee, was established in 1973 as an independent, nonprofit center for public interest energy and environmental research. EPRI brings together members, participants, the Institute's scientists and engineers, and other leading experts to work collaboratively on solutions to the challenges of electric power. These solutions span nearly every area of electricity generation, delivery, and use, including health, safety, and environment. EPRI's members represent over 90% of the electricity generated in the United States. International participation represents nearly 15% of EPRI's total research, development, and demonstration program.

Together...Shaping the Future of Electricity

Program:
Technology Innovation

© 2008 Electric Power Research Institute (EPRI), Inc. All rights reserved. Electric Power Research Institute, EPRI, and TOGETHER...SHAPING THE FUTURE OF ELECTRICITY are registered service marks of the Electric Power Research Institute, Inc.

Printed on recycled paper in the United States of America

1017458

Electric Power Research Institute
3420 Hillview Avenue, Palo Alto, California 94304-1338 • PO Box 10412, Palo Alto, California 94303-0813 USA
800.313.3774 • 650.855.2121 • askepri@epri.com • www.epri.com